

Aus der Klinik für Kardiologie, Pneumologie und Angiologie  
der Heinrich Heine Universität Düsseldorf  
Direktor Prof. Dr. med. Malte Kelm

Nrf2 as a converging node of redox sensing and  
signaling in HUVECs induced by (-)-epicatechin,  
nitric oxide, sulfide and nitrosopersulfide

Dissertation

zur Erlangung des Grades eines Doktors der Medizin  
der Medizinischen Fakultät der Heinrich Heine Universität zu Düsseldorf

vorgelegt von

**David Pullmann**

Düsseldorf, 2018

aus der Klinik für Kardiologie, Pneumologie und Angiologie  
der Heinrich Heine Universität Düsseldorf  
Direktor Prof. Dr. med. Malte Kelm

Als Inauguraldissertation gedruckt mit der Genehmigung der Medizinischen Fakultät der  
Heinrich-Heine-Universität Düsseldorf

Gez.:

Dekan:	Prof. Dr. med. Nikolaj Klöcker
Erstgutachterin	Prof. Dr. rer. nat. Miriam M. Cortese-Krott
Zweitgutachter	Prof. Dr. rer. nat. Wilhelm Stahl (Institut für Biochemie und Molekularbiologie I)

Tag der mündlichen Prüfung: 19.06.2018

Ich möchte diese Arbeit meiner Mutter Heike Pullmann und meinen Großeltern Anton und Maria Bauer widmen. Vielen Dank für eure Unterstützung in meinem Studium und in meinem gesamten Leben. Ohne euch hätte ich nichts von dem geschafft, was ich bisher geschafft habe. Danke, dass ihr mich zu dem gemacht habe was ich bin und dafür, dass ihr mir alle Freiheit gebt zu sein und zu werden was ich will.

Neugier ist der Schlüssel zur Erkenntnis.

Fleiß ist der Schlüssel zum Erfolg.

Freude ist der Schlüssel zum Glück.

Freundschaft ist der Schlüssel zu Unsterblichkeit.

(MGS)

Teile dieser Arbeit wurden veröffentlicht

Cortese-Krott, M. M., Pullmann, D. and Feelisch, M. “Nitrosopersulfide (SSNO(-)) targets the Keap-1/Nrf2 redox system.” (2016) Pharmacol. Res. **113**, 490–499.

## Summary

**Background** Oxidative and electrophilic stress-induced Nrf2 signaling mediates the expression of antioxidant and phase II detoxifying enzymes via binding to the antioxidant response element (ARE). Therefore, Nrf2 plays a crucial role in mammalian cell protection from oxidative and electrophilic insults, which cause cellular dysfunction. Since electrophilic agents are capable of activating Nrf2 it is of great interest whether Keap1-Nrf2-interaction is a common target of these molecules in human endothelial cells and hereby acts as a converging node of sensing electrophilic and oxidative stress and of maintaining cellular redox homeostasis.

**Aims** The aim of this dissertation was to elucidate and compare the effects of the electrophiles (1) (-)-epicatechin, (2) NO<sup>·</sup>, NO<sup>-</sup> and NO<sup>+</sup>, (3) sulfide, (4) the crosstalk of NO and sulfide and (5) their recently described reaction product SSNO<sup>-</sup> on Keap1-Nrf2-interaction in the same cellular model (human umbilical vein endothelial cells – HUVECs).

**Methods** HUVECs were treated with the substances in micromolar concentrations in medium containing 2% inactivated FCS. Nrf2 translocation into the nucleus and binding to ARE was detected by transcription factor binding assays. Additionally, western blots of nuclear extracts were performed. Transcription of phase II antioxidant enzymes (Hmox1, Nqo1 and Gclc) was determined using reverse transcription real time PCR. The formation of reaction products of nitric oxide and sulfide (SSNO<sup>-</sup>) was measured via UV-visible spectrometry.

**Results** (1) Nrf2 binding activity of HUVECs was significantly increased ( $1.48 \pm 0.09$  fold) upon incubation with 10 μM (-)-epicatechin, whereas gene expression of Hmox1, Nqo1 and Gclc was only little affected. (2) Treatment with 1-100 μM concentrations of NO<sup>·</sup>, NO<sup>-</sup> and NO<sup>+</sup> donors showed that NO<sup>·</sup> (released by SPER/NO) increased ARE binding ( $2.05 \pm 0.1$  fold at 100 μM) and Hmox1 gene expression ( $16.26 \pm 1.97$  fold at 20 μM) most potently while the other two redox congeners had weaker but still significant effects. (3) The sulfide donor Na<sub>2</sub>S only exerted significant effects on Nrf2 activation when concentrations were higher than 100 μM ( $1.43 \pm 0.14$  fold at 200 μM,  $2.25 \pm 0.27$  fold at 400 μM) while GYY 4137 had no significant effects at micromolar concentrations. (4) Crosstalk of NO and sulfide led to diverging results. While the Nrf2 activation of the NO<sup>+</sup> donor S-nitroso-N-acetylpenicillamine (SNAP) was attenuated by sulfide, co-incubation with sulfide did not affect SPER/NO derived Nrf2 activation. (5) Treatment of HUVECs with SSNO<sup>-</sup> led to the strongest and most significant activation of Nrf2 ( $1.76 \pm 0.28$  fold at 20 μM,  $2 \pm 0.42$  fold at 40 μM) and transcription of Hmox1 mRNA ( $10.68 \pm 1.31$  fold at 20 μM) among all substances analyzed. Upon coincubation with NO scavengers (cPTIO) and after decomposition of polysulfides (upon coincubation with cysteine) Nrf2 binding activity and Hmox1 gene expression were significantly decreased indicating that NO release and polysulfides contribute to Nrf2 activation of the SSNO<sup>-</sup> mix.

**Conclusion** For the first time Nrf2 activation, translocation and transcription of phase II detoxifying enzymes was directly compared in the same cellular model (HUVECs) after treatment with (-)-epicatechin, NO<sup>·</sup>, NO<sup>-</sup> and NO<sup>+</sup>, sulfide and reaction products of NO and sulfide (SSNO<sup>-</sup>, SULFI/NO, polysulfides). Taken together this study showed that among all substances under investigation NO<sup>·</sup> and SSNO<sup>-</sup> exert the most distinct effects on Nrf2 signaling, whereas effects of SSNO<sup>-</sup> are likely to be mediated by its products of homolysis NO<sup>·</sup> and S<sub>2</sub><sup>·-</sup> of which the later results in formation of polysulfides. Therefore, these molecules emerge to play a key role in redox signaling and should be subject to subsequent studies.

## Zusammenfassung

**Hintergrund** Der durch oxidativen Stress induzierte Nrf2 Signalweg vermittelt die Expression von antioxidativen Phase II Enzymen. Daher spielt Nrf2 eine entscheidende Rolle beim Schutz eukaryotischer Zellen vor oxidativen oder elektrophilen Schäden, die zu zellulärer Dysfunktion führen können und damit zur Pathogenese vieler Krankheiten beitragen. Da elektrophile Substanzen in der Lage sind Nrf2 zu aktivieren ist es von großem Interesse, ob die Keap1/Nrf2 Interaktion auch in menschlichen Endothelzellen ein gemeinsames molekulares Ziel dieser Substanzen ist und einen Knotenpunkt bei der Wahrnehmung und Antwort von elektrophilem und oxidativen Stress darstellt und somit zur Aufrechterhaltung der zellulären Redox Homöostase in humanen Endothelzellen beiträgt.

**Ziel** Die Ziele dieser Dissertation waren demnach den Einfluss von (1) (-)-Epicatechin, (2) NO<sup>•</sup>, NO<sup>-</sup> und NO<sup>+</sup>, (3) Sulfid, (4) einem Wechselspiel von NO und Sulfid und (5) deren vor kurzem beschriebenen Reaktionsprodukts SSNO<sup>-</sup> auf die Aktivierung und Translokation von Nrf2 und die Expression der Phase II Enzyme zu untersuchen und zwar in einem direkten Vergleich im selben zellulären Modell (human umbilical vein endothelial cells – HUVECs).

**Methoden** HUVECs wurden mit den jeweiligen Substanzen in Medium mit 2% inaktiviertem FCS behandelt. Nach 1 h wurde die Nrf2 Translokation und Bindungsaktivität an das *Antioxidative Responsive Element (ARE)* durch Transkriptionsfaktor-Assays und Western-Blots von Kernextrakten bestimmt. Die Genexpression der antioxidativen Phase-II Enzyme Hmox1, NQO1 und GCLC wurden unter Verwendung der *reverse transcription real time PCR* bestimmt. Zelluläre Glutathion Konzentrationen wurden mit Fluoreszenznachweismethoden analysiert. Die Entstehung des Reaktionsproduktes von NO und Sulfid (SSNO<sup>-</sup>) wurde mittels UV-sichtbarer-Spektrometrie gemessen.

**Ergebnisse** (1) die Nrf2 Bindungsaktivität von HUVECs war nach Behandlung der Zellen mit 10µM (-)-Epicatechin signifikant auf das 1.48 ±0.09 fache erhöht wohingegen die Gen Expression von Hmox1, Nqo1 und Gclc nur geringfügig beeinflusst wurde. (2) Behandlung mit 1-100 µM NO<sup>•</sup>, NO<sup>-</sup> und NO<sup>+</sup> Donoren zeigte, dass NO<sup>•</sup> (aus SPER/NO freigesetzt) sowohl die Nrf2 Bindungsaktivität (2.05 ±0.1 fach bei 100 µM) als auch die Hmox1 Genexpression (16.26 ±1.97 fach bei 20 µM) am stärksten beeinflusst während seine Redox Varianten NO<sup>-</sup> und NO<sup>+</sup> nur geringeren jedoch trotzdem signifikanten Einfluss hatten. (3) Der Sulfid Donor Na<sub>2</sub>S erhöhte die Nrf2 Bindungsaktivität nur bei Konzentrationen von über 100 µM signifikant (1.43 ±0.14 fach bei 200 µM, 2.25 ±0.27 fach bei 400 µM) während GYY 4137 in mikromolaren Konzentrationen keinen signifikanten Effekt auf Nrf2 hatte. (4) Das Zusammenspiel von Sulfid und NO zeigte unterschiedliche Ergebnisse. Während die Nrf2 Aktivierung durch den NO<sup>+</sup> Donor S-nitroso-N-acetylpenicillamine (SNAP) von Sulfid abgeschwächt wurde, hatte die Co-Inkubierung von Sulfid und SPER/NO keinen eindeutigen Effekt.

(5) Die Behandlung von HUVECs mit begastem SSNO<sup>-</sup> führte zur stärksten, signifikanten Nrf2 Aktivierung (1.76 ±0.28 fach bei 20 µM, 2 ±0.42 fach bei 40 µM) und Hmox1 Expression (10.68 ±1.31 fach bei 20 µM) unter allen untersuchten Substanzen. Es konnte gezeigt werden, dass die Freisetzung von NO<sup>•</sup> und Entstehung von Polysulfiden durch den Zerfall von SSNO<sup>-</sup> wesentlich zu den SSNO<sup>-</sup> induzierten Effekten auf den Nrf2 Signalweg beitragen, da nach gemeinsamer Inkubierung mit dem NO Scavenger (cPTIO) und nach Zerfall der Polysulfide durch Anwesenheit von millimolarem Cystein die Nrf2 Bindungsaktivität deutlich geschwächt wurde.

**Fazit** Zum ersten Mal wurden die Effekte elektrophiler Substanzen auf den Nrf2 Signalweg und die Gen Expression von Phase II Enzymen im selben zellulären Model verglichen, indem HUVECs mit (-)-Epicatechin,  $\text{NO}^\cdot$ ,  $\text{NO}^-$  und  $\text{NO}^+$ , Sulfid und dem Reaktionsprodukt aus NO und Sulfid ( $\text{SSNO}^-$ , SULFI/NO, Polysulfide) behandelt wurden. Hierbei konnte diese Arbeit zeigen, dass unter allen untersuchten Substanzen  $\text{NO}^\cdot$  und  $\text{SSNO}^-$  die stärksten Effekte auf den Nrf2 Signalweg hatten, wobei diese Effekte sehr wahrscheinlich durch die Zerfallsprodukte  $\text{NO}^\cdot$  und  $\text{S}_2^-$  vermittelt werden. Diese Ergebnisse legen nahe, dass diese beiden Substanzen eine Schlüsselrolle in der Redoxkommunikation spielen könnten. Deshalb sollten sie in weiteren Studien zum Zusammenspiel von NO und Sulfid eingehend untersucht werden.

## Abbreviations

<b>ARE</b>	Antioxidant response element
<b>AS</b>	Angeli's salt
<b>BAEC</b>	Bovine aortic endothelial cells
<b>Ca<sup>2+</sup></b>	Calcium
<b>cDNA</b>	complementary DNA
<b>cPTIO</b>	2-(4-Carboxyphenyl)-4,4,5,5-tetramethylimidazoline-1-oxyl-3-oxide
<b>CTRL</b>	Control
<b>DEA/NO</b>	DiethylaminoNO-NOate
<b>DMSO</b>	Dimethylsulfoxid
<b>DNA</b>	Desoxyribonucleic acid
<b>DTT</b>	Dithiothreitol
<b>ELISA</b>	Enzyme linked immunosorbent assay
<b>eNOS</b>	endothelial nitric oxide synthase
<b>ERK</b>	extracellular signal-regulated kinase
<b>Fig.</b>	Figure
<b>FMD</b>	flow mediated dilation
<b>G</b>	Gravitational force
<b>Gclc</b>	Glutamate-cysteine ligase catalytic subunit
<b>GSH</b>	Glutathione
<b>GSNO</b>	S-nitrosoglutathione
<b>GSSG</b>	Glutathione disulfide
<b>GY 4137</b>	( <i>p</i> -methoxyphenyl)morpholino-phosphinodithioic acid
<b>H<sub>2</sub>O<sub>dd</sub></b>	Double distilled water
<b>H<sub>2</sub>O<sub>2</sub></b>	hydrogen peroxide
<b>HepG2</b>	hepato cellular carcinoma cell line
<b>Hmox1/ HO-1</b>	Hemeoxygenase 1
<b>HRP</b>	Horse radish peroxidase
<b>HS<sup>-</sup></b>	Hydrogen sulfide
<b>HSNO</b>	thionitrite
<b>HUVECs</b>	human umbilical vein endothelial cells
<b>IgG</b>	Immunoglobulin G
<b>IU</b>	International unit
<b>kDa</b>	Kilo dalton
<b>KO</b>	Knock out
<b>L-Arg</b>	L-Arginine
<b>LDL</b>	Low density lipoprotein
<b>L-NAME</b>	N <sup>G</sup> -Nitro-L-arginine-methyl ester. HCl
<b>MAPK</b>	Mitogen-activated protein kinase
<b>max.</b>	Maximum
<b>min.</b>	Minimum

<b>mM</b>	Millimolar
<b>mRNA</b>	messenger RNA
<b>n</b>	Number
<b>N<sub>2</sub>O</b>	nitrous oxide
<b>Na<sub>2</sub>S</b>	Sodium disulfide
<b>NaCl</b>	Potassium chloride
<b>NADP</b>	Nicotinamide adenine dinucleotide phosphate
<b>NF<sub>κ</sub>B</b>	nuclear factor 'kappa-light-chain-enhancer' of activated B-cells
<b>NO<sup>•</sup></b>	nitric oxide
<b>NO<sup>-</sup></b>	nitroxyl
<b>NO<sup>+</sup></b>	nitrosonium
<b>NO<sup>2-</sup></b>	nitrite
<b>NO<sup>3-</sup></b>	nitrate
<b>Nqo1</b>	NAD(P)H dehydrogenase (quinone 1)
<b>Nrf2</b>	Nuclear factor (erythroid-derived 2)-like 2
<b>p</b>	Statistical probability value
<b>Pa</b>	Pascal
<b>PBS</b>	Phosphate buffered saline
<b>PCR</b>	Polymerase chain reaction
<b>Pen</b>	Penicillin
<b>ROS</b>	Reactive oxygen species
<b>RBC</b>	Red blood cell
<b>RNA</b>	Ribonucleic acid
<b>RNS</b>	Reactive nitrogen species
<b>RT</b>	Reverse transcription
<b>SD</b>	standard deviation
<b>SDS PAGE</b>	Sodium dodecyl polyacrylamite gel electrophoresis
<b>SEM</b>	Standard error of the mean
<b>SIN 1</b>	3-morpholinosydnonimine
<b>SMC</b>	Smooth muscle cells
<b>SNAP</b>	S-nitroso-N-acetylpenicillamine
<b>SNP</b>	sodium nitroprusside
<b>SPER/NO</b>	Spermine NONOate
<b>SSNO<sup>-</sup></b>	nitrosopersulfide
<b>Strep</b>	Streptomycin
<b>Tab.</b>	table
<b>tBHQ</b>	Tert-Butyl Hydrochinon
<b>TBS</b>	Tris buffer saline
<b>UV</b>	ultra violet
<b>VEGF</b>	Vascular endothelial growth factor
<b>WT</b>	Wild type

# Content

Summary .....	6
Content .....	10
1 Introduction .....	14
1.1 Oxidative stress signaling in biological systems .....	14
1.2 Keap1 Nrf2 ARE pathway.....	15
1.2.1 Structural basis .....	15
1.2.2 Keap1-Nrf2-ARE interaction .....	16
1.3 (-)-epicatechin.....	18
1.3.1 Beneficial effects.....	18
1.3.2 Chemical structure and properties.....	18
1.3.3 Bioavailability and metabolism.....	18
1.3.4 Effect on Endothelial Cells .....	19
1.4 Nitric oxide.....	20
1.4.1 Nitric oxide sources, circulation and signaling .....	20
1.4.2 Nitric oxide releasing compounds.....	20
1.4.3 Nitric oxide and Nrf2 in endothelial cells .....	21
1.5 Sulfide.....	22
1.5.1 Endogenous production, exogenous sources and metabolism .....	22
1.5.2 Biological activity and influence on endothelial cells .....	23
1.6 Crosstalk of sulfide and nitric oxide.....	24
1.6.1 Biological similarities and cross talk of sulfide and nitric oxide signaling .....	24
1.6.2 Keap1-Nrf2-signaling as a potential target of sulfide and nitric oxide crosstalk.....	25
1.7 Aims of the dissertation.....	26
2 Material .....	27
2.1 Cells.....	27
2.2 Media und Antibiotics .....	27
2.3 Western blot - Solutions and Buffer .....	27

2.4	Synthetic Primers.....	28
2.5	Reverse transcription real time PCR .....	28
2.6	siRNA.....	28
2.7	Antibodies.....	28
2.8	Chemicals .....	28
2.9	Consumables.....	29
2.10	Equipement .....	30
2.11	Kits.....	31
2.12	Software .....	31
3	Methods.....	32
3.1	Cell culture .....	32
3.1.1	Cells.....	32
3.1.2	Incubation and population of the cells .....	32
3.1.3	Freezing and thawing of the cells.....	32
3.1.4	Trypsinization of the cells (splitting protocol).....	33
3.1.5	Cell growth control .....	33
3.1.6	Cell count .....	33
3.2	Substance solutions and mix preparation .....	33
3.3	Synthesis and UV-visible spectrometry of SSNO <sup>-</sup> .....	35
3.3.1	Incubation of SSNO <sup>-</sup> with Zn .....	35
3.3.2	Gassing of SSNO <sup>-</sup> .....	37
3.3.3	Identification of the increased absorbance at 250 to 310 nm.....	38
3.4	Protein level analysis.....	39
3.5	Transcription factor analysis .....	41
3.6	mRNA level analysis.....	43
3.7	Glutathione assay.....	44
3.8	RNA Interference .....	45
3.9	Statistic analysis .....	46

3.10	Citation manager.....	47
4	Results.....	48
4.1	Plan of the study and experimental setup .....	48
4.2	Pre-experiments and evaluation .....	49
4.2.1	Treatment of HUVECs passage $\geq 3$ .....	49
4.2.2	Toxicity tests of treatments .....	50
4.2.3	Transfection with siRNA .....	53
4.3	Effects of (-)-epicatechin on Nrf2 in HUVECs .....	54
4.3.1	Nrf2 transcription factor binding assay .....	54
4.3.2	Western blots of nuclear extracts .....	55
4.3.3	Gene expression .....	56
4.4	Effects of NO $\cdot$ , NO $^-$ and NO $^+$ on Nrf2 in HUVECs .....	58
4.4.1	SPER/NO, SNAP and Angeli's salt .....	58
4.4.2	Treatment with DEA/NO .....	60
4.4.3	Compared Nrf2 activation by nitroxyl, S-nitrosothiol and NO.....	61
4.5	Effects of sulfide on Nrf2 in HUVECs.....	62
4.5.1	Treatment with GYY 4137.....	62
4.5.2	Treatment with Na $_2$ S .....	63
4.6	Modulation of nitric oxide effects on Nrf2 by sulfide in HUVECs .....	64
4.6.1	Treatment with GYY and SPER/NO .....	64
4.6.2	Treatment with GYY and SNAP.....	65
4.6.3	Treatment with sulfide and DEA/NO .....	66
4.6.4	Treatment with GYY and L-NAME .....	67
4.7	Effects of SSNO $^-$ on Nrf2 in HUVECs.....	68
4.7.1	Formation of SSNO $^-$ .....	68
4.7.2	Treatment with SSNO $^-$ .....	68
4.7.3	Treatment with SSNO $^-$ incubated with Zn.....	69
4.7.4	Treatment with gassed SSNO $^-$ .....	71

4.7.5	Influence of nitric oxide and polysulfides on Nrf2 activation by SSNO <sup>-</sup> .....	73
4.7.6	Concentration dependent treatment of HUVECs with gassed SSNO <sup>-</sup> .....	76
4.8	Comparison of HS, NO and SSNO <sup>-</sup> effects on Nrf2 signaling .....	79
4.8.1	Nrf2 activation by nitroxyl, S-nitrosothiol, NO, sulfide and SSNO <sup>-</sup> .....	79
4.8.2	Hmox1 expression by nitroxyl, S-nitrosothiol, NO, sulfide and SSNO <sup>-</sup> .....	80
5	Discussion .....	82
5.1	Major findings .....	82
5.2	Methods measuring Nrf2 activation – advantages and limitations .....	84
5.3	Influence of (-)-epicatechin on Nrf2 signaling in human endothelial cells.....	84
5.4	Influence of nitroxyl, S-nitrosothiols and NO on Nrf2 signaling in human endothelial cells	85
5.5	Influence of sulfide on Nrf2 signaling in human endothelial cells .....	86
5.6	Comparison and Crosstalk of sulfide with NO.....	88
5.7	Formation of SSNO <sup>-</sup> and influence on Nrf2 signaling.....	89
5.7.1	SSNO <sup>-</sup> increases Nrf2 binding activity and Hmox1 gene expression in human endothelial cells.....	89
5.7.2	Sulfide in excess does not contribute to SSNO <sup>-</sup> mediated effects on Nrf2 .....	90
5.7.3	SULFI/NO is not likely to account for SSNO <sup>-</sup> derived effects on Nrf2 signaling.....	90
5.7.4	Nitric oxide plays a crucial role in SSNO <sup>-</sup> signaling.....	91
5.7.5	Polysulfides contribute to SSNO <sup>-</sup> derived effects on Nrf2 signaling .....	92
5.7.6	Who does account for SSNO <sup>-</sup> derived signaling now?.....	92
5.8	Could SSNO <sup>-</sup> be formed endogenously and exert effects on Nrf2 <i>in vivo</i> ?.....	93
5.9	Conclusion, significance and outlook.....	94
6	Literature .....	96

# 1 Introduction

## 1.1 Oxidative stress signaling in biological systems

Oxidative stress is defined as “an imbalance between oxidants and antioxidants in favor of the oxidants, potentially leading to damage” (Sies 1985). These damages include structural impairments on a broad variety of biological compound most importantly nucleic acids, proteins, carbohydrate and lipids (Sies 1986) and they appear to be a keystone to systemic impairments and pathophysiology in form of carcinogenesis (Trachootham, Alexandre et al. 2009), neurodegeneration (Andersen 2004, Shukla, Mishra et al. 2011), diabetes (Paravicini and Touyz 2006), arteriosclerosis (Stocker and Keaney 2004) and aging (Haigis and Yankner 2010). Since sources of oxidative stress are manifold and include metabolic oxidative stress, environmental oxidative stress, photooxidative stress, drug-dependent oxidative stress and nitrosative stress (Encyclopedia of stress, Fink and Fink 2000, volume 3, chapter "oxidative stress", H. Sies and D. Jones), oxidative stress occurs ubiquitous in all cells at both physiological and pathological conditions. Therefore, all cells require sufficient mechanisms to maintain redox homeostasis. These mechanisms include non-enzymatic systems (tocopherole, ascorbate, glutathione etc.) as well as enzymatic systems (superoxide dismutase, glutathione peroxidase, glutathione-disulfide reductase etc.), of which the later account for the major part of antioxidant defense, and in its entirety is described by the term *redox signaling* (Sies 1993). Therefore, the “discovery of master switch systems” (Sies 2015) was particularly important. These systems include nuclear factor 'kappa-light-chain-enhancer' of activated B-cells (NFκB) (Schreck, Rieber et al. 1991) and Nrf2/Keap1 (Itoh, Chiba et al. 1997) amongst others summarized in (Lukosz, Jakob et al. 2010). However, amongst all these pathways nuclear factor (erythroid-derived 2)-like 2 (Nrf2) signaling seems to play a key role in reactive oxygen species derived oxidative stress response (Dhakshinamoorthy, Long et al. 2000, Jaiswal 2004, Kobayashi and Yamamoto 2006, Zhang 2006) and was therefore put to focus of this work.

## 1.2 Keap1 Nrf2 ARE pathway

### 1.2.1 Structural basis

Nrf2 is a basic leucine zipper transcription factor with a cap'n'collar (Moi, Chan et al. 1994, Itoh, Igarashi et al. 1995) domain and highly conserved in most species (Kobayashi, Itoh et al. 2002).

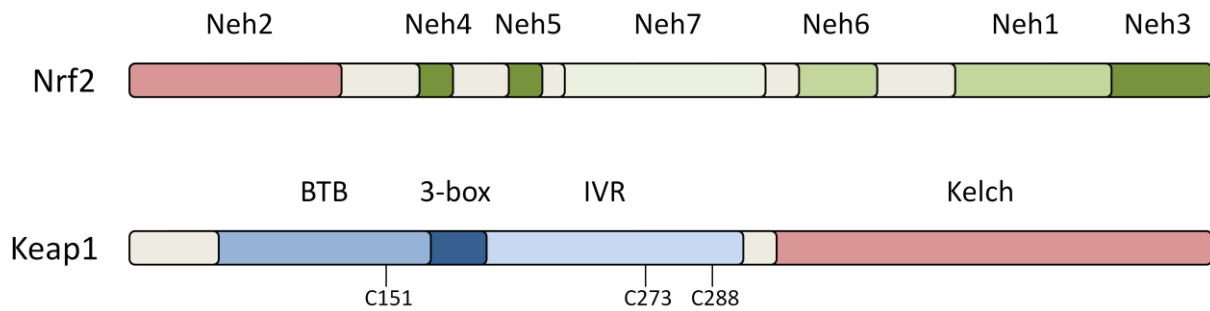


Fig. 1 Domain architecture of human KEAP1 and Nrf2 protein. Modified from Canning et al. and Saito et al. (Canning, Sorrell et al. 2015, Saito, Suzuki et al. 2015)

As Fig. 1 shows Nrf2 consists of seven Neh (Nrf2-ECH homology) domains. With its cap'n'collar basic leucine zipper domain Neh1 allows heterodimerization with small musculoaponeurotic fibrosarcoma proteins (small Maf) (Motohashi, Katsuoka et al. 2004). Neh2 contains the DLG and ETGE degrons which are substrates to Kelch-like ECH-associated protein 1 (Keap1) binding sites (Tong, Padmanabhan et al. 2007). Neh 3-5 are essential for transcription (Katoh, Itoh et al. 2001, Nioi, Nguyen et al. 2005) whereas Neh 6 was described as a redox independent degron which is not bound by Keap1 (McMahon, Thomas et al. 2004). Function of Neh7 is not clear yet.

Keap1 however contains three main domains. The N-terminal BTB (Broad complex, Tramtrack, Bric à brac) mediates Keap1 homodimerization and Cul 3 interaction (Cleasby, Yon et al. 2014). The 3-box motif belongs to the IVR part, whereas the C-terminal Kelch domain is the binding site for Nrf2 via its ETGE and DLG motives (Lo, Li et al. 2006, Padmanabhan, Tong et al. 2006, Tong, Padmanabhan et al. 2007, Fukutomi, Takagi et al. 2014).

ARE, also referred to as electrophile response element (*ERE*), is a *cis*-regulatory element or enhancer sequence and acts as the promoter region of many phase II detoxifying enzymes such as heme oxygenase 1 (HO-1), glutathione S-transferase (GST) and NAD(P)H quinone reductase (NQO) amongst others. Rushmore et al. were the first to describe its sequence as 5'-puGTGACNNNGC-3' (Rushmore, Morton et al. 1991). Bach1 is a transcriptional repressor and competes against Nrf2 for ARE binding (Dhakshinamoorthy, Jain et al. 2005).

### 1.2.2 Keap1-Nrf2-ARE interaction

Nrf2 is abundant in almost all tissues and cells of the human body (Chan, Han et al. 1993, Moi, Chan et al. 1994, McMahon, Itoh et al. 2001) and considered to play a crucial role in mediating antioxidant response (Kobayashi and Yamamoto 2006) and therefore maintaining redox homeostasis.

Keap1 was discovered as the suppressor protein of Nrf2 (Itoh, Wakabayashi et al. 1999). Under physiological conditions Keap1 forms homodimers that are able to bind to the Neh2 part of Nrf2 with their C-terminal Kelch domains. In this coupled state Nrf2 and Keap1, which is an E3 ubiquitin ligase can be targeted to undergo proteasomal degradation (Itoh, Ishii et al. 1999, McMahon, Thomas et al. 2006).

Thus, Keap1 modulation releases Nrf2 from the coupled state to escape proteasomal degradation. Hereafter, Nrf2 accumulates and translocates to the nucleus to form heterodimers with small Mafs and bind to the antioxidant response element (ARE) (Itoh, Chiba et al. 1997). This leads to transcription of ARE dependent genes of phase II enzymes (Rushmore, Morton et al. 1991, Ishii, Itoh et al. 2000) such as Nqo1, Hmox1, Gclc amongst others, which account for detoxifying and antioxidant effects (Kaspar, Niture et al. 2009, Baird and Dinkova-Kostova 2011).

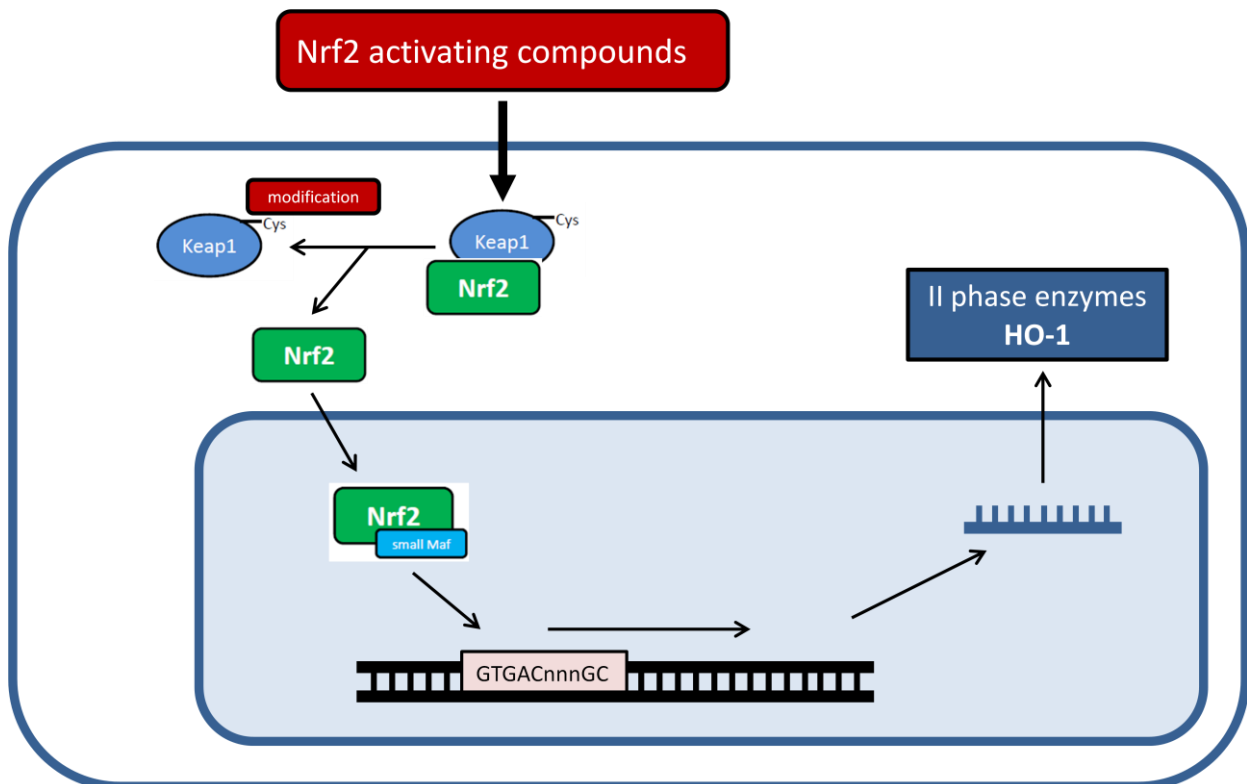


Fig. 2 Keap1-Nrf2-ARE pathway in eukaryotic cells

Since Keap1 modulation is essential for Nrf2 activation it is of great interest by which molecular mechanisms Keap1 is affected. Due to the fact that substances activating Nrf2 belong to different chemical classes but share the same characteristic of readily reacting with protein thiols it was proposed that one or more of the cysteine residues of Keap 1 act as the molecular target of Nrf2 inducers (Dinkova-Kostova, Massiah et al. 2001). In following studies their research group showed sulfhydryl groups of Keap1 to be the major sensors of induced Nrf2 activation (Dinkova-Kostova, Holtzclaw et al. 2002) and proposed a critical role for Cys273 and Cys288 due to their high reactivity and ability to form disulfide bridges. (Wakabayashi, Dinkova-Kostova et al. 2004).

Zhang et al. were also able to identify Cys273 and Cys288 as critical cysteine residues in Keap1, which are required for Keap1-dependent ubiquitination of Nrf2. They also described a third cysteine residue (Cys151) that plays a crucial role for Keap1 inhibition by sulforaphane and oxidative stress (Zhang and Hannink 2003). Further studies reported that Cys151 modification inhibits Cul3 interaction, which is required for E3 ligase activity (Kobayashi, Kang et al. 2004, Rachakonda, Xiong et al. 2008, Cleasby, Yon et al. 2014).

However, while Cys 273, Cys288, and Cys151 were identified as key targets for electrophilic Nrf2 activators (Hong, Freeman et al. 2005) it remained unclear how these cysteine residues are modulated chemically.

Cys151 was reported to play the major key role in electrophile sensing by Keap1 (Zhang and Hannink 2003) and McMahon et al. considered direct adduction of electrophiles to Cys151 as the most likely molecular basis of it. Hereby, the negative charge of the thiolate anion could be removed leading to structural changes in the protein fold (McMahon, Lamont et al. 2010).

NO was also shown to be sensed by Cys151. Mutation of Keap1 (C151S) lead to diminished Nrf2 levels after treatment of mouse embryonic fibroblast cells (MEF) with the NO donor acetoxymethylated diethylamine-NONOate (DEA-NO/AM) (McMahon, Lamont et al. 2010). As the molecular mechanism for NO sensing by Keap1, they suggested S-nitrosylation as the most likely mechanism.

After Nishida et al. described electrophile sulfhydration properties of sulfide (Nishida, Sawa et al. 2012) S-sulfhydration at cysteine 151 could be shown for sulfide and S-nitrosothiol mediated Nrf2 activation (Yang, Zhao et al. 2013). An alternative mechanisms was proposed by Hourihan et al. in which sulfide leads to formation of a disulfide bond between Cys226 and Cys613 inactivating the Keap1 ubiquitin ligase substrate adaptor (Hourihan, Kenna et al. 2012).

## 1.3 (-)-epicatechin

### 1.3.1 Beneficial effects

Accumulating epidemiological evidence shows flavonoids and especially flavanols to mediate beneficial effects on the vasculature amongst other organs and systems. It could be shown, that flavanoids reduce the risk of cardiovascular disease and mortality (Mulvihill and Huff 2010, McCullough, Peterson et al. 2012, Toh, Tan et al. 2013). Therefore their sources, their metabolism, and their molecular effects are of great interest of current investigations.

### 1.3.2 Chemical structure and properties

Flavanoids are natural molecules from sources like cocoa, tea, whine, fruits, and vegetables and belong to the group of polyphenols, which are all derived from the flavan-structure. They distinguish each other by variation of side groups and oxidation status of the carbon rings.

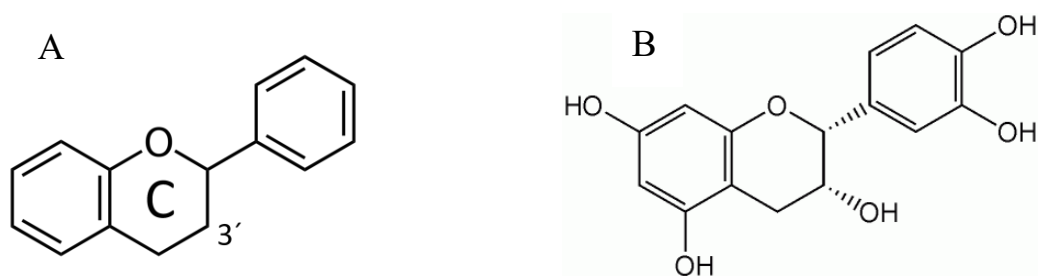


Fig. 3 chemical structures and properties of (A) Flavan structure; (B) (-)-epicatechin with hydroxyl group on 3' position

Flavan-3-ols like (-)-epicatechin share a hydroxyl group on position 3' of the C ring. In plants they serve as chromophoric molecules or protect against UV light or herbivores. Additionally, they have direct antioxidant properties due to their ability to accept one or two electrons to form a semichinon or chinon.

### 1.3.3 Bioavailability and metabolism

Work by Schroeter and Ottaviani et al. (Schroeter, Heiss et al. 2006, Ottaviani, Momma et al. 2011) could show that intake of flavanol monomers has beneficial effects on vascular function in humans indicated by flow-mediated dilation (FMD). Since Ottaviani et al. were also able to detect and measure flavanol-monomers and their methylated, glucuronidated or sulfated metabolites in human blood, (-)-epicatechin was shown to have the greatest bioavailability and bioactive potential (Ottaviani, Momma et al. 2012).

### 1.3.4 Effect on Endothelial Cells

After (-)-epicatechin and its metabolites were found out to have beneficial effects on vascular function in humans (Schroeter, Heiss et al. 2006) there were several studies investigating on the molecular short and long-term mechanisms as reviewed in (Brossette, Hundsdörfer et al. 2011). As one cause especially of these long-term effects cellular redox-homeostasis was considered, not only in vascular research. Flavanols are assumed to provide their influence on cellular signaling by different mechanisms including direct anti-oxidative effects and indirect anti-oxidative effects via cell membrane signaling or intracellular signaling molecules (Fraga and Oteiza 2011).

Flavanoids in general but also Flavanols like (-)-epicatechin were described by some authors to have scavenging activities towards reactive oxygen species (ROS) (Chen, Zheng et al. 1990, Sichel, Corsaro et al. 1991) as well as reactive nitrogen species (RNS) (Haenen, Paquay et al. 1997) depending on their chemical structure. They are able to prevent oxidation by direct anti-oxidative effects. Direct ROS scavenging activity of the flavan-3-ol (-)-epicatechin was described in HUVECs in only one study (Ruijters, Weseler et al. 2013). Though, concentrations applied in this study, which are required for direct antioxidant effects *in vivo*, are not provided by dietary flavanols in most tissues and are lower compared to other antioxidant compounds like glutathione, albumin, ascorbate and tocopherols. Therefore, indirect anti-oxidative effects are much more likely to mediate the beneficial outcome (Fraga and Oteiza 2011).

The intracellular signaling mechanisms described for (-)-epicatechin include mainly NF $\kappa$ B (Mackenzie, Carrasquedo et al. 2004, Mackenzie and Oteiza 2006, Mackenzie, Adamo et al. 2008), MEK/ERK pathway (Kang, Lee et al. 2008) and Nrf2 (Nehlig 2013, Chang, Cho et al. 2014) amongst others (Lukosz, Jakob et al. 2010).

However, due to its electrophilic properties (-)-epicatechin makes a good candidate for Keap1-Nrf2-signaling and therefore was chosen for this study.

For neurons and astrocytes Nrf2 activation and Hmox1 expression was already shown after treatment with (-)-epicatechin in cell culture (Bahia, Rattray et al. 2008) and animal experiments (Shah, Li et al. 2010). Effects could be abolished in Nrf2  $\neg/\neg$  mice (Shah, Li et al. 2010).

However, evidence that (-)-epicatechin accounts for Nrf2 activation in endothelial cells was missing so far.

## **1.4 Nitric oxide**

### **1.4.1 Nitric oxide sources, circulation and signaling**

Since its discovery as endothelium-derived relaxing factor (Ignarro, Buga et al. 1987, Palmer, Ferrige et al. 1987) nitric oxide has been the focus of a broad field of research. It has unique chemical properties that account for its role in cellular signaling. With its unpaired electron nitric oxide is able to bind to ferrous heme parts of proteins like soluble guanylat cyclase (sGC) (Denninger and Marletta 1999) or cytochrome C oxidase (Cooper and Giulivi 2007) by a reaction called nitrosylation. Nitric oxide can also promote nitrosation of proteins mainly by reaction with cysteine residues (Zhang and Hogg 2005). Those nitroso groups can be further transferred to other proteins called transnitrosation.

Due to its short half-life (Thomas, Liu et al. 2001) mechanisms of endogenous generation, transport and release are of crucial importance. Nitric oxide synthetase (NOS) could be identified as the major physiological source of NO, which converts L-arginine and molecular oxygen to citrulline and NO in a calcium dependent manner (Bredt and Snyder 1990). In addition to the endothelial NOS (eNOS) an inducible isoform (iNOS) present in macrophages and monocytes (Siedlar, Mytar et al. 1999) and a neuronal isoform (nNOS) found in neuronal tissues (Rothe, Huang et al. 1999) could be identified. In addition, Cortese-Krott et al. could show that eNOS is not only abundant in the endothelium but is also present and consistently active in red blood cells (Cortese-Krott, Rodriguez-Mateos et al. 2012).

### **1.4.2 Nitric oxide releasing compounds**

For exogenous application of nitric oxide there are many different sources. Some of them already became essential pharmacological therapeutics like glyceryl trinitrate, ISMN, ISDN, nitroprussid sodium and molsidomin.

N-Diazeniumdiolates (NONOate) like Spermine NONOate (SPER/NO) and DiethylaminoNONOate (DEA/NO) can be synthesized from amines and nitric oxide (Hrabie and Keefer 2002) and decompose to NO or nitrosonium by protonation of the NONOate moiety (Keefer 2011, Riccio and Schoenfisch 2012). Therefore, they do not require redox activation and release nitric oxide at first order rates that can easily be dissolved in cell culture media (Keefer 2011).

S-nitrosothiols are considered as one physiological mean of systemic NO circulation (Rassaf, Feelisch et al. 2004). Therefore, the small SNAP molecule serves as a good model for physiological nitric oxide or nitrosonium interaction, which could easily be acquired and administered in cell culture. Angeli's salt (sodium trioxodinitrate) is a nitroxyl donor decomposing at physiological pH whereas nitric oxide could be a reaction product at acidic conditions (pH<4) (DuMond and King 2011) or in the presence of superoxide dismutase (SOD) (Cortese-Krott, Kuhnle et al. 2015).

### **1.4.3 Nitric oxide and Nrf2 in endothelial cells**

Naughton et al. were the first ones to show Nrf2 activation by nitric oxide. They described interaction of heme with nitroxyl and nitric oxide leading to Nrf2 derived Hmox-1 amplification in cardiac cells (Naughton, Hoque et al. 2002). Due to this involvement there were several studies focusing on nitric oxide-Nrf2 interrelation. A significant increase in Hmox-1 mRNA levels could be shown after treatment of BAEC with SNAP, sodium nitroprusside (SNP) and diethylenetriamine-NONOate (DETA/NO) (Foresti, Hoque et al. 2003). SPER/NO was also found to affect Nrf2 activation as well as HO-1 and total GSH levels in BAEC (Buckley, Marshall et al. 2003). Complementary, nitric oxide and peroxynitrite interaction with Nrf2 was described for macrophages (Abbas, Breton et al. 2011), rat aortic SMC (Liu, Peyton et al. 2007) and rat aortic ECs (Cortese-Krott, Suschek et al. 2009).

However, although different NO donors and its redox switches were already shown to activate Nrf2 signaling in endothelial cells it remains unknown if NO activates Nrf2 signaling in human endothelial cells and how different NO redox congeners would affect Nrf2 signaling in direct comparison to each other in the same cellular model.

## 1.5 Sulfide

### 1.5.1 Endogenous production, exogenous sources and metabolism

In mammalian cells sulfide is mainly generated from L-cysteine or homocysteine by cystathionine beta-synthase (CBS) and cystathionine gamma-lyase (CSE) (Wang 2012). As Yang et al. could demonstrate both enzymes contribute to endogenous cellular H<sub>2</sub>S levels, which are significantly lowered in CSE knockout mouse embryonic fibroblasts (MEF) and after CSE/CBE inhibition (Yang, Zhao et al. 2013).

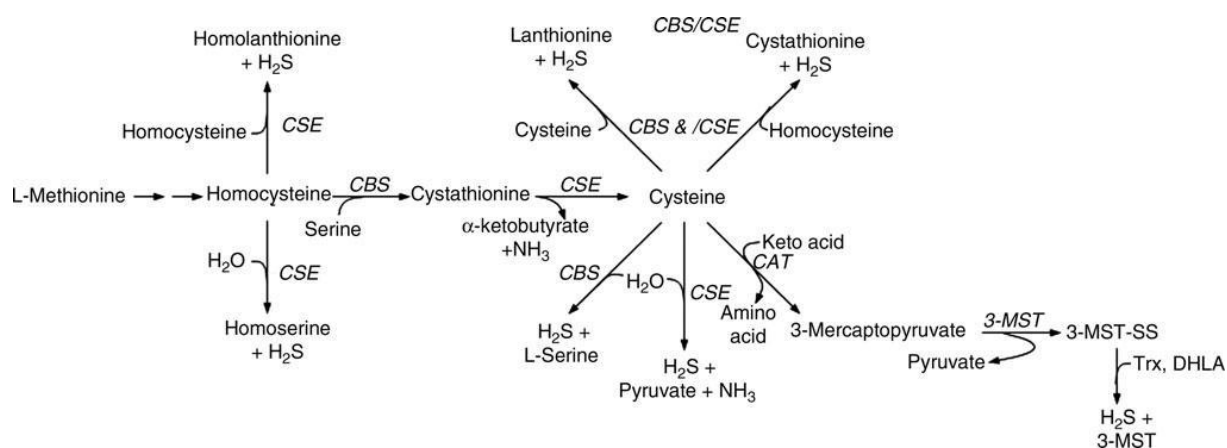


Fig. 4 pathways of H<sub>2</sub>S biosynthesis (Olson 2012) DHLA, dihydrolipoic acid; CAT, cysteine aminotransferase; CBS, cystathionine b-synthase; CSE, cystathionine c-ligase; ST, sulfur transferase; TR, thiosulfate reductase; Trx, thioredoxin; 3-MST, 3-mercaptopyruvate sulfur transferase.

As summarized by Olson (Olson 2012) exogenous application of sulfide in experimental conditions is most commonly made by the sulfide salts NaHS and Na<sub>2</sub>S. Due to its pK<sub>a1</sub> of 7.0 and pK<sub>a2</sub> of 17.0 Wang et al. estimated that this will account for an intracellular equilibrium of about  $\frac{1}{2}$  undissociated H<sub>2</sub>S,  $\frac{1}{2}$  HS<sup>-</sup> and a negligible rest of S<sup>2-</sup> at physiological pH and 37°C. In extracellular fluid and plasma this equilibrium is shifted to 20% H<sub>2</sub>S and 80% HS<sup>-</sup> (Wang 2012). At physiological conditions Olson describes an absolute concentration of 191 μM of dissolved H<sub>2</sub>S in a 1 mM Na<sub>2</sub>S solution (Olson 2012). However, this equilibrium will be referred to as “sulfide” in the following.

GY 4137 is a water-soluble and cell-permeable sulfide releasing molecule that was characterized by Li et al. (Li, Whiteman et al. 2008) next to other sulfide releasing agents (Zhao, Biggs et al. 2014). Those agents and especially GY 4137 release sulfide slower and more sustained, making it eligible for chronic treatment and pharmaceutical approaches.

### 1.5.2 Biological activity and influence on endothelial cells

Over the last years sulfide could be shown to provide a great many of beneficial effects on blood pressure, angiogenesis and response to hypoxemia (Kajimura, Fukuda et al. 2010, Liu, Lu et al. 2012) amongst many other biological effects (Wang 2012). Levitt et al. could show that the vasculature contains the highest concentration of free sulfide in rodents (Levitt, Abdel-Rehim et al. 2011) and in line with that, a growing number of publications could attribute the above mentioned effects to direct or indirect influence of sulfide on endothelial cells.

Considering that those effects might be at least in part mediated by NO, influence on endothelial NO release and therefore vasodilatory effects were hypothesized to account for those protective effects. While eNOS phosphorylation was considered and described as one possible origin for these effects (Coletta, Papapetropoulos et al. 2012, Altaany, Yang et al. 2013) Ondrias et al. could also show direct NO release from nitrosothiols by sulfide (Ondrias, Stasko et al. 2008). On the other hand Nrf2 was proposed to be the converging node of sulfide derived signaling in endothelial cells (Calvert, Jha et al. 2009, Hourihan, Kenna et al. 2012, Liu, Wang et al. 2012). Calvert et al. described increased nuclear Nrf2 levels for at least 2 h in cardiac cells treated with sulfide. Cellular Hmox1 gene expression was also increased by sulfide in wild-type mice but not in Nrf2<sup>-/-</sup> mice indicating that the increase of HO-1 in cardiac cells was Nrf2 dependent (Calvert, Jha et al. 2009). Decreased endogenous H<sub>2</sub>S production in CSE deficient MEF cells was recently described to lower nuclear Nrf2 levels and to account for less GCLC, GCLS and GR mRNA, as well as decreased cellular GSH concentration. In consequence, oxidative stress was increased and cellular senescence was fastened. In contrast, exogenous application of H<sub>2</sub>S reversed those effects in knockout and wild type cells (Yang, Zhao et al. 2013). As the underlying molecular mechanism of sulfide mediated Nrf2 activation they suggested S-sulfhydration at cysteine 151 (Yang, Zhao et al. 2013). In line with that, Hourihan et al. reported Keap1 inactivation by sulfide but credited formation of a disulfide bond between Cys226 and Cys613 for those effects (Hourihan, Kenna et al. 2012). Due to those findings and since Nishida et al. showed electrophile sulfhydration properties of sulfide (Nishida, Sawa et al. 2012) sulfide can be assumed to strongly activate Keap1-Nrf2-signaling also in human endothelial cells. However, as described in the previous chapter, NO release and activation of Nrf2 signaling are not contradictory theses. Therefore, this study aimed to investigate on Nrf2 activation and Hmox1 gene expression induced by sulfide in HUVECs. Additionally it aimed to compare those effects to the ones of nitric oxide and a sulfide-NO-crosstalk (as described in chapter 1.6) in the same cellular model.

## 1.6 Crosstalk of sulfide and nitric oxide

### 1.6.1 Biological similarities and cross talk of sulfide and nitric oxide signaling

While sulfide was disclosed to have major effects on different cellular signaling systems (see chapter 1.5.2) it became noticeable that its properties were similar to those of nitric oxide like vasorelaxation (Hosoki, Matsuki et al. 1997, Ali, Ping et al. 2006), cardioprotection (Cohen, Yang et al. 2006, Jones and Bolli 2006, Sivarajah, McDonald et al. 2006) and anti-proliferation (van der Veen, Dietlin et al. 1999, Du, Hui et al. 2004). Therefore, the possibility of a “cross talk” between sulfide and NO was proposed (Moore, Bhatia et al. 2003, Wang 2003).

As the cause of these similarities different molecular mechanism were suggested. Some authors described that sulfide was able to release NO<sup>•</sup> from S-nitrosothiols (Ondrias, Stasko et al. 2008, Teng, Scott Isbell et al. 2008) while others described direct chemical interaction of the two small molecules to form a new nitrosothiol, which could not yet be identified (Whiteman, Li et al. 2006).

Recent work by Cortese-Krott et al. (Cortese-Krott, Fernandez et al. 2014) brought back to mind that the smallest nitrosothiol HSNO was already described by the German chemist Goehring in 1950 (Goehring and Messner 1950). However, this compound was never studied in great detail afterwards except in the 1980s when Müller and Nonella could report that HSNO and its isomers can only be characterized unstable and at extreme conditions (Müller, Nonella et al. 1984). But due to currently increasing interest, research on direct sulfide-NO-interaction was resumed and one recent publication reported HSNO formation at physiological conditions via 15N-NMR (Filipovic, Miljkovic et al. 2012). The authors claimed that HSNO was stable for less than 1 h and therefore speculated that it might play a major role in cellular sulfide S-nitrosothiol crosstalk.

Though, due to its reactivity and disputable stability Cortese-Krott et al. doubted the biological relevance of HSNO and suggested nitrosopersulfide (SSNO<sup>-</sup>) to be a more likely biological mediator (Cortese-Krott, Fernandez et al. 2015). Referring to older work by Seel et al. (Seel and Wagner 1988) they could provide evidence of its formation and stability at physiological conditions via UV–visible spectroscopy and mass spectrometry (Cortese-Krott, Fernandez et al. 2014), which could be successfully reproduced in this work. In subsequent studies they described formation of another S/N hybrid molecule dinitrososulfite ([ONN(O)–SO<sub>3</sub>]<sup>2-</sup> or “SULFI/NO”) at physiological pH and could show that homolysis of SSNO<sup>-</sup> strongly releases NO<sup>•</sup> and leads to formation of polysulfides (S<sub>x</sub><sup>2-</sup>), colloidal sulfur (S<sub>8</sub>) and sulfide (Cortese-Krott, Kuhnle et al. 2015).

Most recent publications showed that  $SSNO^-$  (and its byproducts) potentially influence vasodilation in a NO-analog fashion. In their 2015 publication Cortese-Krott et al. showed that  $SSNO^-$  accounts for increased NO bioavailability and lowers blood pressure in rats (Cortese-Krott, Kuhnle et al. 2015). Berenyiova et al. showed that the reaction products of sulfide and NO relax precontracted isolated rings of rat thoracic aorta but not if coincubated with the NO scavenger cPTIO or the inhibitor of soluble guanylyl cyclase ODQ (Berenyiova, Grman et al. 2015). Therefore,  $SSNO^-$  formation must be considered whenever addressing sulfide and NO interaction.

### **1.6.2 Keap1-Nrf2-signaling as a potential target of sulfide and nitric oxide crosstalk**

Since NO (Naughton, Hoque et al. 2002) and sulfide (Calvert, Jha et al. 2009) were shown to potentially activate Nrf2 activation, leading to increased Hmox1 gene expression, the Nrf2 pathway was suggested to act as a converging node of these effects (Liu, Wang et al. 2012). Taking in account that sulfide affects NO release from S-nitrosothiols (Ondrias, Stasko et al. 2008) and directly interacts with NO to form  $SSNO^-$ , SULFI/NO and polysulfides, which themselves were described to either directly affect Nrf2 activation (Koike, Ogasawara et al. 2013, Kimura 2014) or mediate NO release (Berenyiova, Grman et al. 2015, Cortese-Krott, Kuhnle et al. 2015), it is much likely that sulfide and nitric oxide strongly influence each other in Nrf2 activation. However, it has not been shown yet if sulfide application alters NO derived effects on Nrf2 signaling or vice versa, nor were effects of their reaction products on Nrf2 activation ever studied before. Therefore this study aimed to investigate on Nrf2 activation and Hmox1 gene expression upon meanwhile application of sulfide and nitric oxide congeners from different sources and compare these effects within the same cellular model. It also aimed to analyze the impact of  $SSNO^-$  on Nrf2 signaling in endothelial cells and elucidate which one of the possible reaction/decomposition products of  $SSNO^-$  accounts for its biological effects.

## 1.7 Aims of the dissertation

Oxidative stress induced Nrf2 signaling mediates the expression of several antioxidant and phase II detoxifying enzymes. Therefore, Nrf2 plays a crucial role in mammalian cell protection from oxidative and electrophilic insults implicating cellular dysfunction in aging, cardiovascular and neurodegenerative disease among other pathologies. Hence, activators of this pathway are considered as promising therapeutics.

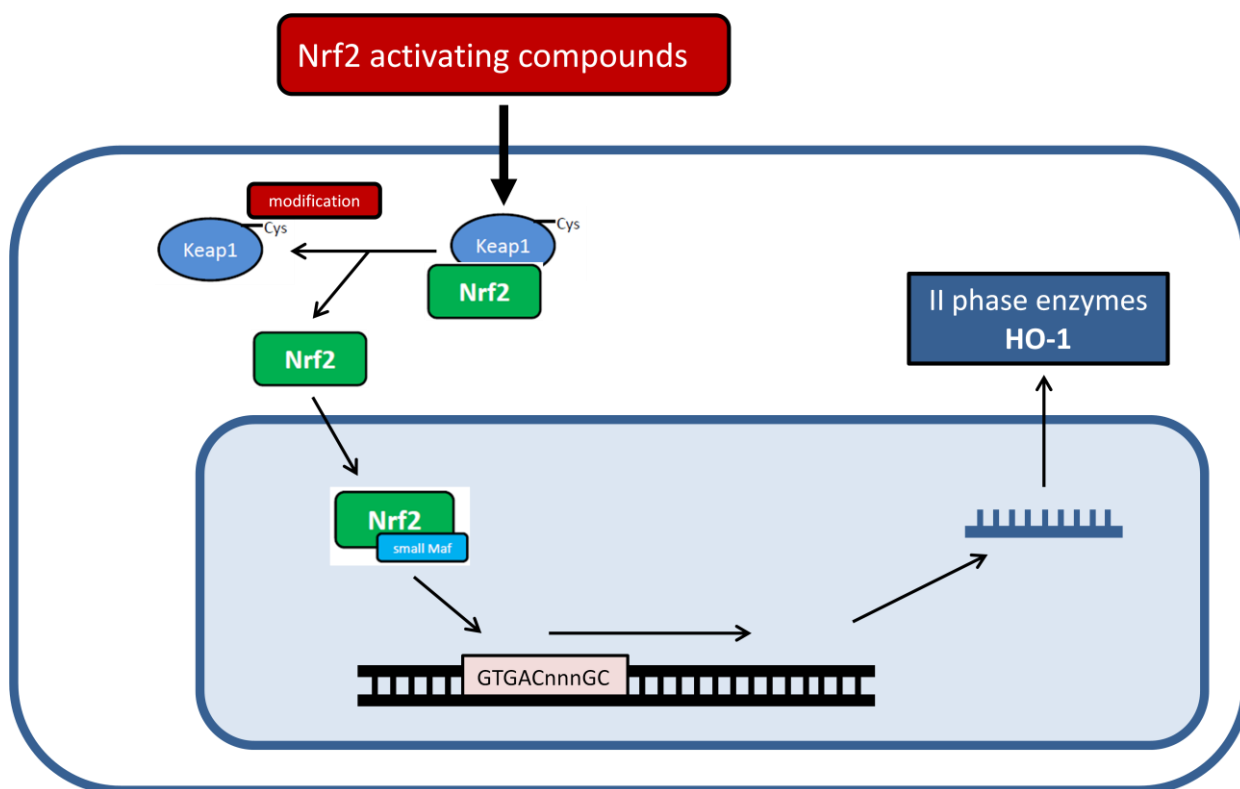


Fig. 5 Major hypothesis - Nrf2 as a converging node of redox sensing and signaling in HUVECs induced by (-)-epicatechin, NO, sulfide and NO-sulfide-crosstalk.

This study aimed to investigate on the role of Nrf2 signaling as a converging node in defense against redox induced damage in human primary endothelial cells. Since Keap1-Nrf2 interaction is a susceptible target of electrophiles and other redox active molecules, this work compared the effects of different electrophiles on Nrf2 signaling.

Therefore, the impact of (1) (-)-epicatechin, (2)  $\text{NO}^{\cdot}$ ,  $\text{NO}^{-}$  and  $\text{NO}^{+}$ , (3) sulfide, (4) the crosstalk of NO and sulfide and (5) their recently described reaction product  $\text{SSNO}^{-}$  on Nrf2 activation and translocation to the nucleus, ARE binding and transcription of phase II detoxifying enzymes was analyzed and compared within the same cellular system.

## 2 Material

### 2.1 Cells

HUVECs Lot 1110701 (used for major parts of this work)	PromoCell	Heidelberg, DE
HUVECs Lot 1122701 (used for subsequent experiments)	PromoCell	Heidelberg, DE

### 2.2 Media und Antibiotics

DMEM	PromoCell	Heidelberg, DE
Dulbeccos PBS	PAA/GE Healthcare	Buckinghamshire, UK
Endothelial Cell Basal Medium	PromoCell	Heidelberg, DE
Endothelial Cell Growth Medium Supplement Mix	PromoCell	Heidelberg, DE
FCS	PromoCell	Heidelberg, DE
human Fibronectin	Biochrom/Merck KGaA	Darmstadt, Germany
Penicillin/Streptomycin	PAA/GE Healthcare	Buckinghamshire, UK
Trypsin EDTA	PAA/GE Healthcare	Buckinghamshire, UK

### 2.3 Western blot - Solutions and Buffer

NuPage 3-8% Tris-Acetate Gel	Novex	California, USA
Tris Acetat running buffer	Novex	California, USA
Transfer buffer	Novex	California, USA
Image Quant	GE healthcare	Buckinghamshire, UK
Membrane	GE healthcare	Buckinghamshire, UK
Whatman paper	GE healthcare	Buckinghamshire, UK
MagicMark <sup>TM</sup> 220 / 120 / 100 / 80 / 60 / 50 / 40 / 30 / 20 kDa, unstained	life technologies	Carlsbad, USA
TBS (20x) pH 7,4	1 l	Trizma base NaCl H <sub>2</sub> O <sub>dd</sub>
T-TBS	50 ml 1 ml 950 ml	TBS (20x) Tween 20 H <sub>2</sub> O <sub>dd</sub>
Running buffer	50 ml 950 ml	Tris Acetat running buffer(20x) H <sub>2</sub> O <sub>dd</sub>
Inner chamber buffer	200 ml 1 ml	running buffer antioxidant
Transfer buffer	50 ml 25 ml 425 ml	Methanol running buffer (20x) H <sub>2</sub> O <sub>dd</sub>

## 2.4 Synthetic Primers

18S (Hs03003631_g1)	life technologies	Carlsbad, USA
NQO 1 (Hs01045993_g1)	life technologies	Carlsbad, USA
HMOX 1 (Hs01110250_m1)	life technologies	Carlsbad, USA
GCLC (00892604_m1)	life technologies	Carlsbad, USA
Rplp0 (Mm01974474_gH)	life technologies	Carlsbad, USA
HMOX 1 (Mm00516005_m1)	life technologies	Carlsbad, USA

## 2.5 Reverse transcription real time PCR

Abi Prism 7900 HAT Sequence detection system	invitrogen	Carlsbad, USA
MicroAmp® Optical Adhesive Film	invitrogen	Carlsbad, USA
MicroAmp® Optical Film Compression Pad	invitrogen	Carlsbad, USA
Proteinase K	QIAGEN	Hilden, DE
QuantiTect Reverse Transcription Kit	QIAGEN	Hilden, DE
Rneasy Mini Kit	QIAGEN	Hilden, DE
TagMan gene expression master mix	invitrogen	Carlsbad, USA
TissueRuptor	QIAGEN	Hilden, DE

## 2.6 siRNA

RNAi Human/Mouse Starter Kit	QIAGEN	Hilden, DE
------------------------------	--------	------------

## 2.7 Antibodies

Anti-Nrf2 (ab62352) Dilution 1:200	abcam	Cambridge, UK
Anti-Nrf1 (ab90524) Dilution 1:1000	abcam	Cambridge, UK
Anti-Lamin A (ab8980) Dilution 1:500	abcam	Cambridge, UK
Anti-alpha Tubulin (ab4074) Dilution 1:1000	abcam	Cambridge, UK
Goat-anti-rabbit IgG 1:5000	BD Bioscience	New Jersey, USA
Goat-anti-mouse IgG 1:5000	BD Bioscience	New Jersey, USA

## 2.8 Chemicals

(-)-Epicatechin	Sigma-Aldrich	St. Louis, USA
10x PVP-Solution	Mecatronic	Netherlands
acetic acid	Carl Roth GmbH	Karlsruhe, Germany
Aqua bidest	Merck Millipore	Darmstadt, DE
beta-Mercaptoethanol	Sigma-Aldrich	St. Louis, USA
Bovine serum albumin	Sigma-Aldrich	St. Louis, USA
Calciumchlorid (CaCl <sub>2</sub> )	Sigma-Aldrich	St. Louis, USA
Dimethyl Sulfoxide (DMSO)	Sigma-Aldrich	St. Louis, USA
Ethanol	Merck KGaA	Darmstadt, Germany
GYG 4137	Cayman	Michigan, USA
Hybond P membrane	GE healthcare	Buckinghamshire, UK

Hydrochloride acid (HCl) 25%	Merck KGaA	Darmstadt, Germany
Hydrogen peroxide 30% (H <sub>2</sub> O <sub>2</sub> );	Carl Roth GmbH	Karlsruhe, Germany
L-Arginin	Carl Roth GmbH	Karlsruhe, Germany
L-NAME	Enzo Life Sciences GmbH	Lörrach, Germany
Magic Mark XP Western Protein Standard	Invitrogen	Carlsbad, USA
Magnesium sulfate (MgSO <sub>4</sub> )	Sigma-Aldrich	St. Louis, USA
Methanol	Merck KGaA	Darmstadt, Germany
Methanol, $\beta$ -Nicotinamide adenine dinucleotide 2'-phosphate reduced tetrasodium salt hydrate	Sigma-Aldrich	St. Louis, USA
Milkpowder blotting grade	Sigma-Aldrich	St. Louis, USA
Na <sub>2</sub> S	Sigma-Aldrich	St. Louis, USA
Neutralred	Sigma-Aldrich	St. Louis, USA
NuPAGE LDS Sample Buffer	Invitrogen	Carlsbad, USA
NuPAGE Reducing Agent	Invitrogen	Carlsbad, USA
NuPAGE Transferbuffer	Invitrogen	Carlsbad, USA
NuPAGE Tris acetate running buffer	Invitrogen	Carlsbad, USA
Potassium chloride (KCl)	Sigma-Aldrich	St. Louis, USA
Potassium hydrogen phosphate (KH <sub>2</sub> PO <sub>4</sub> )	Sigma-Aldrich	St. Louis, USA
Protease-Phosphatase-Inhibitor Cocktail	Bio-Rad	Munich, Germany
SNAP	Cayman	Michigan, USA
Sodium chloride (NaCl)	Sigma-Aldrich	St. Louis, USA
Sodium dihydrogen phosphate (NaH <sub>2</sub> PO <sub>4</sub> )	Sigma-Aldrich	St. Louis, USA
Sodium hydrogencarbonat (NaHCO <sub>3</sub> )	Sigma-Aldrich	St. Louis, USA
Sodium hydroxide (NaOH)	Merck KGaA	Darmstadt, Germany
SpermineNONOate		
tBHQ	Sigma-Aldrich	St. Louis, USA
Trizma(R) Base (Tris)	Sigma-Aldrich	St. Louis, USA
Trypsin EDTA	PAA/GE Healthcare	Buckinghamshire, UK

## 2.9 Consumables

12 well plates	Greiner Bio One	Frickenhausen, DE
12 well plates	Corning	NY, USA
6 well plates	Greiner Bio One	Frickenhausen, DE
6 well plates	Corning	NY, USA
cell scraper 18mm blade	Becton, Dickinson and Company (BD)	Franklin Lakes, USA
petridishes 100mm	Greiner Bio One	Frickenhausen, DE
96-well-micro-plates black, flat bottom, fluotrac200	Greiner Bio One	Frickenhausen, DE
96-well-micro-plates clear, flat bottom	Greiner Bio One	Frickenhausen, DE
96-well-micro-plates white , flat bottom	Greiner Bio One	Frickenhausen, DE
Falcons 15ml	Greiner Bio One	Frickenhausen, DE
Falcons 50ml	Greiner Bio One	Frickenhausen, DE
NuPage 3-8% Tris-Acetate Gel	Novex	California, USA
NuPage 7% Tris-Acetate Gel	Novex	California, USA
Gloves, nitril powder free	Ansell	Tamworth, UK

Nitrocellulose Membrane Ammersham Hybond-P	GE Healthcare	Buckinghamshire, UK
Parafilm "M"	Bemis	Wisconsin, USA
Pipette filter tip	Star Lab	Hamburg,DE
Pipette tip TipOne 10µl	Star Lab	Hamburg,DE
Pipette tip TipOne 100µl	Star Lab	Hamburg,DE
Pipette tip TipOne 1000µl	Star Lab	Hamburg,DE
Safe-Lock tubes 2,0ml	Eppendorf	Hamburg,DE
Single-use Syringes 10ml	B. Braun AG	Melsungen, DE
Single-use Syringes 20ml	B. Braun AG	Melsungen, DE
Single-use Syringes 5ml	B. Braun AG	Melsungen, DE
Stripetten Costar® 10ml	Corning	NY, USA
Stripetten Costar® 25ml	Corning	NY, USA
Stripetten Costar® 5ml	Corning	NY, USA

## 2.10 Equipement

Autoclave Systec DX-90	Systec	Linden, DE
Centrifuge 5417 R	Eppendorf	Hamburg, DE
Centrifuge Mikro 200R	Hettich	Kirchlengern,DE
Centrifuge Rotina 380R	Hettich	Kirchlengern,DE
Centrifuge Rotina 35R	Hettich	Kirchlengern,DE
Incubator Heraeus BBD 6220	Thermo Scientific	Massachusetts, USA
Incubator Heracell 240	Thermo Scientific	Massachusetts, USA
Laminar air flow	Clean Air	Illinois, USA
Fluostar Omega	BMG Labtech GmbH	Ortenberg, DE
Millipore Filter	Merck Millipore	Darmstadt, DE
Micro pippets	Eppendorf	Hamburg, DE
Vortex	scientific industries	New York, USA
Heating cabinet TH15	Edmund Bühler	Tübingen, DE
Heating oven	Memmert GmbH & CO. KG	Schwabach, DE
ImageQuant LAS400	GE Healthcare	Buckinghamshire, UK
pH Meter Lab870	Schott Instruments	Mainz, DE
Pipet boy comfort	Integra Bioscience	Biebertal, DE
Testtube heater	Stuart Scientific	Staffordshire, UK
Master Cycler	Eppendorf	Hamburg, DE
ABI Prism 7900HT Sequence Detection System	applied biosystems	Carlsbad, USA

## 2.11 Kits

Glutathione (GSH) Colorimetric Detection Kit	arbor assays	Michigan, USA
Nuclear extraction kit	active motif	Carlsbad,USA
TransAM® Nrf2	active motif	Carlsbad,USA
DC Protein Assay	BioRad	Munich, Germany

## 2.12 Software

MS excel	microsoft	Albuquerque, USA
MS word	microsoft	Albuquerque, USA
MS powerpoint	microsoft	Albuquerque, USA
Zotero	Roy Rosenzweig Center for History and New Media	Virginia, USA
EndNote	Thomson Reuters (Scientific) LLC	New York City, USA
GraphPad Prism	GraphPad Software, Inc.	La Jolla, CA, USA
Image J	Open source	
ImageQuant TL	GE Healthcare	Buckinghamshire, UK
OMEGA	BMG Labtech	Ortenberg, Germany

## **3 Methods**

### **3.1 Cell culture**

#### **3.1.1 Cells**

For all cell culture experiments HUVECs c-pooled by PromoCell (Cat No. C-12203) with Lot numbers 1110701 (used for major parts of this work) and 1122701 (used for subsequent experiments) were used. All processes and treatments of the cells were performed under a laminar airflow bench.

#### **3.1.2 Incubation and population of the cells**

HUVECs were incubated at 37°C, 21% O<sub>2</sub>, 5% CO<sub>2</sub> and 78% H<sub>2</sub>O saturation in a heraeus incubator. The surface of the 100 mm diameter Petri dishes used was coated with a fibronectin layer from a 10 µg/ml fibronectin/PBS stock solution.

After thawing and seeding the cells (see chapter 3.1.3) they were incubated in 8 ml of PromoCell growth medium. After 24 h hours the medium was changed with 8 ml fresh medium. At day 4 the cells reached a confluence of 90 %. They were split 1:3 and incubated in a Petri dish with 8 ml of fresh growth medium. After another 3 days their confluence reached 90%. Cells were then trypsinized again, their number was determined (see chapter 3.1.6) and they were seeded on Petri dishes or 6 or 12-well plates depending on the up-coming experiment (see chapters 0, 0, 0 and 0 for cell numbers and plate sizes). Therefore all experiments could be performed with second passage cells.

#### **3.1.3 Freezing and thawing of the cells**

HUVECs were cryopreserved in liquid nitrogen prior to use. To thaw the cells according to the manufacturer's protocol, they were put in a 37°C water bath for 90 seconds. After that the cryovial was disinfected with 70% ethanol. Under a laminar airflow bench cells were transferred into a falcon tube together with 5 ml of complete growth medium. The falcon tube was then centrifuged for 10 min at 300g and 20°C. After removing the supernatant the cell pellet was re-suspended in 1 ml of complete growth medium and added to a Petri dish with another 9 ml of complete growth medium.

The cells were not frozen again at any point.

### **3.1.4 Trypsinization of the cells (splitting protocol)**

To split the cells they were washed one time with 37 °C warm Dulbecco's PBS and then incubated with 3 ml of trypsin at 37°C for maximum 5 min. As stop solution 8 ml of DMEM (containing 2% FCS and 1% penicillin/streptomycin) was used. The suspensions of all Petri dishes were pooled in two falcon tubes and then centrifuged for 10 min at 300g and 20°C. After removing the supernatant the cell pellets were re-suspended in 1,5 ml (per Petri) of complete growth medium and their number was determined with a *Neubauer Zählkammer* as described below (3.1.6 "cell count").

### **3.1.5 Cell growth control**

To control their growing process the cells were observed daily by light microscopy. Their confluence was determined on the days of trypsinization and before every experiment.

### **3.1.6 Cell count**

At passages 0 and 1 cell numbers were estimated and described by their confluence. Prior to experiments a *Neubauer Zählkammer* was used to determine the number of cells in suspended state. 10 µl of cell suspension were put on both counting areas of the counting chamber. All cells inside of the 16 squares and all of those cells who touched the left or upper border of the squares were counted together in all 4 areas and the mean of the four areas times 10<sup>4</sup> makes the cell number per µl.

## **3.2 Substance solutions and mix preparation**

Stock solutions were prepared as described in the following. Further dilutions were made in Dulbeccos PBS if not otherwise mentioned.

### **(-)-Epicatechin**

(-)-Epicatechin stock solution was prepared in DMSO in a concentration of 50 mM.

### **Tert-Butylhydrochinon (tBHQ)**

tBHQ stock solution was prepared in DMSO in a concentration of 50 mM.

### **GY Y 4137**

GY Y 4137 stock solution was prepared in DMSO in a concentration of 40 mM.

### **L-N<sup>G</sup>-Nitroarginine methyl ester (L-NAME)**

L-Name stock solution was prepared in 0,01 M NaOH in a concentration of 50 mM.

### **S-nitroso-N-acetylpenicillamine (SNAP)**

SNAP stock solution was prepared in DMSO in a concentration of 200 mM.

### **DiethylaminoNO-NOate (DEA/NO)**

DEA/NO stock solution was prepared in 0.01 M NaOH in a concentration of 50 mM.

### **Spermine NONOate (SPER/NO)**

SPER/NO stock solution was prepared in 0.01 M NaOH in a concentration of 50 mM.

### **Angeli's salt (AS)**

AS stock solution was prepared in 0.01 M NaOH in a concentration of 50 mM.

### **Sodium sulfide (Na<sub>2</sub>S)**

Na<sub>2</sub>S stock solution was prepared in double distilled water (H<sub>2</sub>O<sub>dd</sub>) at concentration of 500 mM.

### **SSNO<sup>-</sup> Mix**

To obtain a 1 mM stock solution of SSNO<sup>-</sup>, 200 μl of 50 mM Na<sub>2</sub>S was added to a 1 mM SNAP solution, dissolved in 800 μl of a 1 mM TRIS buffer. The eppendorf tube was incubated 10 min protected from direct light. SSNO<sup>-</sup> formation was detected as described in chapter 3.3.

### **SSNO<sup>-</sup> Zinc mix**

To eliminate the remaining Na<sub>2</sub>S of the stock solution, 20 μl of a 500 mM ZnCl<sub>2</sub> solution were added to the prepared SSNO<sup>-</sup> mix. It was then incubated for 2 min at room temperature to allow formation of complexes. Afterwards it was centrifuged for 1 min at 10000 g and 20°C. The supernatant was used for experiments or further procedure (see chapter 3.3.1).

### **Gassed SSNO<sup>-</sup>**

The second protocol to eliminate the remaining Na<sub>2</sub>S of the stock solution was to gas the ready prepared SSNO<sup>-</sup> sample with nitrogen for 10 min (see chapter 3.3.2 for further details).

### **TPEN**

TPEN was prepared as a stock solution of 50 mM, which was then added to the supernatant of the SSNO<sup>-</sup> Zinc mix in a final concentration of 1 mM, in order to eliminate the remaining zinc.

### **Carboxy-PTIO potassium salt (cPTIO)**

cPTIO was prepared as a stock solution of 50 mM in DMSO.

### **L-cysteine**

L-cysteine stock solution of 3 mM was prepared by solving L-cysteine HCl in PBS.

### **Dithiothreitol (DTT)**

DTT was prepared as a stock solution of 100 mM in H<sub>2</sub>O<sub>dd</sub>.

### **Dinitrososulfite (SULFI/NO)**

SULFI/NO stock solution was prepared in 0,01 M NaOH in a concentration of 50 mM.

### 3.3 Synthesis and UV-visible spectrometry of SSNO<sup>-</sup>

Following the protocol of Cortese-Krott et al. (Cortese-Krott, Fernandez et al. 2014) 1 mM SNAP was incubated with 10 mM of Na<sub>2</sub>S to obtain a 1 mM SSNO<sup>-</sup> mix. As buffer 100 mM hydrogen phosphate or 100 mM TRIS (data not shown) was used. This lead to formation of a stable yellow compound, which showed an increase of absorbance with peaks at 260 nm and 412 nm as well as increased absorbance at 250 to 310 nm in UV-visible spectroscopy (Fig.6). As proposed by Cortese-Krott et al. this reaction product will be referred to as SSNO<sup>-</sup> in the following.

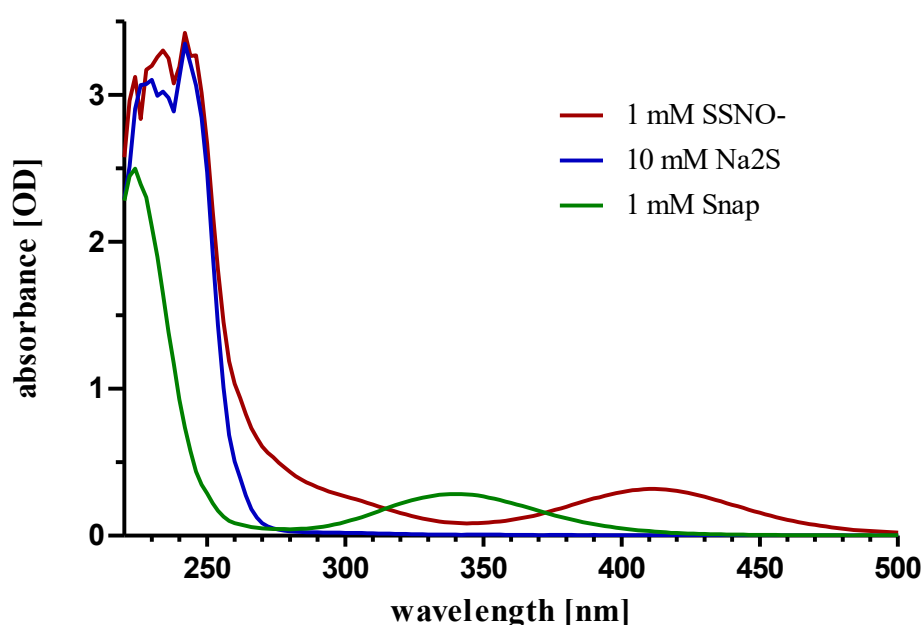


Fig. 6 Absorbance spectrum of 1 mM SNAP in hydrogen phosphate buffer (green), 10 mM Na<sub>2</sub>S in hydrogen phosphate buffer (blue) and the mix of 1 mM SNAP and 10 mM Na<sub>2</sub>S in hydrogen phosphate buffer (SSNO<sup>-</sup>) after 10 min of incubation at room temperature (red). The spectrum of SSNO<sup>-</sup> shows a huge peak of 3,2 OD at 220 – 250 nm similar to Na<sub>2</sub>S, an increase of absorbance at 250 to 310 nm and a second peak of 0,3 OD at 412 nm, while the peak at 340 nm disappeared.

#### 3.3.1 Incubation of SSNO<sup>-</sup> with Zn

To proof that the peaks of < 250 nm in SSNO<sup>-</sup> and Na<sub>2</sub>S solution were caused by excessive Na<sub>2</sub>S and to remove it two different methods were used.

On the one hand ZnCl<sub>2</sub> was used in equimolar concentration to Na<sub>2</sub>S to form complexes, which could then be eliminated by spinning them down. Therefore 10 mM ZnCl<sub>2</sub> were put to the SSNO<sup>-</sup> solution and as a control also to the Na<sub>2</sub>S solution and those mixes were incubated for 2 min. After centrifuging those mixes at 12000 g and 20°C for 1 min white pellets could be observed and absorbance was measured again and compared to the “crude” SSNO<sup>-</sup> mix.

As shown in Fig. 7 incubation of both, the  $\text{Na}_2\text{S}$  and the  $\text{SSNO}^-$  solution with  $\text{ZnCl}_2$  lead to absence of the  $<250$  nm peak in the samples. While the  $\text{Na}_2\text{S}$  zinc mix hereafter was not showing any absorbance at all indicating complete removal of the  $\text{Na}_2\text{S}$  part, the  $\text{SSNO}^-$  zinc mix still showed increased absorbance from 250 to 310 nm and the 412 nm absorbance peak.

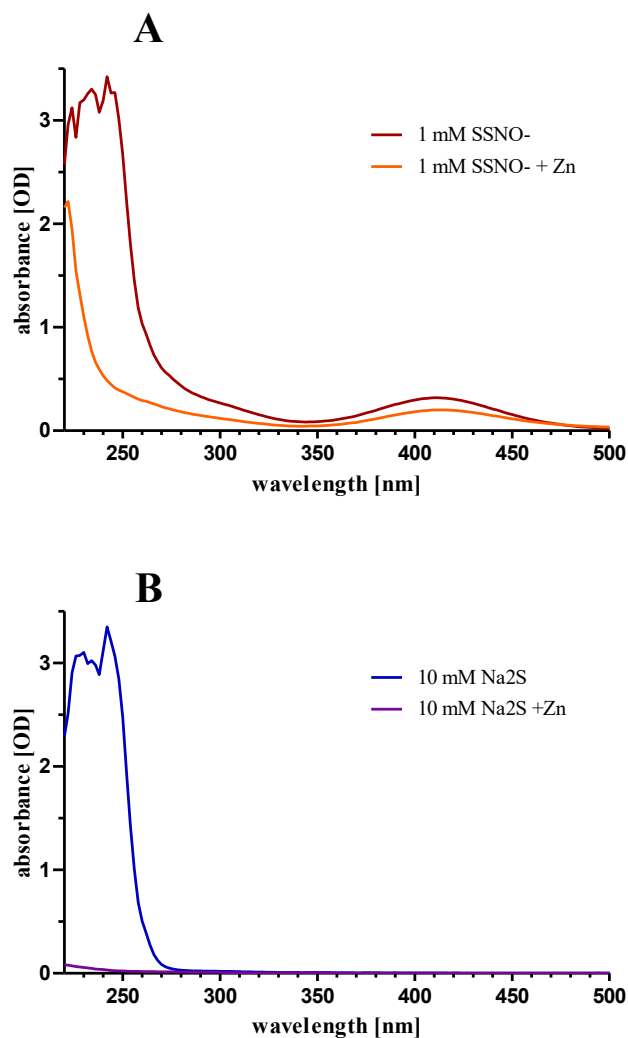


Fig. 7 (A) Absorbance spectrum of 1 mM  $\text{SSNO}^-$  after 10 min of incubation at room temperature (red) and 1 mM  $\text{SSNO}^-$  additionally incubated with 10 mM of  $\text{ZnCl}_2$  and centrifuged (orange). (B) 10 mM  $\text{Na}_2\text{S}$  (blue) and 10 mM  $\text{Na}_2\text{S}$  additionally incubated with 10 mM of  $\text{ZnCl}_2$  and centrifuged (purple). All mixes prepared in 100 mM Hydrogen phosphate buffer. (A) The spectrum of  $\text{SSNO}^-$  incubated with  $\text{ZnCl}_2$  shows a depletion of the huge peak at 250 nm and below which is to be seen in regular  $\text{SSNO}^-$  solution.  $\text{SSNO}^-$  plus  $\text{ZnCl}_2$  still shows the increase of absorbance at about 280 nm and the second peak at 412 nm. (B) 10 mM  $\text{Na}_2\text{S}$  incubated with 10 mM of  $\text{ZnCl}_2$  and centrifuged was showing less than 0,2 OD absorbance in the UV-spectrum.

### 3.3.2 Gassing of SSNO<sup>-</sup>

The second method to remove excessive Na<sub>2</sub>S was gassing the SSNO<sup>-</sup> mix with N<sub>2</sub> for 10 min as described by Cortese-Krott et al. (Cortese-Krott, Fernandez et al. 2014). Sulfide (HS<sup>-</sup>) is in equilibrium with its undissociated form H<sub>2</sub>S and its twice dissociated form S<sup>2-</sup> (see equation 1)



By gassing the sample with nitrogen the gaseous H<sub>2</sub>S is displaced from the solution. In consequence, sulfide will be removed completely from the solution after 10 min. Fig. 8 shows elimination of the < 250 nm peak from the SSNO<sup>-</sup> spectrum.

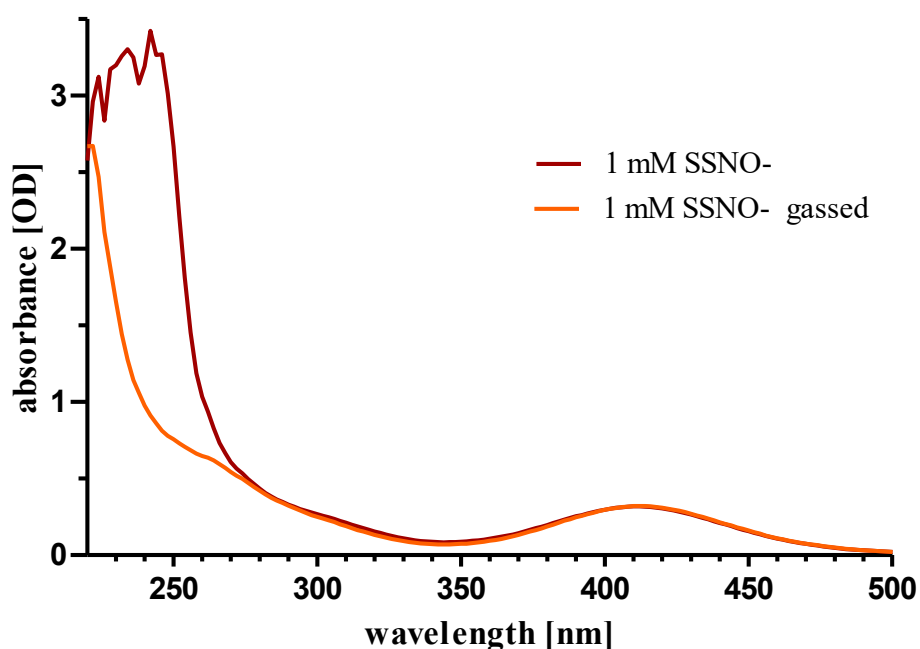


Fig. 8 Absorbance spectrum of 1 mM SSNO<sup>-</sup> after 10 min of incubation at room temperature (red) and 1 mM SSNO<sup>-</sup> additionally gassed with nitrogen for 10 min (orange). The spectrum of SSNO<sup>-</sup> gassed with nitrogen shows a depletion of the huge peak at 250 nm and below which is to be seen in regular SSNO<sup>-</sup> solution, while still showing the increase of absorbance at 250 to 310 nm and the second peak at 412 nm.

For cell culture experiments this method had the advantage that it is free of Zn compounds, which themselves have a significant effect on Nrf2 signaling (Cortese, Suschek et al. 2008) also found in our experiments (see chapter 4.7.3 and chapter 4.2.2).

### 3.3.3 Identification of the increased absorbance at 250 to 310 nm

As described by Cortese-Krott et al. (Cortese-Krott, Fernandez et al. 2014, Cortese-Krott, Fernandez et al. 2015) reaction of sulfide and nitric oxide also leads to formation of dinitrososulfite (SULFI/NO) and polysulfides ( $\text{HS}_x^-$ ). Therefore, we reproduced the identification of the increased absorbance at 250 to 310 nm via UV-visible spectroscopy. To disclose  $\text{HS}_x^-$  in the mix 1 mM of the polysulfide scavenger DTT was added to the  $\text{SSNO}^-$  sample. Fig. 10 shows how the gassed  $\text{SSNO}^-$  samples lowered their absorbencies at 250 to 310 nm in presence of DTT. SULFI/NO was detected to generate an absorbance peak of 259 nm, which also matches the absorbance increase of  $\text{SSNO}^-$  as to be seen in Fig. 9.

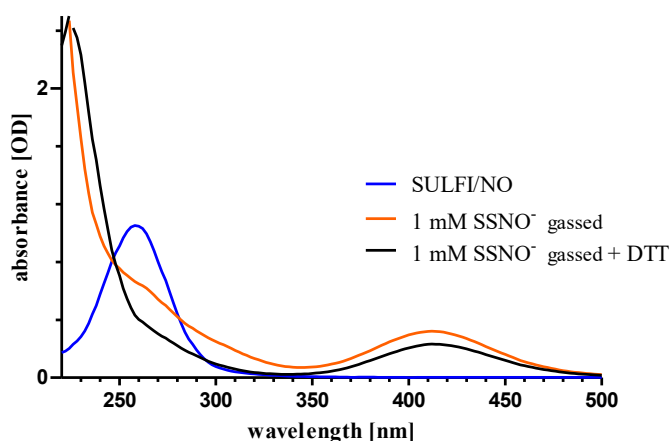


Fig. 9 Absorbance spectrometry of SULFI/NO. The compound shows an absorbance peak of 259 nm.

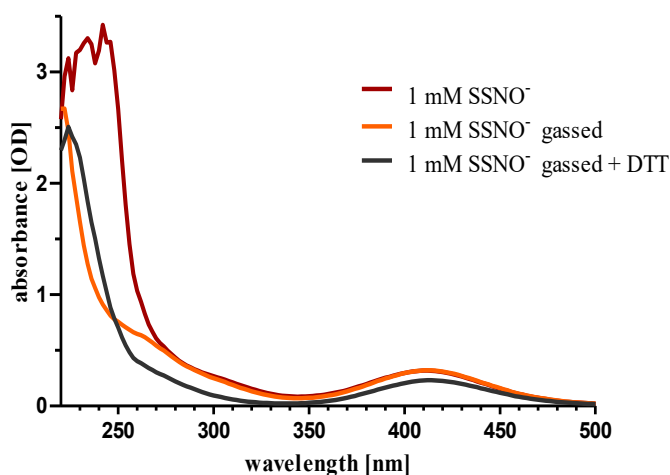


Fig. 10 Absorbance spectrum of 1 mM  $\text{SSNO}^-$  after 10 min of incubation at room temperature (red) and 1 mM  $\text{SSNO}^-$  additionally gassed with nitrogen for 10 min (orange). Addition of DTT (black) shows decrease of the absorbance from 250 nm to 310 nm which is to be seen in regular  $\text{SSNO}^-$  solution, while still showing the increase of absorbance at 412 nm.

### **3.4 Protein level analysis**

#### **Treatment of HUVECs for 12 h**

For plasma protein analysis HUVECs ( $2 \times 10^5$ ) were incubated 24 h in 6 well plates with 2 ml growth medium. Hereafter, medium was changed to 1.5 ml of FBS inactivated medium and cells were incubated 12 h with the respective treatments and thereafter lysed and processed as described below.

#### **Lysis**

To lyse HUVECs for further protein assays a 200 mM RIPA buffer was used. Every well was washed one time with Dulbeccos PBS and then flooded with 350  $\mu$ l of RIPA. With help of cell scrapers cells were collected in eppendorf tubes and frozen at  $-20^\circ\text{C}$

#### **Protein assay**

NanoQuant assay was used to determine protein concentrations in whole cell lysates. This absorbance based assay calculates protein levels by comparing the quotient  $\text{OD}_{590}/\text{OD}_{450}$  of sample absorbencies to the ones of a prepared standard row in aqueous solutions. Hereafter corrections for any dilution of the sample were made and total protein levels were calculated using OMEGA software or MS excel.

#### **Western blot**

Western Blotting was performed to compare levels of cellular proteins. Samples were prepared and operated as described below and analysis was made using “Image J” software.

#### **SDS-Page**

Samples were diluted in double distilled water ( $\text{H}_2\text{O}_{\text{dd}}$ ) to a final concentration of 15  $\mu\text{g}$  protein in 16.25  $\mu$ l of  $\text{H}_2\text{O}_{\text{dd}}$ . 6.25  $\mu$ l of NuPage 4x LDS sample buffer and 2.5  $\mu$ l of NuPage 10x sample reducing agent were added and those mixes were incubated for 10 min at  $70^\circ\text{C}$  without shaking or vortexing.

Meanwhile the 1x running buffer (Tris acetate) was made (see chapter 2.3). 200 ml of the buffer were separated and 500  $\mu$ l of sample oxidant was added to obtain the buffer for the inner chamber. The gel was put into the chamber and after the buffers were added to the chambers, the comb was removed and the slots were washed one time with inner chamber buffer.

The molecular weight marker was put into the first slot and the incubated samples were applied to the other ones. To start the SDS-Page the running module was connected to a continuous current of 200 mV for 40 to 50 minutes.

## **Blotting**

After the SDS-Page the gel was unpacked and put on a wet Whatman paper. The blotting membrane was activated in methanol and put on top of the gel. The side of molecular weight marker (the left side of the gel) was marked with a small cut on the edge of the membrane. Another Whatman paper was put onto the membrane and the whole package was pressed one time with an empty falcon tube to avoid air bubbles between gel and membrane. Surrounded by 4 sponges the pack was then put into the transfer module. The inner chamber was filled with transfer buffer (10% methanol, 5% 20x transfer buffer diluted in H<sub>2</sub>O<sub>dd</sub>) while the outer chamber was filled with H<sub>2</sub>O<sub>dd</sub>. The whole blot module was connected to a continuous current of 30 mV for one hour.

## **Ponceau S staining and blocking**

To detect if the transfer was successful and to lock the proteins the membrane was incubated in a Ponceau S solution for 5 min and washed with H<sub>2</sub>O<sub>dd</sub> several times. To block unspecific bands the membrane was put into a 5% skim milk/T-TBS solutions at room temperature for 2 hours.

## **Primary antibody incubation**

After 15 min washing in TBS solution the membrane was incubated at 4°C over night with different concentrations of primary antibodies (see chapter 2.7) diluted in 5% BSA/T-TBS solution also containing 0.03% of NaN<sub>3</sub> for conservation.

## **Secondary antibody incubation**

Membranes were washed 5 times 5 min in T-TBS. Hereafter they were incubated with a 1:5000 diluted secondary antibody solution (see chapter 2.7) in 5% BSA/T-TBS buffer.

## **Chemiluminescence and detection**

Membranes were washed another 5 times 5 min in T-TBS and then put on a wet Whatman paper. To detect the protein lanes they were dyed with SuperSignal™ West Pico Chemiluminescent Substrate and the chemiluminescence signal was measured with ImageQuant LAS 4000.

## **Stripping of membranes**

To strip the membranes they were put in stripping buffer (see chapter 2.3) at 70°C for 30 min and then washed 5 times in TBS.

## **Densitometry analysis**

Densitometry analysis was made using ImageJ software (see chapter 3.9).

### **3.5 Transcription factor analysis**

#### **Treatment of the cells for 1 h**

To analyze nuclear translocation of transcription factors HUVECs ( $10^6$ ) were incubated 24 h in 100 mm diameter Petri dishes with 8 ml growth medium. Hereafter, medium was changed to 8 ml of FBS inactivated medium and cells were incubated with the respective treatments for 1 h and thereafter lysed and processed as described in chapter 0.

#### **Nuclear extraction**

Nuclear extraction was performed using the Active Motif Nuclear Extraction Kit. After 1 hour treatment in 100 mm diameter Petri dishes, cells were put on iced underground and washed one time in ice cold PBS. With the help of cell scrapers they were collected in ice cold PBS and centrifuged at 500 g and 4°C for 10 min. Supernatant was removed and cells were re-suspended in 500 µl pre-cooled hypotonic buffer for 15 min to allow lysis of the cytoplasmatic fraction. After those 15 min the detergent was added to the vials and the samples were vortexed at highest setting for 10 s then centrifuged at 10000 g 4°C for 30s. The cytoplasmatic fraction in the supernatant was put to another vial and immediately stored in liquid nitrogen. The remaining nuclear pellet was re-suspended in 50 µl complete lysis buffer vortexed once at highest setting and then incubated for 30 min on ice on a rocking platform at 150 rpm. After another vortexing at highest setting for 30 s the samples were again centrifuged at 10000 g 4°C for 10 min. The supernatant including the nuclear fraction could now be separated and 5 µl aliquots for protein detection and 40 µl aliquots for sample processing were frozen in liquid nitrogen. All samples were then stored at -80°C.

#### **Protein determination**

Protein concentrations of nuclear extracts were determined using the BioRad protein detection assay. In this colorimetric assay Coomassie brilliant blue G-250 dye changes its color in response to various concentrations of protein because the dye binds to primarily basic and aromatic amino acid residues (Bradford 1976). Protein levels are calculated by comparing the absorbance at 595 nm of the sample to the ones of a prepared standard row using OMEGA software or MS excel.

### **Nrf2 transcription factor binding assay**

To detect activated Nrf2 levels in nuclear extracts TransAM<sup>®</sup> Nrf2 transcription factor assay by active motif was used. The DNA-binding ELISA for activated Nrf2 transcription factor was performed according to the company's protocol using 10 µg of protein per well. As blank 10 µl complete lysis buffer was used, as positive control the 1.25 µl COS-7 solution diluted in 10 µl of complete lysis buffer was used. All measurements were performed in duplicates.

Controls and samples (10 µg of protein in 40 µl full lysis buffer) were pipetted to an intransparent microplate, to whose base ARE oligonucleotides (5'-GTCACAGTGACTCAG-CAGAATCTG-3') are bound. Incubation of 1h on a rocking platform (100 rpm) at room temperature allows activated nuclear Nrf2 to bind to those oligonucleotides. After discarding the sample solutions and 3 times washing the wells with 200 µl of a PBS buffer they were again incubated for 1 h with 100 µl of a 1:1000 diluted Nrf2 antibody at room temperature. After discarding the Nrf2 antibody solution and 3 times washing the wells with a PBS buffer they were again incubated for 1 h with 100 µl of a 1:1000 horseradish peroxidase (HRP) linked anti-Nrf2-antibody at room temperature. After discarding the HRP antibody solution and 4 times washing the wells with a PBS buffer they were incubated with a developing solution containing a substrate of the HRP. After 5-15 min peroxidase activity was stopped and absorbance could be read at 450 nm with a reference wavelength of 655 nm. Nrf2 binding activity was calculated as % of control or  $\Delta\%$  of control.

### **Western blot of nuclear extracts**

Importantly, western blots of nuclear extracts were made to prove that nuclear Nrf1 levels were not increased by treatment with the respective substances. Western blots were performed as described in chapter 0 using 15 µg of protein per slot.

### **3.6 mRNA level analysis**

#### **Treatment of the cells for 6 h**

To analyze effects of the substances on gene expression of phase II detoxifying enzymes HUVECs ( $2 \times 10^5$ ) were incubated 24 h in 6 well plates with 2 ml growth medium. Hereafter, medium was changed to 1.5 ml of FBS inactivated medium and cells were incubated for 6 h with the respective treatment and thereafter lysed and processed as described below.

#### **RNA extraction of HUVECs**

RNA extraction of cells was performed with RNeasy mini kit. Cells were lysed in 350  $\mu$ l RLT buffer containing 1% beta-mercaptoethanol per well and collected in eppendorf tubes with help of cell scrapers. A volume of 350  $\mu$ l 70% ethanol was added to the tubes and mixed by pipetting up and down several times. Samples were then put into the RNeasy spin columns and centrifuged at 8000 g for 15 s. Collection tubes were depleted and spin columns were filled with 700  $\mu$ l of RW1 washing buffer, then centrifuged again at 8000 g for 15 s. Collection tubes were depleted again and 500  $\mu$ l of RPE washing buffer was added to the spin columns, before they were centrifuged at 8000 g for 15 s. This last step was repeated once with centrifugation at 8000 g for 2 min this time. Afterwards the columns were carefully removed from collection tubes. If completely dry they were put into 1,5 ml eppendorf tubes and 40  $\mu$ l  $H_2O_{dd}$  was added to the columns to dilute the RNA. In a final centrifugation step at 8000 g for 1 min the diluted RNA was collected in the eppendorf tubes.

#### **RNA quantification**

To determine the yield of RNA extraction performed sample absorbance was measured using the NanoDrop ND 2000 spectrophotometer.

#### **RNA quality control**

To estimate the quality of the RNA extracted, Agilent bioanalysis was performed by the BMFZ (Universitätsstraße 1, Geb. 23.12.E2 40225 Düsseldorf).

#### **Reverse transcription**

Reverse transcription was performed with the QuantiTect Reverse Transcription Kit. Samples were diluted to a quantity of 1  $\mu$ g RNA in 12  $\mu$ l  $H_2O_{dd}$ . To eliminate gDNA 2  $\mu$ l of gDNA wipe out buffer were added to the samples and they were incubated at 42°C for 2 min and hereafter put on ice again. A RT-masternix was prepared containing 1 part Quantiscript Reverse Transcriptase, 4 parts 5x Quantiscript RT Buffer and 1 part RT Primer Mix. To every sample 6  $\mu$ l of RT-masternix were added. Additionally there was one pre-RT control, which underwent the gDNA wipeout, but no reverse transcription to test the efficiency of the wipeout performed.

All samples were then incubated at 42°C for 15 min to allow reverse transcription. Thereafter temperature was risen to 95°C for 3 min in order to inactivate Quantiscript reverse transcriptase. Obtained cDNA samples were then put on ice again and processed further or stored at -20°C.

### **Realtime polymerase chain reaction (rt-PCR)**

To detect mRNA quantity real time PCR with the TaqMan gene expression assay was used. Samples were diluted to a concentration of 2 ng/μl and 5 μl (10 ng) cDNA per well was applied to a 96-well microplate. Every sample measurement was performed in triplets. Reaction mixture (20 μl per well) contained 1.25 μl 20x concentrated target assay mix (see chapter 2.4 for primer overview), 12.5 μl 2x concentrated TaqMan gene expression mastermix and 6.25 μl H<sub>2</sub>O<sub>dd</sub>. The reaction mixture was added to the samples leading to a total volume of 25 μl per well.

Real time PCR was then performed in the ABI Prism 7900HT sequence detection system. Primer activity was detected by FAM (6-FAM-phosphoramidit) reporter and the number of cycles needed to reach the threshold was measured to obtain Ct-values for each sample.

### **Statistical analysis of gene expression**

The values measured by reverse transcription real time PCR were analyzed with  $\Delta\Delta\text{CT}$  method. Ct-values of the target genes were first compared to Ct-values of housekeeping gene 18 S (“ $\Delta\text{CT}$ ”). Then these differences were compared to those of the untreated control (“ $\Delta\Delta\text{CT}$ ”). To calculate x-fold gene expression from those results the base 2 was raised to the power of the differences in Ct-values [ $2^{\Delta\text{Ct}(\text{untreated control}) - \Delta\text{Ct}(\text{sample})}$ ].

## **3.7 Glutathione assay**

### **Treatment of the cells for 24 h**

To detect differences in cellular glutathione levels cells ( $2 \times 10^5$ ) were incubated 24 h in 6 well plates with 2 ml growth medium. Hereafter, medium was changed to 1.5 ml of FBS inactivated medium and cells were treated with the respective substances for another 24 h and lysed after this.

### **Lysis**

Cells were lysed in 200 μl of 100 mM HCl buffer per well. With the help of cell scrapers whole cell lysates were collected in 1.5 ml eppendorf tubes.

### **Protein assay**

Samples were diluted 1:20 and buffered in a 100 mM TRIS buffer. To detect cellular protein levels NanoQuant protein assay was chosen. This absorbance based assay calculates protein levels by comparing the quotient  $OD_{590}/OD_{450}$  of sample absorbencies to the ones of a prepared standard row in aqueous solutions. Hereafter corrections for any dilution of the sample were made and total protein levels were calculated using OMEGA software or MS excel.

### **Glutathione assay**

Total GSH and GSSG levels were determined by an Arbor Assays<sup>®</sup> GSH detection kit according to the company's protocol. The fluorescence based assay uses a proprietary nonfluorescent molecule (ThioStar<sup>®</sup>), which will form fluorescent product after binding to the free thiol group of GSH. After mixing the sample or standard with ThioStar and incubating at room temperature for 15 minutes the fluorescent product is read at 510 nm in a fluorescent plate reader with excitation at 390 nm and intensity is compared to a GSH standard to calculate free GSH. Hereafter, GSSG is measured by a glutathione reductase reaction mixture, which converts the remaining GSSG to GSH. After incubating the converted samples with ThioStar for another 15 min at room temperature the fluorescent signal is again read at 510 nm with excitation at 390 nm and intensity is again compared to a GSH standard. After measuring free GSH and GSSG concentration suitable correction for any dilution of the sample were made using the OMEGA software and total GSH levels could be calculated from GSH and GSSG.

## **3.8 RNA Interference**

### **siRNA Transfection**

RNA interference was planned to knock down Nrf1, Nrf2 and Keap1 and to elucidate which one of these proteins contributes most to electrophile induced Nrf2 signaling. As transfection kit the Qiagen RNAi Human/Mouse Starter Kit and HiPerFect transfection reagent were used. For effective knock-down HUVECs ( $10^5$ ) were incubated 24 h in 12-well plates with 1 ml growth medium. Hereafter, medium was changed to 1 ml of FBS inactivated medium and cells were treated with 5 or 10 nM siRNA oligonucleotides and 8, 12 or 18  $\mu$ l of HiPerFect transfection reagent for 24 h. After this time cells were lysed (compare to chapter 0) and gene expression of target genes was monitored as described in chapters 0 and 0.

### **Negative control and mock control**

Knock down of target genes was compared to its expression in untreated cells and to cells which were treated with transfection reagent only (mock control).

### **Cell death control**

Qiagen Cell death control was used to check transfection effectiveness. Cells were incubated with AllStars Hs Cell Death Control siRNA from the kit and HiPerFect transfection reagent in the same concentrations as used in MAPK1 transfection. Incubation was prolonged to 72 h as proposed by the manufacturer's protocol. Dying cells then showed effective knock down.

### **MAPK1 transfection control**

In order to quantify transfection effectiveness the expression of the housekeeping gene MAPK1 was monitored by rt-PCR after knocking down its corresponding mRNA. siRNA was transfected in concentrations of 5 and 10  $\mu$ M using 6, 12 and 18  $\mu$ l of HiPerFect transfection reagent per ml of medium.

### **Monitoring of gen knockdown**

Knockdown was monitored by rt-PCR as suggested by the manufacturer. As primer hs\_MAPK1 was chosen with FAM signaling. As mastermix TaqMan gene expression mastermix was used (compare to chapter 3.6). Knockdown was analyzed according to  $\Delta\Delta$ CT method comparing knocked down MAPK1/18S CT-ratio to untreated control MAPK1/18S CT-ratio (compare to chapter 3.6).

## **3.9 Statistic analysis**

### **Statistical analysis of ARE binding assays**

The values measured by UV-visible absorbance spectrometry were first blank corrected to the absorbance of the lysis buffer used. Blank corrected values were then presented as raw data or compared to control as % of control (value/CTRL) or  $\Delta\%$  of control  $[(\text{sample}-\text{CTRL})/\text{CTRL}]$ .

### **Statistical analysis of gene expression**

The values measured by reverse transcription real time PCR were analyzed with  $\Delta\Delta$ CT method. Ct-values of the target genes were first compared to Ct-values of housekeeping gene 18 S (“ $\Delta$ CT”). Then these differences were compared to those of the untreated control (“ $\Delta\Delta$ CT”). To calculate x-fold gene expression from those results the base 2 was raised to the power of the differences in Ct-values  $[2^{\Delta\text{Ct}(\text{untreated control}) - \Delta\text{Ct}(\text{sample})}]$ .

### **Presentation of results**

All values are reported as means with standard errors of the means (SEM). Comparisons were performed via two tailed T-test or one-way ANOVA with Tukey post hoc tests for multiple comparisons. Differences were considered significant when  $p < 0.05$ .

**Microsoft Excel**

Assay analysis, descriptive statistics and RNA analysis was performed with Microsoft Excel. For RNA analysis  $\Delta\Delta\text{CT}$  method was applied. Hereby

**GraphPad Prism 5**

Major parts of descriptive and all inference statistics were performed with GraphPad Prism 5.

**3.10 Citation manager**

For citation managing Zotero (Version 4.0.27.1) and EndNote (Version X7.3.1) were used.

## 4 Results

### 4.1 Plan of the study and experimental setup

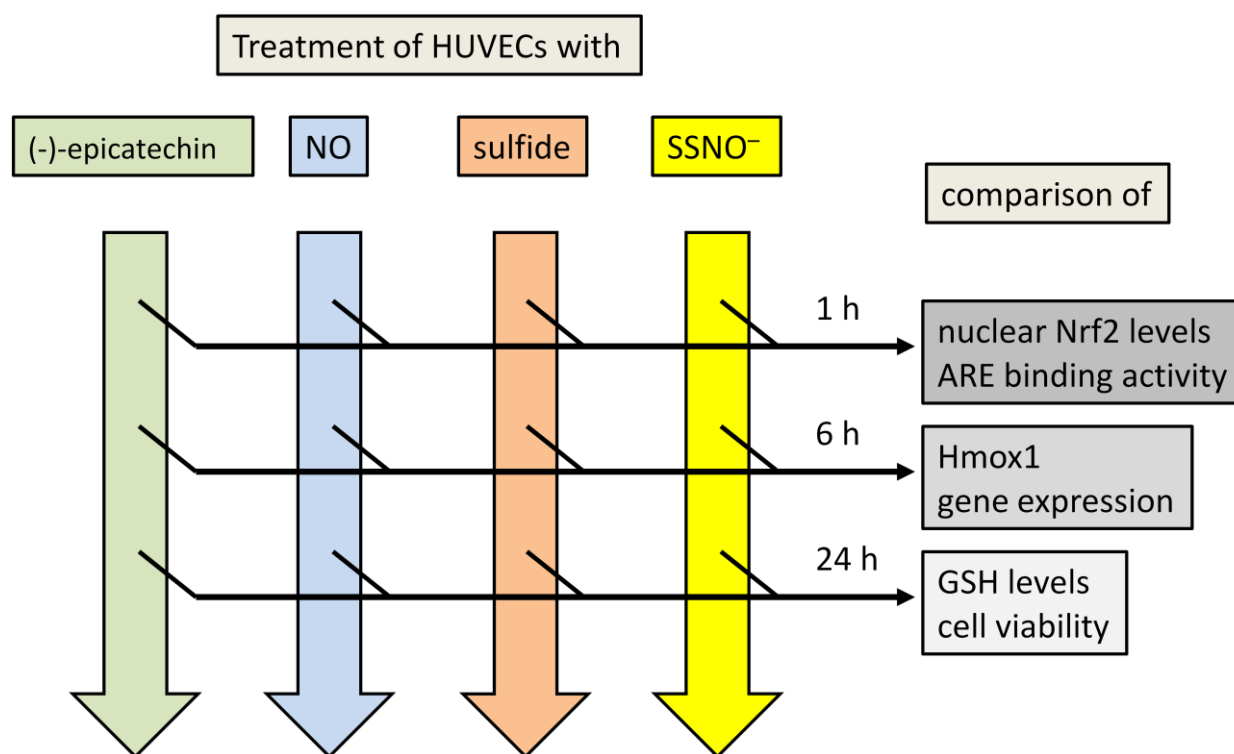


Fig. 11 experimental setup for the comparison of (-)-epicatechin, NO, sulfide and SSNO<sup>-</sup>

This work aimed to compare the effects of (-)-epicatechin, NO, sulfide, the crosstalk of NO and sulfide and nitrosopersulfide (SSNO<sup>-</sup>) on Nrf2 activation and translocation to the nucleus, ARE binding, transcription of phase II detoxifying enzymes and cell viability in human endothelial cells. To do so, HUVECs were treated with those substances and analyzed at different levels of the Nrf2 pathway as shown by Fig. 11. Nuclear extracts were obtained after 1 h of incubation and were analyzed by western blots and staining for Nrf1, Nrf2 and Lamin A (as loading control). Nuclear extracts were also analyzed with an ELISA-based transcription factor binding assay for Nrf2. Hmox-1 gene expression was determined after 6 h of treatment using reverse transcription real time PCR. Cellular GSH levels were measured after 24h of incubation by fluorescence detection assay and cell viability was determined by neutral red staining.

## 4.2 Pre-experiments and evaluation

### 4.2.1 Treatment of HUVECs passage $\geq 3$

Nrf2 signaling is dependent on cell type, cellular redox status and culture conditions. To prove eligible conditions the cells responsiveness to tert-butylhydroquinone (t-BHQ) was compared, because this substance was already characterized as a strong inhibitor of Keap1 (Wakabayashi, Dinkova-Kostova et al. 2004). Hereby, pooled HUVECs from the same lot number and same passage were found to be necessary for best comparability. Otherwise responsiveness to t-BHQ was inconsistent (data not shown). We also found that the cells should not be split to passages higher than two, they should not be maintained in culture for more than one day once full confluence was reached, and they should all be cultured under the same standardized growing conditions (see chapter 3.1).

Under these conditions we found an increased ARE-binding activity upon treatment with 10  $\mu\text{M}$  t-BHQ as shown in Fig. 12 (no statistical significance due to  $n=2$ ). Additionally we found that treatment with the hydrophobic solvent DMSO that was used for stock preparation (see chapter 3.2) did not have any significant effects on Nrf2 activation.

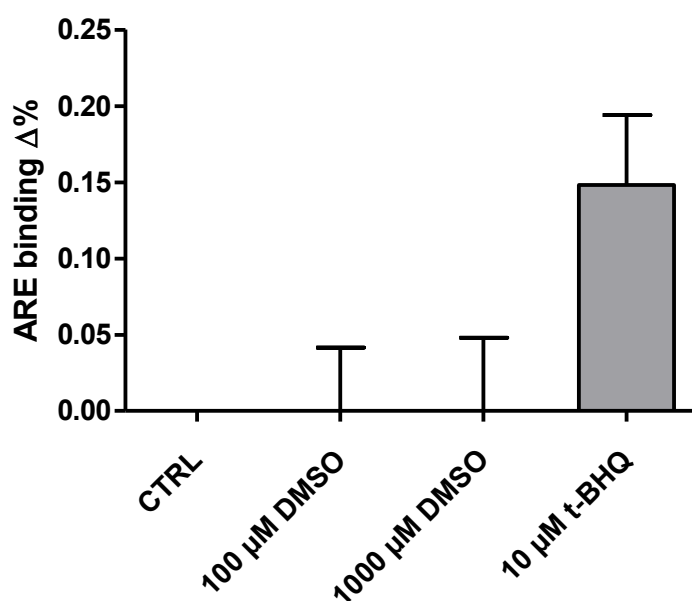


Fig. 12 treatment of HUVECs passage  $\leq 2$  with positive control t-BHQ and solvent DMSO. In HUVECs passage  $\leq 2$  t-BHQ showed increased ARE binding while DMSO had no influence. Scatter is shown as SEM. Statistical significance was tested by one-way ANOVA ( $n=2$ ;  $P=0.13$  [95% CI for t-BHQ -0.3792 to 0.08267])

## 4.2.2 Toxicity tests of treatments

To make sure that the compounds and its concentrations used have no toxic effects on HUVECs neutral red staining experiments were performed. Cells were treated for 24 h with all compounds used in this work (for treatments and concentrations see figures below) and stained with neutral red afterwards. Fig. 13,

Fig. 14 and Fig. 15 show the absorbance of 450 nm correspondent to HUVECs viability after treatment.

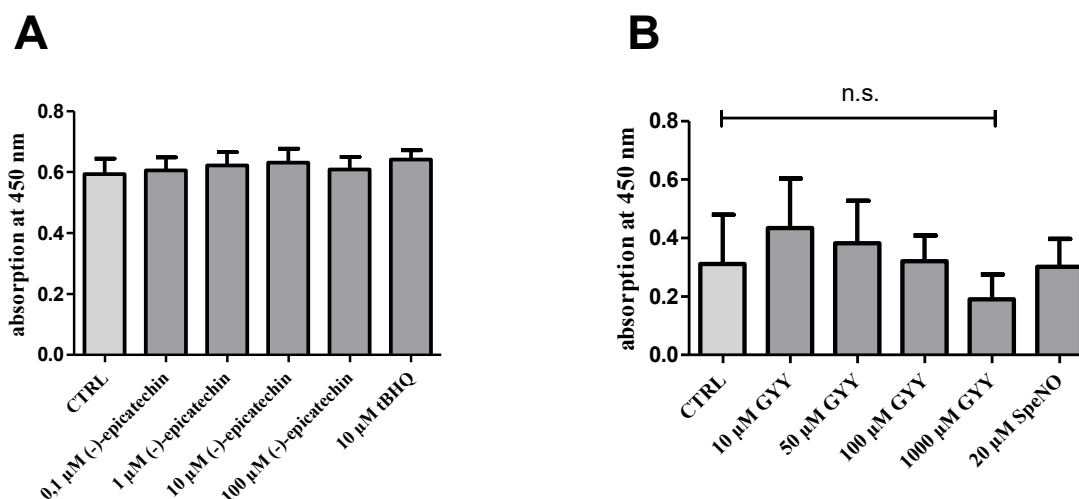


Fig. 13 Cellular viability after 24 h incubation with (A) (-)-epicatechin, tBHQ and (B) GYY 4137 and SPE/NO. Viability was determined by neutral red staining. The graph shows absorbance at 450 nm equivalent to cell viability. Scatter is shown as SEM. Statistical significance was tested by one-way ANOVA (n=5; n.s.= no statistical difference in ANOVA and additional single t-test)

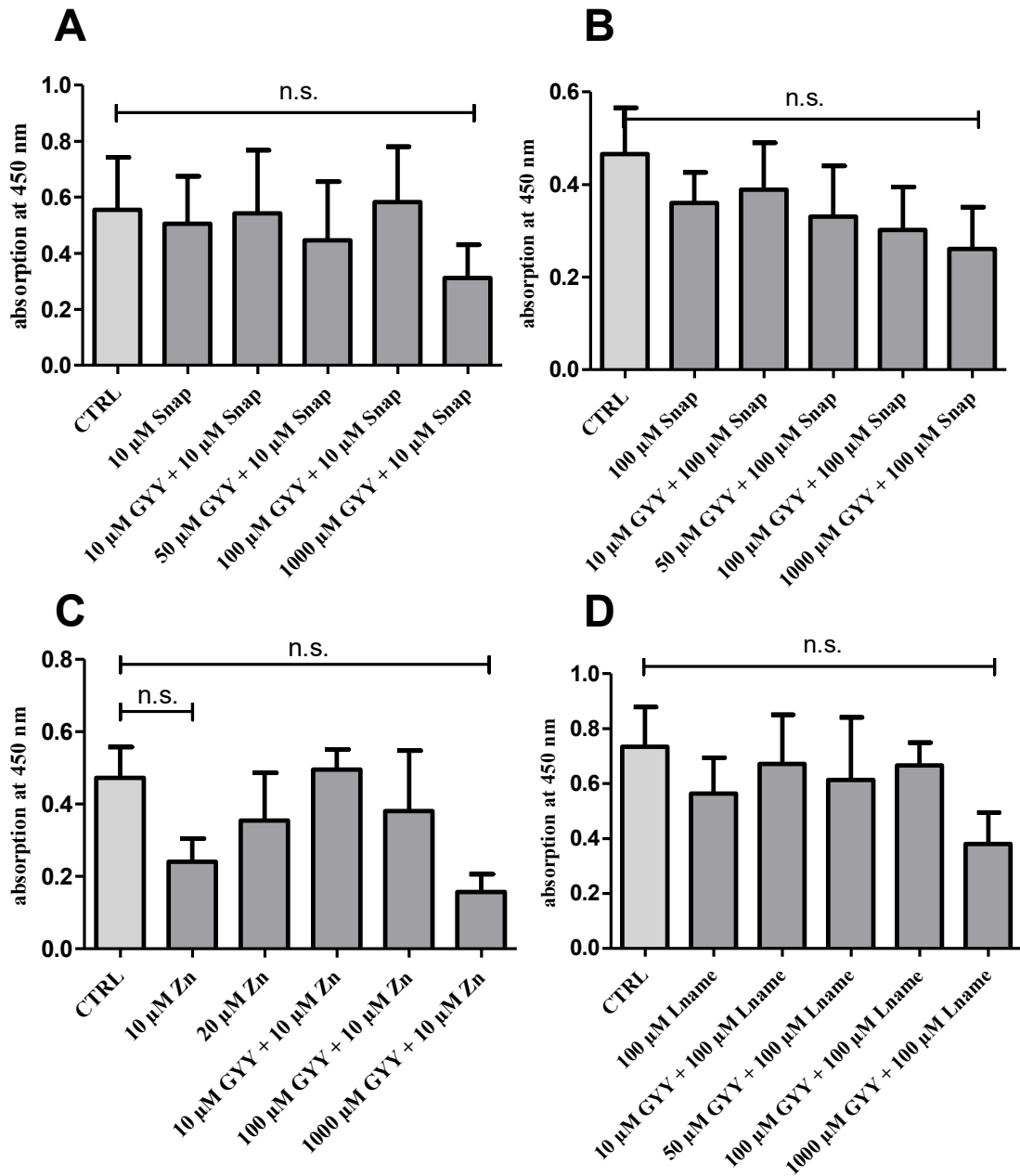


Fig. 14 Cellular viability after 24 h incubation with GYY 4137 in combination with SNAP, L-NAME and  $Zn^{2+}$ . Viability was determined by neutral red staining. The graph shows absorbance at 450 nm equivalent to cell viability. Scatter is shown as SEM. Statistical significance was tested by one-way ANOVA (n=5; n.s.= no statistical difference in ANOVA and additional single t-test)

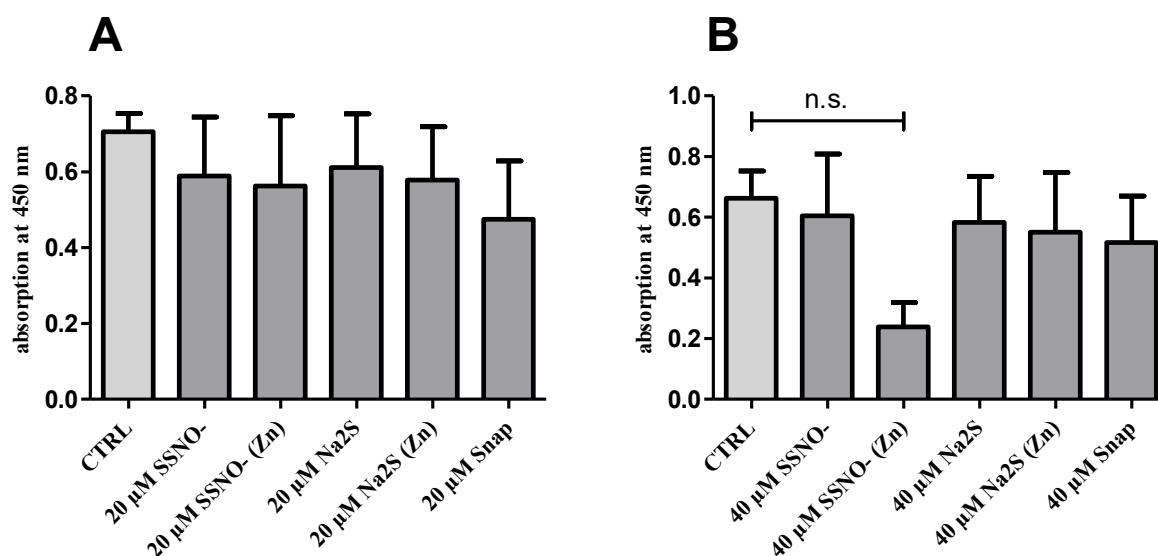


Fig. 15 Cellular viability after 24 h incubation with different concentrations of SSNO<sup>-</sup> and Na<sub>2</sub>S, with and without zinc. Viability was determined by neutral red staining. The Graph shows absorbance at 450 nm equivalent to cell viability. Scatter is shown as SEM. Statistical significance was tested by one-way ANOVA (n=5; n.s.= no statistical difference in ANOVA and additional single t-test)

Neutral red staining experiments showed that the selected treatments of HUVECs overall did not affect their viability at the concentrations used. However, GYY 4137 showed decreased cell viability at concentrations of 1000 μM. These findings were consistent with observations via microscopy (not displayed) in which changes in cell morphology were seen after administration of 1000 μM GYY 4137 to the medium. Additionally, decreased cell viability could be observed within incubations with zinc which don't seem to follow a specific rule since 10 μM zinc seem to harm the cells while 20 μM do not. On the other side, mix 2 on concentration of 40 μl per ml medium shows decreased viability, while lower concentrations or segregation of zinc (mix 4) had no effect on cell survival. However, differences were not significant at any treatment. Taken together, most treatments did not affect cell viability. While treatments with 1000 μM GYY 4137 and some treatments with zinc seemed to decrease cell viability there were no statistical differences observed.

### 4.2.3 Transfection with siRNA

RNA interference experiments were planned to knock down Nrf1, Nrf2 and Keap1 and to elucidate to what extent they contribute to electrophile induced Nrf2 signaling. As transfection kit the Qiagen RNAi Human/Mouse Starter Kit and HiPerFect transfection reagent were used. For effective knock-down HUVECs ( $10^5$ ) were incubated 24 h in 12-well plates with 1 ml growth medium. Hereafter, medium was changed to 1 ml of FBS inactivated medium and cells were treated with 5 or 10 nM siRNA oligonucleotides and 8, 12 or 18  $\mu$ l of HiPerFect transfection reagent for 24 h. After this time cells were lysed and gene expression of target genes was monitored as described in detail in chapters 3.6 and 3.8.

To establish the protocol siRNA for MAPK1 (NM\_002745) was chosen. Fig. 16 shows expression of MAPK1 after transfection as calculated by  $\Delta\Delta$ CT method. Sufficient knock down would significantly reduce MAPK1 gene expression.

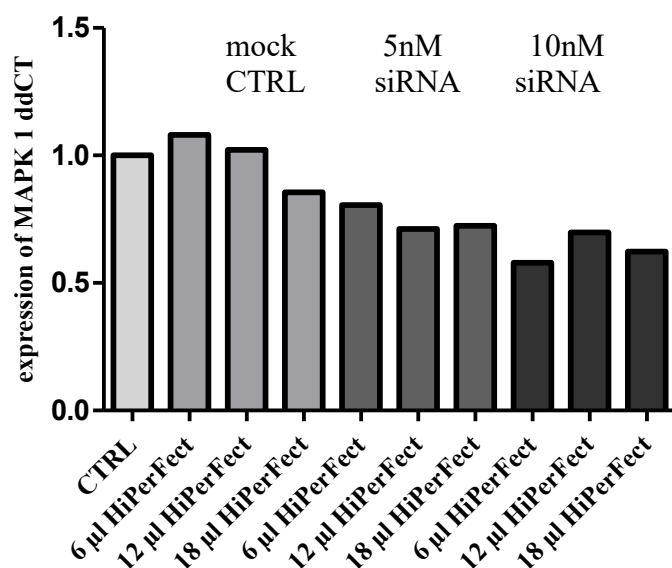


Fig. 16 Real time RT-PCR of RNA extracts from HUVECs transfected with MAPK1 siRNA and HiPerFect reagent in different concentrations. Cellular mRNA concentration was detected by real time RT-PCR (10 ng cDNA per well) using primers for 18S as housekeeping gene. CT values were analyzed according to  $\Delta\Delta$ CT method. Values represent the mean  $\pm$ SEM (n=1)

MAPK1 expression was at most reduced to 0.58 fold expression (when treated with 10 nm siRNA) as compared to untreated control. Although this was only n=1, siRNA-transfection was considered incomplete since cell viability controls of the transfection with AllStars Hs Cell Death Control siRNA were also insufficient (not displayed). Therefore, this protocol for human primary endothelial cells RNA interference was not studied further and still has to be optimized.

### 4.3 Effects of (-)-epicatechin on Nrf2 in HUVECs

#### 4.3.1 Nrf2 transcription factor binding assay

To analyze the effects of (-)-epicatechin on Nrf2 signaling HUVECs were treated with concentrations from 0.1 to 100  $\mu\text{M}$  (-)-epicatechin for one hour. After preparation of nuclear extracts activated Nrf2 levels were determined using the transcription factor binding assay measuring ARE binding. Fig. 17 shows the absorbance at 450 nm and absorbance relative to control corresponding to activated nuclear Nrf2 levels.

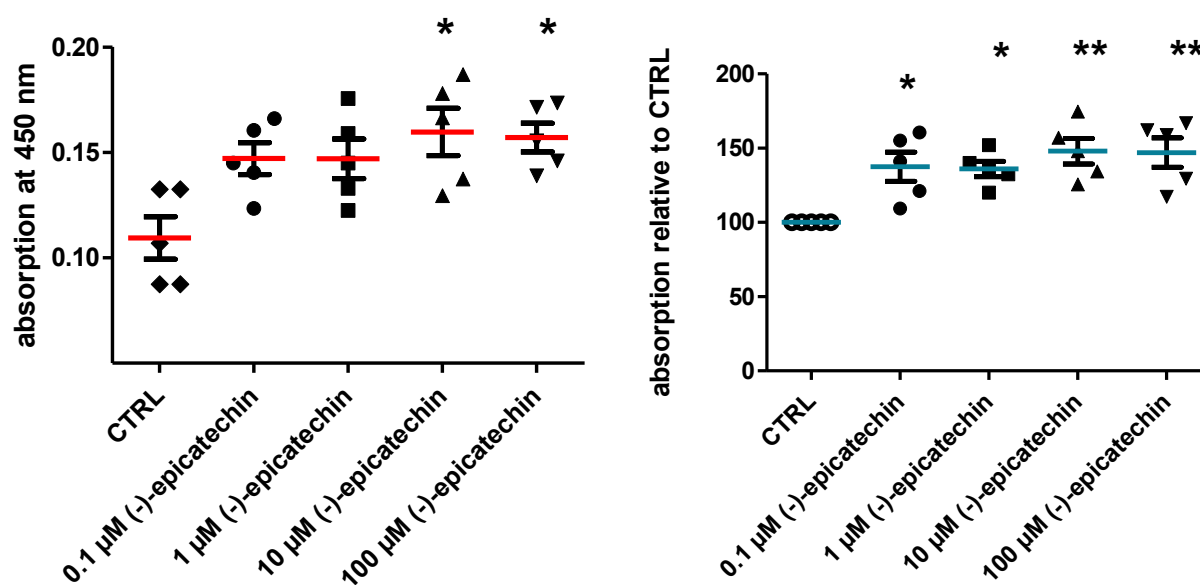


Fig. 17 Transcription factor binding assay of nuclear extracts from HUVECs treated with (-)-epicatechin. The graphic shows the absorbance at 450 nm and relative to control corresponding to activated nuclear Nrf2 levels. Treatment for 1 h with (-)-epicatechin shows increased absorbance dependent on concentration. Significant differences were observed at all concentrations. Each measurement was performed in duplicates. Scatter is shown as SEM. Statistical significance was tested by one-way ANOVA followed by Tukey post hoc multiple comparison test (n=5; \*P<0.05, \*\*P<0.01)

Treatment for 1 h with (-)-epicatechin shows increased absorbance dependent on concentration. ARE binding was augmented up to  $1.48 \pm 0.09$  fold intensity (at concentration of 10  $\mu\text{M}$ ) indicating up to 50% increase in nuclear Nrf2 levels. Significant differences to control treatment were observed at concentrations of 10 and 100  $\mu\text{M}$  when comparing raw data.

### 4.3.2 Western blots of nuclear extracts

To analyze translocation of Nrf2 western blots of the same nuclear extracts were made. Nrf2 levels were detected at a molecular weight of 100 kDa (see discussion) (Lau, Tian et al. 2013). Fig. 18 shows one representative western blot. Fig. 19 shows the densitometry analysis of western blots.

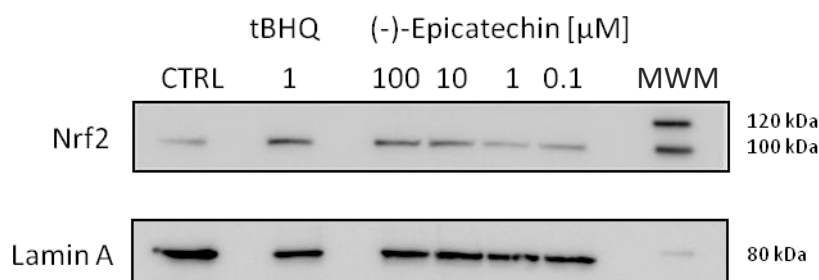


Fig. 18 Western blot of nuclear extracts from HUVECs treated with (-)-epicatechin. The graphic shows bands at 100 kDa after staining with Anti-Nrf2 (ab63252) corresponding to activated nuclear Nrf2. Treatment for 1 h with (-)-epicatechin shows increased incidence of Nrf2 in the nucleus in a concentration dependent manner. The second staining was made with Lamin A (ab8980) as a loading control. Slots were loaded with 15  $\mu\text{g}$  protein.

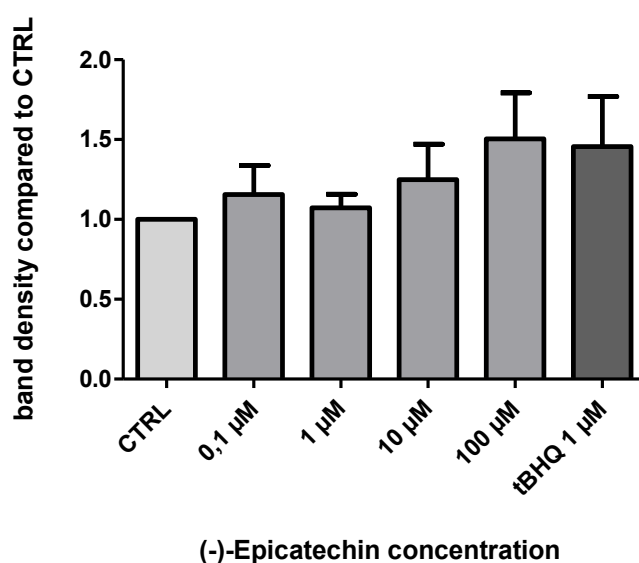


Fig. 19 Densitometry analysis of western blots of nuclear extracts from HUVECs treated with (-)-epicatechin. The graphic shows the band density of the treatments compared to control. Treatment for 1 h with (-)-epicatechin shows increased translocation of Nrf2 into the nucleus in a concentration dependent manner (error bars show SEM, n=5).

Western blot analysis of nuclear activated Nrf2 levels could also show a concentration dependent translocation of Nrf2 into the nucleus that was strongest for (-)-epicatechin at 100  $\mu\text{M}$  concentration, though not statistically significant.

### 4.3.3 Gene expression

To determine the effects on transcription of phase II detoxifying enzymes by (-)-epicatechin mRNA expression was detected after 6 h of treatment using reverse transcription real time PCR. As target enzymes of Nrf2 Nqo1, Hmox1 and Gclc were chosen. Fig. 20 shows the logCT values compared to housekeeping genes and compared to CTRL gene expression ( $\Delta\Delta CT$ ) of Nqo1, Hmox1 and Gclc.

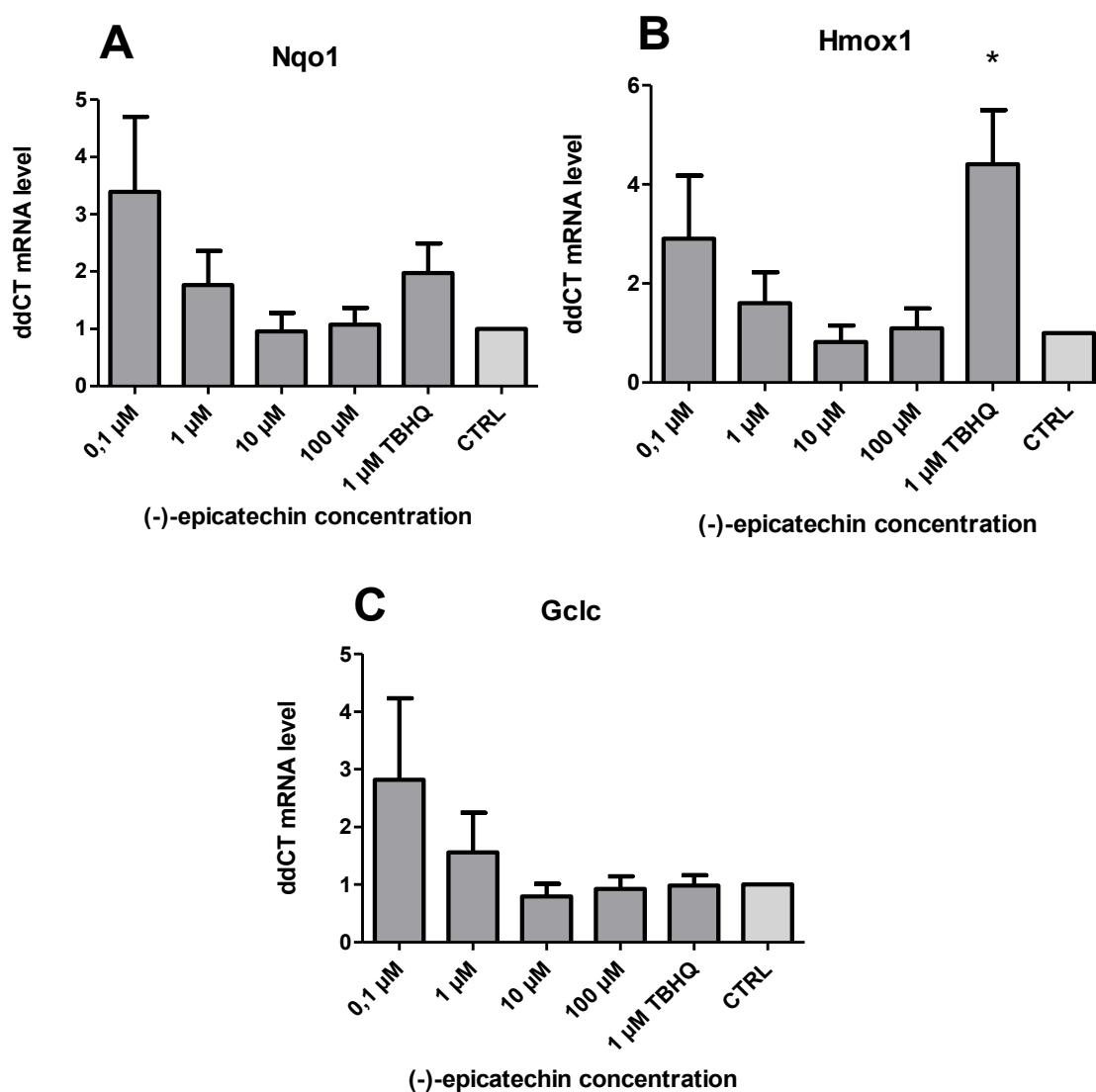


Fig. 20 Real time RT-PCR of RNA extracts from HUVECs treated with (-)-epicatechin for 6 h. Cellular mRNA concentration was detected by real time RT-PCR (10 ng cDNA per well) using primers for (A) Nqo1 (Hs01045993\_g1), (B) Hmox1 (Hs01110250\_m1), (C) Gclc (00892604\_m1) as target genes and 18S (Hs03003631\_g1) as housekeeping gene. CT values were analyzed according to  $\Delta\Delta CT$  method. Values represent the mean  $\pm$ SEM; Statistical significance was tested by one-way ANOVA followed by Tukey post hoc multiple comparison test (n=5; \*P<0.05)

Reverse transcription real time PCR showed a non significant increase of cellular phase II enzymes mRNA levels. Treatments with 0.1  $\mu\text{M}$  (-)-epicatechin led to  $3.39 \pm 1.31$  fold up-regulation of Nqo1 mRNA levels, to  $2.91 \pm 1.28$  fold up-regulation of Hmox1 mRNA levels and to  $2.8 \pm 1.41$  fold up-regulation of Gclc mRNA levels. However, gene expression of the phase II genes was only weakly increased by 1  $\mu\text{M}$  (-)-epicatechin and hardly increased by 10  $\mu\text{M}$  and 100  $\mu\text{M}$  treatment. Statistically significant differences were only measured for the positive control t-BHQ.

## 4.4 Effects of NO<sup>·</sup>, NO<sup>-</sup> and NO<sup>+</sup> on Nrf2 in HUVECs

### 4.4.1 SPER/NO, SNAP and Angeli's salt

An important goal of this study was to compare Nrf2 activation by Angeli's salt (nitroxyl-donor), SNAP (S-nitrosothiol), SPER/NO and DEA/NO (both NO<sup>·</sup> releasing chemicals) in the same cellular system. Upon exposure to NO<sup>·</sup>, NO<sup>-</sup> and NO<sup>+</sup> for 1 h Nrf2 activation and translocation was measured via ARE binding assays of nuclear extracts. Fig. 21 shows the absorbance at 450 nm and absorbance relative to control corresponding to activated nuclear Nrf2 levels.

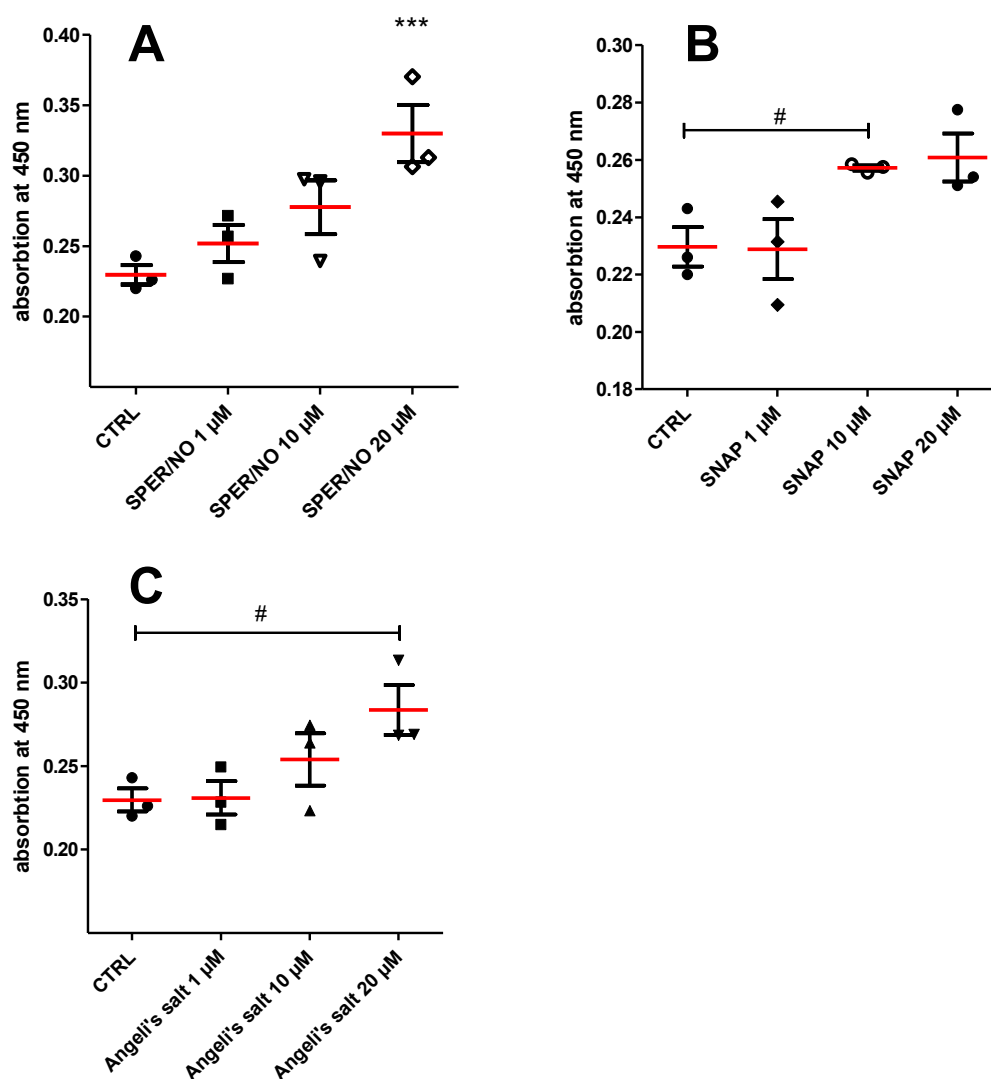


Fig. 21 Transcription factor binding assay of nuclear extracts from HUVECs treated for 1 h with (A) SPER/NO (1-20 μM), (B) SNAP (1-20 μM) and (C) Angeli's salt (1-20 μM). Treatments of HUVECs with SPER/NO showed the strongest increase in ARE binding. Nrf2 is activated in a concentration dependent fashion with significant increase at 20 μM SPER/NO. Angeli's salt and SNAP also augmented Nrf2 activation in a concentration dependent fashion but in less potent way. Each measurement was performed in duplicates. Scatter is shown as SEM. Statistical significance was tested by one-way ANOVA followed by Tukey post hoc multiple comparison test and/or two way T-test (n=3; \*P<0.05, \*\*P<0.01, # indicates P<0.05 in additional T-test)

Treatments of HUVECs with SPER/NO, SNAP and Angeli's salt all showed a dose responding increase in ARE binding. The highest and significant increase was observed for 20  $\mu$ M of SPER/NO ( $0.33 \pm 0.02$  absorbance compared to CTRL  $0.23 \pm 0.01$ ). Angeli's salt and SNAP also augmented Nrf2 activation in a concentration dependent fashion but in less potent way.

To determine the effects on transcription of Hmox-1 induced by SPER/NO, SNAP, and Angeli's salt, mRNA expression was detected after 6 h of treatment using reverse transcription real time PCR. Fig. 22 shows the logCT values compared to housekeeping genes and compared to control gene expression ( $\Delta\Delta$ CT) of Hmox-1.

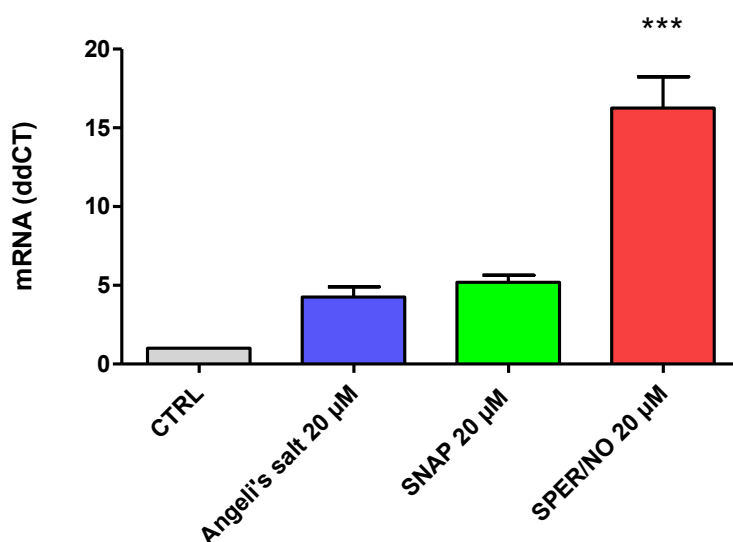


Fig. 22 Hmox1 gene expression in HUVECs treated for 6 h with SPER/NO (20  $\mu$ M), SNAP (20  $\mu$ M) and Angeli's salt (20  $\mu$ M). Treatments of HUVECs with 20  $\mu$ M SPER/NO showed significantly increased Hmox1 gene expression ( $16.26 \pm 1.97$  fold increase). Angeli's salt and SNAP also augmented cellular Hmox1 mRNA levels but in less potent way. Cellular mRNA concentrations were detected by real time RT-PCR (10 ng cDNA per well) using primers for Hmox1 (Hs01110250\_m1) as target genes and 18S (Hs03003631\_g1) as housekeeping gene. CT values were analyzed according to  $\Delta\Delta$ CT method. Bars represent the mean  $\pm$ SEM. Statistical significance was tested by one-way ANOVA followed by Tukey post hoc multiple comparison test ( $n=3$ ; \* $P<0.05$ , \*\* $P<0.01$ )

SPER/NO at a concentration of 20  $\mu$ M showed a significant increase in cellular mRNA levels of Hmox-1 ( $16.26 \pm 1.97$  fold expression compared to untreated control). Augmentation of cellular Hmox1 mRNA levels by Angeli's salt and SNAP were less potent and statistically not significant ( $4.26 \pm 0.64$  fold expression by Angeli's salt vs.  $5.19 \pm 0.46$  fold expression by SNAP)

#### 4.4.2 Treatment with DEA/NO

In addition DEA/NO was used to measure the influence of nitric oxide (NO<sup>·</sup>) on HUVECs. Upon exposure to NO<sup>·</sup> for 1 h Nrf2 activation and translocation was measured via ARE binding assays of nuclear extracts. Fig. 23 shows the absorbance at 450 nm and absorbance relative to control corresponding to activated nuclear Nrf2 levels.

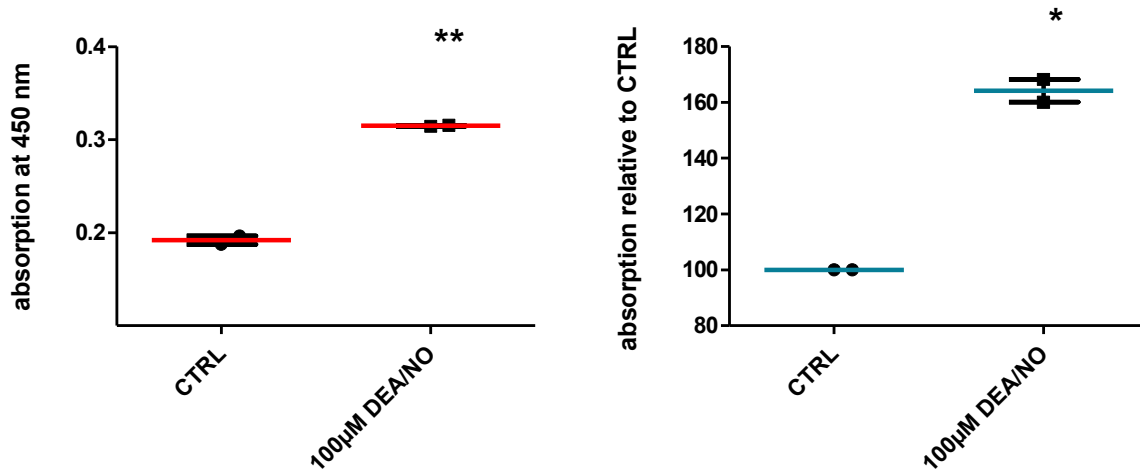


Fig. 23 Transcription factor binding assay of nuclear extracts from HUVECs treated with DEA/NO. The graphic shows the absorbance at 450 nm corresponding to activated nuclear Nrf2 levels and absorbance relative to control. Treatment for 1 h with DEA/NO shows increased absorbance. Each measurement was performed in duplicates. Scatter is shown as SEM. Statistical significance was tested by non-paired, two tailed t-tests (n=2; \*P<0.05, \*\*P<0.01)

Treatment for 1 h with DEA/NO showed  $1.64 \pm 0.041$  fold increased absorbance.

#### 4.4.3 Compared Nrf2 activation by nitroxyl, S-nitrosothiol and NO

In order to better compare the effect sizes on Nrf2 activation by nitroxyl, S-nitrosothiol and NO<sup>•</sup> raw data were normalized. ARE binding data were first compared to untreated control within the same experiment as  $\Delta\%$  of CTRL [(sample-CTRL)/CTRL]. Hereafter data were pooled and reanalyzed for better comparability.

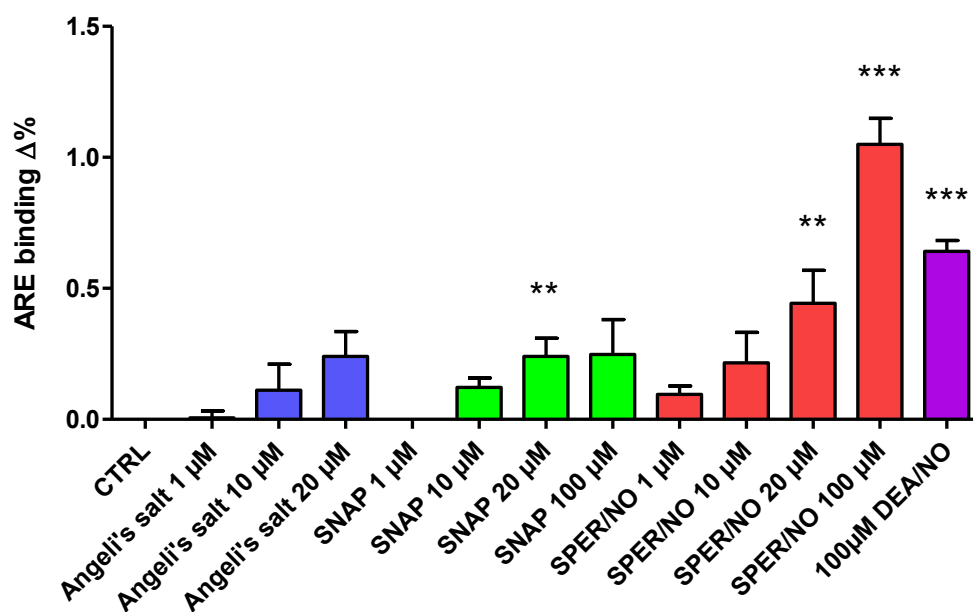


Fig. 24 normalized and pooled data of transcription factor binding assays from HUVECs treated for 1 h with SPER/NO (1-100  $\mu\text{M}$ ), DEA/NO (100  $\mu\text{M}$ ), SNAP (1-100  $\mu\text{M}$ ) and Angeli's salt (1-20  $\mu\text{M}$ ). Treatments of HUVECs with SPER/NO showed the strongest increase in ARE binding. Nrf2 is activated in a concentration dependent fashion with significant increases at 20  $\mu\text{M}$  and 100  $\mu\text{M}$  SPER/NO. DEA/NO also showed significant increased ARE binding. Angeli's salt and SNAP also augmented Nrf2 activation in a concentration dependent fashion but in less potent way. Each measurement was performed in duplicates. Scatter is shown as SEM. Statistical significance was tested by one-way ANOVA followed by Tukey post hoc multiple comparison test (n=3; n=12 for SNAP 20 $\mu\text{M}$ ; \*P<0.05, \*\*P<0.01)

Treatment of HUVECs with SPER/NO showed the strongest increase in ARE binding ( $44\% \pm 13\%$  at 20  $\mu\text{M}$  and  $105\% \pm 10\%$  at 100  $\mu\text{M}$ ) and the most distinct increase in Hmox1 expression ( $16.26 \pm 1.97$  fold expression at 20  $\mu\text{M}$  – see Fig. 22). Angeli's salt and SNAP also augmented Nrf2 activation in a concentration dependent fashion but in less potent way ( $24\% \pm 10\%$  at 20  $\mu\text{M}$  Angeli's salt and  $24\% \pm 7\%$  at 20  $\mu\text{M}$  SNAP). Similar results were shown for Hmox1 expression (see chapter 4.4.1)

Taken together, this work showed Nrf2 activation and increase in cellular mRNA levels of phase II enzyme Hmox1 in HUVECs. By direct comparison of NO<sup>•</sup>, NO<sup>-</sup> and NO<sup>+</sup> strongest effects were shown for SPER/NO indicating NO<sup>•</sup> to be the most potent Nrf2 activator among those three.

## 4.5 Effects of sulfide on Nrf2 in HUVECs

### 4.5.1 Treatment with GYY 4137

To analyze the effects of sulfide on Nrf2 translocation and ARE binding HUVECs were treated with the slow sulfide donor GYY 4137 for one hour. After preparation of nuclear extracts activated Nrf2 levels were determined using the transcription factor binding assay. Fig. 25 shows the absorbance at 450 nm and absorbance relative to control corresponding to activated nuclear Nrf2 levels.

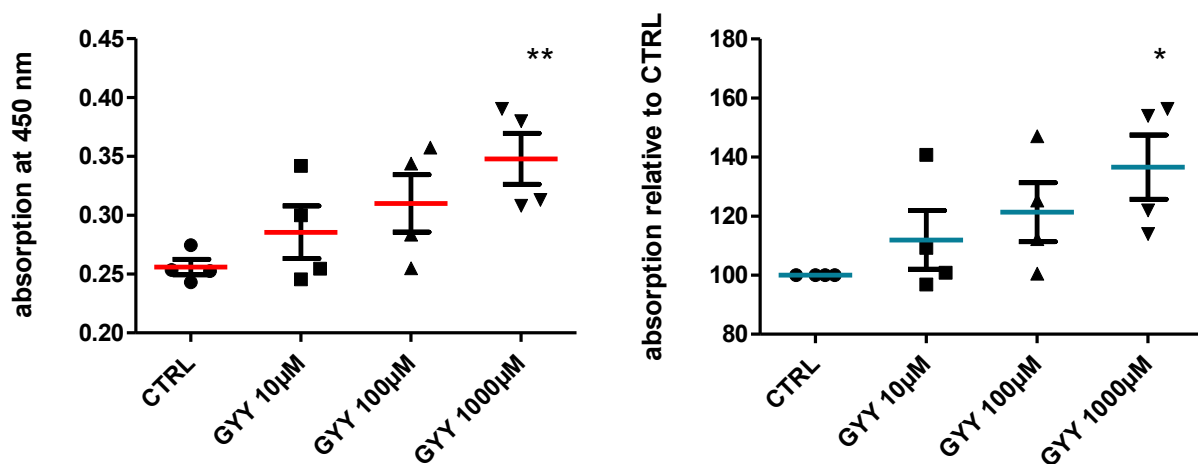


Fig. 25 Transcription factor binding assay of nuclear extracts from HUVECs treated with GYY4137. The graphic shows the absorbance at 450 nm corresponding to activated nuclear Nrf2 levels and absorbance relative to control. Treatment for 1 h with GYY shows increased absorbance dependent on concentration. Significant differences were observed at 1000  $\mu$ M concentration of GYY. Each measurement was performed in duplicates. Scatter is shown as SEM. Statistical significance was tested by one-way ANOVA followed by Tukey post hoc multiple comparison test (n=4; \*P<0.05, \*\*P<0.01)

Treatment for 1 h with GYY shows concentration-dependent increased absorbance. Significant differences were only observed at 1000  $\mu$ M concentration of GYY.

#### 4.5.2 Treatment with Na<sub>2</sub>S

Additionally HUVECs were treated with increasing concentrations of sulfide by dilution of Na<sub>2</sub>S for 1 h. After preparation of nuclear extracts activated Nrf2 levels were determined using the transcription factor binding assay. Fig. 26 shows the absorbance at 450 nm and absorbance relative to control corresponding to activated nuclear Nrf2 levels.

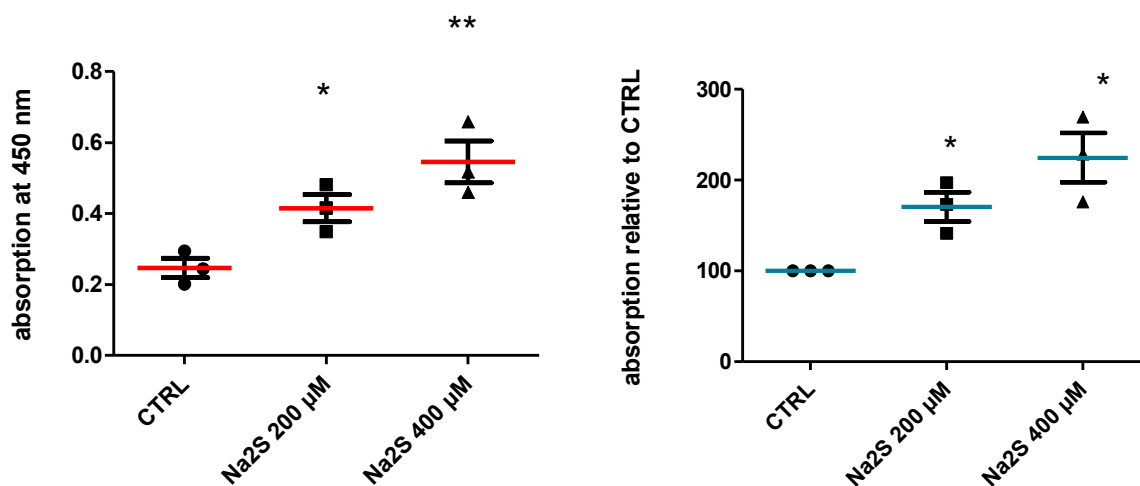


Fig. 26 Transcription factor binding assay of nuclear extracts from HUVECs treated with Na<sub>2</sub>S. The graphic shows the absorbance at 450 nm corresponding to activated nuclear Nrf2 levels and absorbance relative to control. Treatment for 1 h with Na<sub>2</sub>S shows increased absorbance dependent on concentration. Significant differences were observed at 200 μM and 400 μM concentration of Na<sub>2</sub>S. Each measurement was performed in duplicates. Scatter is shown as SEM. Statistical significance was tested by one-way ANOVA followed by Tukey post hoc multiple comparison test (n=3; \*P<0.05, \*\*P<0.01).

Treatment for 1 h with Na<sub>2</sub>S shows increased absorbance dependent on concentration.

Significant differences were only observed at 200 μM and 400 μM concentration of Na<sub>2</sub>S.

## 4.6 Modulation of nitric oxide effects on Nrf2 by sulfide in HUVECs

### 4.6.1 Treatment with GYY and SPER/NO

To investigate on a potential crosstalk between sulfide and nitric oxide HUVECs were treated with GYY 4137 in combination with SPER/NO for 1h. After preparation of nuclear extracts activated Nrf2 levels were determined using the transcription factor binding assay. Fig. 27 shows the absorbance at 450 nm and absorbance relative to control corresponding to activated nuclear Nrf2 levels.

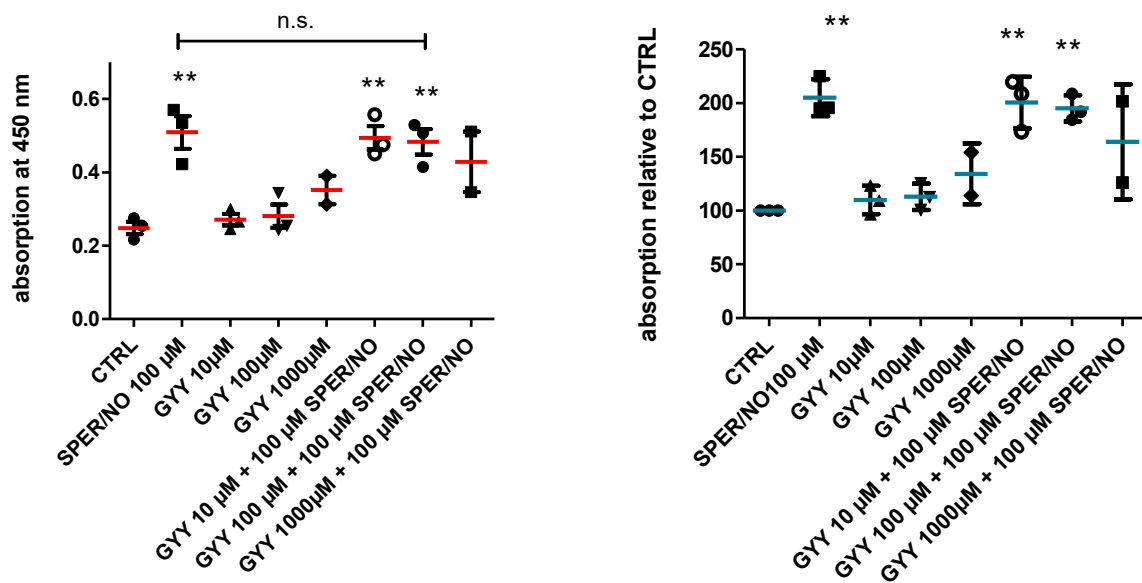


Fig. 27 Transcription factor binding assay of nuclear extracts from HUVECs treated with SPER/NO in combination with GYY 4137. The graphic shows the absorbance at 450 nm corresponding to activated nuclear Nrf2 levels and absorbance relative to CTRL. Treatment for 1 h with SPER/NO shows increased absorbance. In combination with rising concentrations of GYY 4137 absorbance is decreasing. Each measurement was performed in duplicates. Scatter is shown as SEM. Statistical significance was tested by one-way ANOVA followed by Tukey post hoc multiple comparison test (n=3; \*P<0.05, \*\*P<0.01)

Treatment for 1 h with 100 µM SPER/NO shows  $2.05 \pm 0.1$  fold increased absorbance. In combination with 100 µM GYY 4137 Nrf2 binding activity is  $1.95 \pm 0.08$  fold increased while there are no significant differences to treatment with only SPER/NO.

#### 4.6.2 Treatment with GYY and SNAP

To investigate on a potential crosstalk between sulfide and S-nitrosothiols respectively nitrosonium ( $\text{NO}^+$ ) HUVECs were treated with GYY 4137 in combination with SNAP for 1h. After preparation of nuclear extracts activated Nrf2 levels were determined using the transcription factor binding assay. Fig. 28 shows the absorbance at 450 nm and absorbance relative to control corresponding to activated nuclear Nrf2 levels.

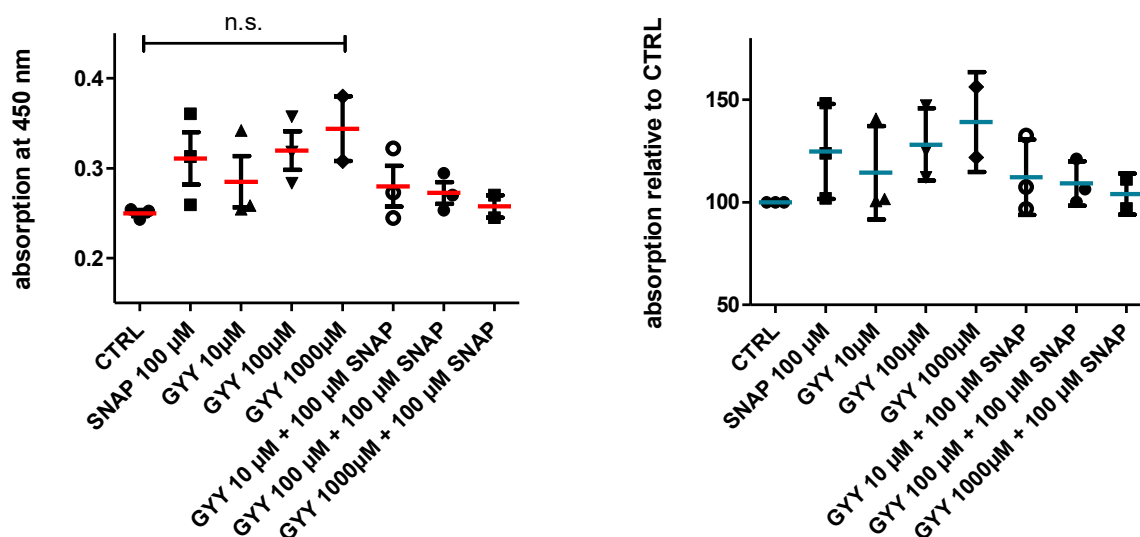


Fig. 28 Transcription factor binding assay of nuclear extracts from HUVECs treated with SNAP in combination with GYY 4137. The graphic shows the absorbance at 450 nm corresponding to activated nuclear Nrf2 levels and absorbance relative to CTRL. Treatment for 1 h with SNAP shows increased absorbance although not significant. In combination with GYY 4137 absorbance is almost decreased to levels of control when concentration of GYY 4137 is rising. Each measurement was performed in duplicates. Scatter is shown as SEM. Statistical significance was tested by one-way ANOVA followed by Tukey post hoc multiple comparison test ( $n=3$ ;  $*P<0.05$ ,  $**P<0.01$ )

Treatment for 1 h with SNAP did not show significantly increased absorbance in this experiment. However, Nrf2 binding activity tends to raise upon incubation with 100  $\mu\text{M}$  SNAP while combination of SNAP with GYY 4137 decreases Nrf2 activation.

### 4.6.3 Treatment with sulfide and DEA/NO

To obtain further insights into the crosstalk between sulfide and NO<sup>•</sup> cells were incubated with DEA/NO with and without Na<sub>2</sub>S for 1 h. After preparation of nuclear extracts activated Nrf2 levels were determined using the transcription factor binding assay.

Fig. 29 shows the absorbance at 450 nm and absorbance relative to control corresponding to activated nuclear Nrf2 levels.

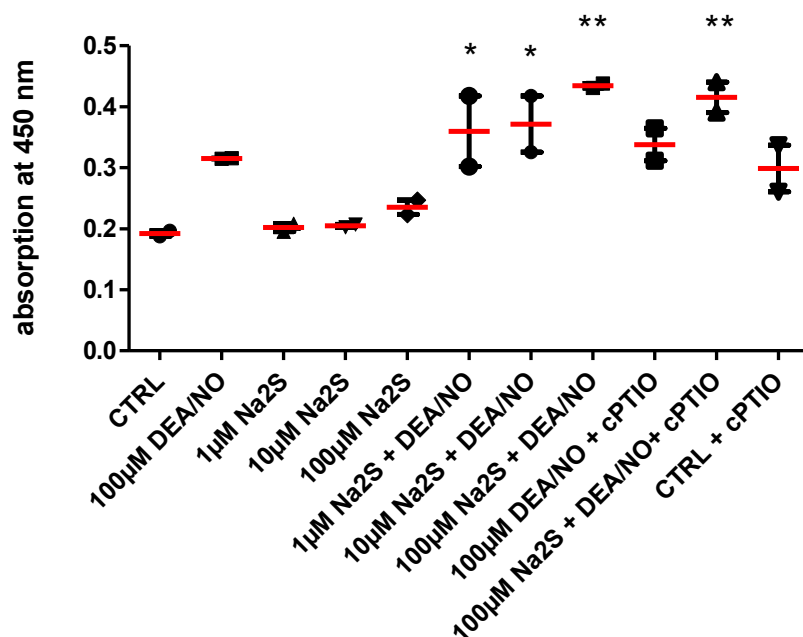


Fig. 29 Transcription factor binding assay of nuclear extracts from HUVECs treated with DEA/NO in combination with Na<sub>2</sub>S. The graphic shows the absorbance at 450 nm corresponding to activated nuclear Nrf2 levels and absorbance relative to CTRL. Treatment for 1 h with DEA/NO shows increased absorbance. In combination with Na<sub>2</sub>S absorbance shows a 2-fold increase compared to levels of control while concentration of Na<sub>2</sub>S is rising. Each measurement was performed in duplicates. Scatter is shown as SEM Statistical significance was tested by one-way ANOVA followed by Tukey post hoc multiple comparison test (n=2; \*P<0.05, \*\*P<0.01)

Treatment for 1 h with DEA/NO showed  $1.64 \pm 0.041$  fold increased absorbance. In combination with Na<sub>2</sub>S ARE binding levels were risen up to  $2.26 \pm 0.035$  fold absorbance.

#### 4.6.4 Treatment with GYY and L-NAME

To clarify if treatment with sulfide has any effects on Nrf2 signaling in the absence of intracellular NO, cells were pre-incubated with L-N<sup>G</sup>-Nitroarginine methyl ester (L-NAME) to inhibit cellular NO production. Fig. 30 shows the absorbance at 450 nm corresponding to activated nuclear Nrf2 levels.

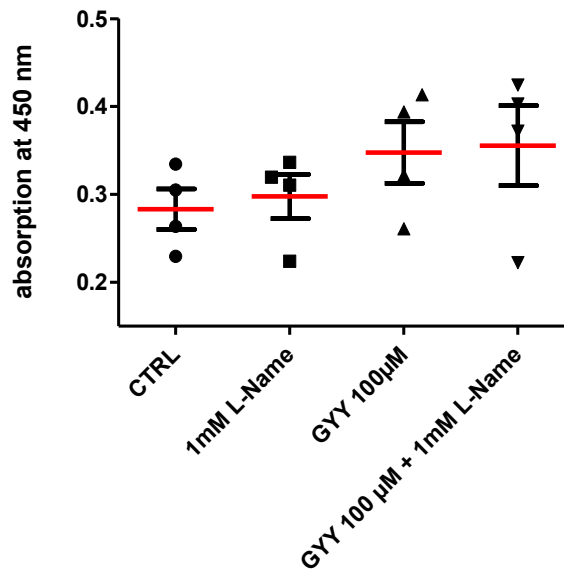


Fig. 30 Transcription factor binding assay of nuclear extracts from HUVECs treated with L-NAME in combination with GYY 4137. The graphic shows the absorbance at 450 nm corresponding to activated nuclear Nrf2 levels and absorbance relative to CTRL. Treatment for 1 h with L-NAME shows no significant change in absorbance. In combination with GYY 4137 absorbance is increased but without significant changes. Each measurement was performed in duplicates. Scatter is shown as SEM. Statistical significance was tested by one-way ANOVA followed by Tukey post hoc multiple comparison test (n=4; \*P<0.05, \*\*P<0.01)

Pre-incubation with L-Name for 30 min did not affect absorbance levels compared to control. In combination with GYY 4137 ARE binding is also not altered significantly.

## 4.7 Effects of SSNO<sup>-</sup> on Nrf2 in HUVECs

### 4.7.1 Formation of SSNO<sup>-</sup>

In this study SSNO<sup>-</sup> was synthesized from sulfide and an S-nitrosothiol at physiological pH monitored by UV–visible spectroscopy following the protocol of Cortese-Krott et al. (Cortese-Krott, Fernandez et al. 2014). Incubation of 10 mM Na<sub>2</sub>S with 1 mM SNAP led to formation of a yellow compound at 412 nm, that was stable for >30 min. Additionally an increase of absorbance at 250 to 310 nm with a second peak at 260 nm was observed. The 250 to 310 nm increase of absorbance was assumed to be polysulfides (HS<sub>n</sub><sup>-</sup>) because it could be removed by the polysulfide scavenger DTT. The peak at 260 nm however emerges from SULFI/NO formation, which is another reaction byproduct also described by Cortese-Krott et al. (Cortese-Krott, Kuhnle et al. 2015). For further information see chapter 3.3.

Since sulfide in excess was used to obtain the SSNO<sup>-</sup> solution, the remaining educts (visible at 250 nm and below) had to be removed to study the reaction products individually. This was performed via two different protocols (see chapter 3.3). The sulfide in excess could be removed (1) via gassing with N<sub>2</sub> for 10 min and (2) via application of 10 mM zinc, which led to formation of zinc complexes, which then could be removed from the solution by centrifugation. Following both protocols the sulfide in excess was removed successfully.

Thereby we obtained a Na<sub>2</sub>S free SSNO<sup>-</sup> solution stable for more than 30 minutes, which could be administered to the cells.

### 4.7.2 Treatment with SSNO<sup>-</sup>

To investigate on activation of Nrf2 signaling by SSNO<sup>-</sup> solutions, HUVECs were incubated with the mixes (described in chapter 3.3) prepared immediately prior to treatment. Effects on Nrf2 activation and translocation were analyzed by ARE binding in nuclear extracts after treating the cells for 1h with SSNO<sup>-</sup> and different controls.

Fig. 31 shows the absorbance at 450 nm and absorbance relative to control corresponding to activated nuclear Nrf2 levels. Treatment for 1 h with SSNO<sup>-</sup> showed up to 2.11 ±0.15 fold increased absorbance at concentrations of 20 μM. Significant differences were observed compared to CTRL as well as to Na<sub>2</sub>S at concentrations of 200 μM.

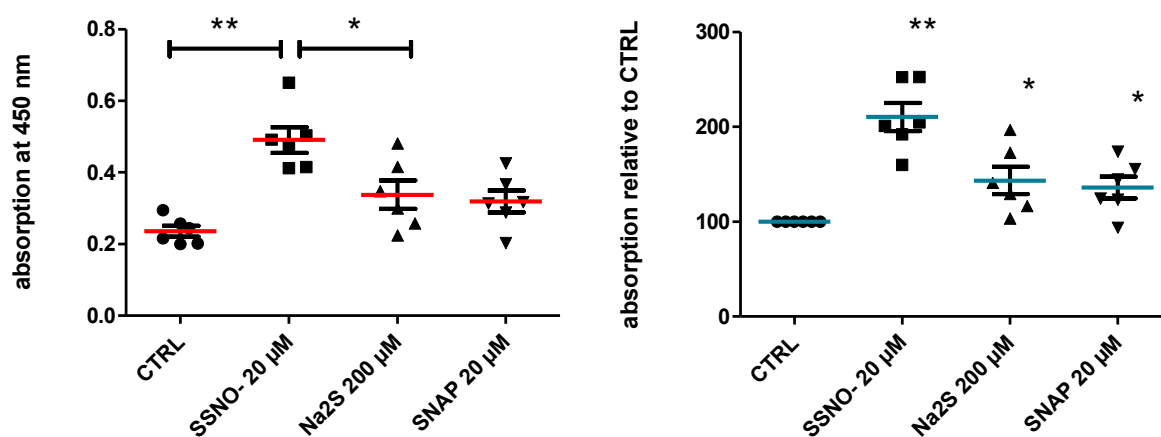


Fig. 31 Transcription factor binding assay of nuclear extracts from HUVECs treated with 20  $\mu\text{M}$  SSNO<sup>-</sup>, 200  $\mu\text{M}$  Na<sub>2</sub>S and 20  $\mu\text{M}$  SNAP. The graph shows the absorbance at 450 nm corresponding to activated nuclear Nrf2 levels and absorbance relative to CTRL. Treatment for 1 h with SSNO<sup>-</sup> shows 2.11  $\pm$  0.15 fold increased absorbance with high significance compared to CTRL. Na<sub>2</sub>S treatment also shows significantly increased absorbance. SSNO<sup>-</sup> shows significant higher absorbance than Na<sub>2</sub>S. Each measurement was performed in duplicates. Scatter is shown as SEM. Statistical significance was tested by one-way ANOVA followed by Tukey post hoc multiple comparison test (n=3; \*P<0.05, \*\*P<0.01)

#### 4.7.3 Treatment with SSNO<sup>-</sup> incubated with Zn

To remove sulfide in excess from the SSNO<sup>-</sup> solution, the SSNO<sup>-</sup> mix was incubated with 10 mM ZnCl<sub>2</sub> for 2 min to allow formation of sulfide Zn complexes, which could then be spun down by centrifugation. As a control the Na<sub>2</sub>S solution was processed the same way (for further details see chapter 3.3). HUVECs were incubated with the supernatant of those mixes.

Fig. 32 shows the absorbance at 450 nm and absorbance relative to control corresponding to activated nuclear Nrf2 levels.

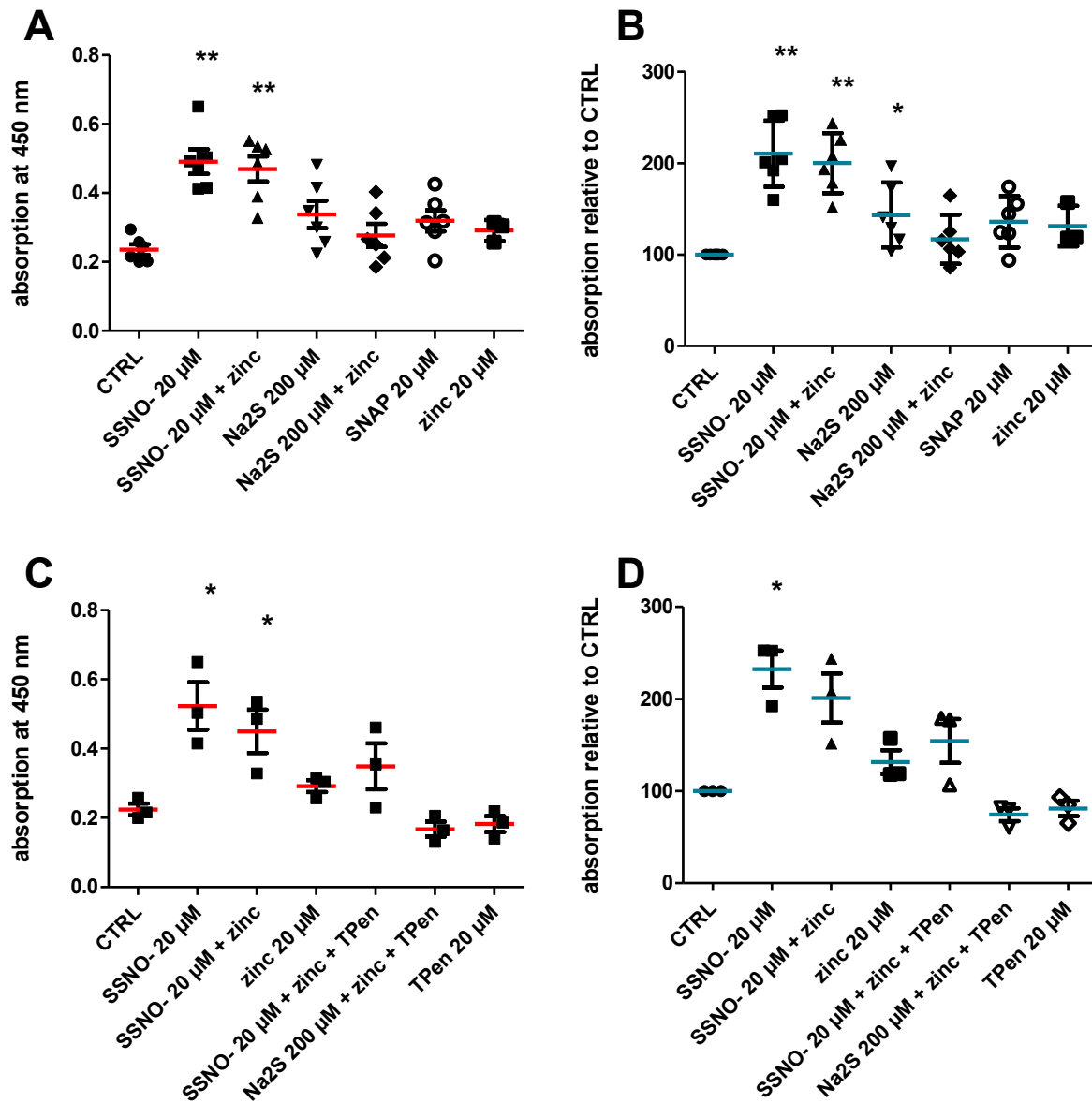


Fig. 32 Transcription factor binding assay of nuclear extracts from HUVECs treated with the supernatant of SSNO<sup>-</sup> and Na<sub>2</sub>S incubated with ZnCl<sub>2</sub>. The graphic shows the absorbance at 450 nm corresponding to activated nuclear Nrf2 levels (A and C) and absorbance relative to CTRL (B and D). Treatment for 1 h with SSNO<sup>-</sup> showed 2.11 ±0.15 and treatment with SSNO<sup>-</sup> incubated with zinc showed 2.0 ±0.13fold increased absorbance with high significance. Na<sub>2</sub>S treatment also shows significantly increased absorbance, while Na<sub>2</sub>S plus zinc shows minor increases. Each measurement was performed in duplicates. Scatter is shown as SEM. Statistical significance was tested by one-way ANOVA followed by Tukey post hoc multiple comparison test (n=3; \*P<0.05, \*\*P<0.01)

Treatment for 1 h with SSNO<sup>-</sup> showed 2.11 ±0.15 and treatment with SSNO<sup>-</sup> incubated with zinc showed 2.0 ±0.13fold increased absorbance with high significance. Na<sub>2</sub>S treatment also shows significantly increased absorbance, while Na<sub>2</sub>S plus zinc shows minor increases. Zinc itself had minor, non significant effects on Nrf2 signaling, which were completely abolished upon coincubation with the chelator TPEN.

#### 4.7.4 Treatment with gassed SSNO<sup>-</sup>

The second protocol to deplete the effects of Na<sub>2</sub>S in excess abundant in the SSNO<sup>-</sup> solution and to investigate on its effects on Nrf2 activation, was to gas the SSNO<sup>-</sup> mix with nitrogen for 10 min. HUVECs were incubated with both gassed and non-gassed SSNO<sup>-</sup> at a concentration of 20 μM. Fig. 33 shows the absorbance at 450 nm corresponding to activated nuclear Nrf2 levels.

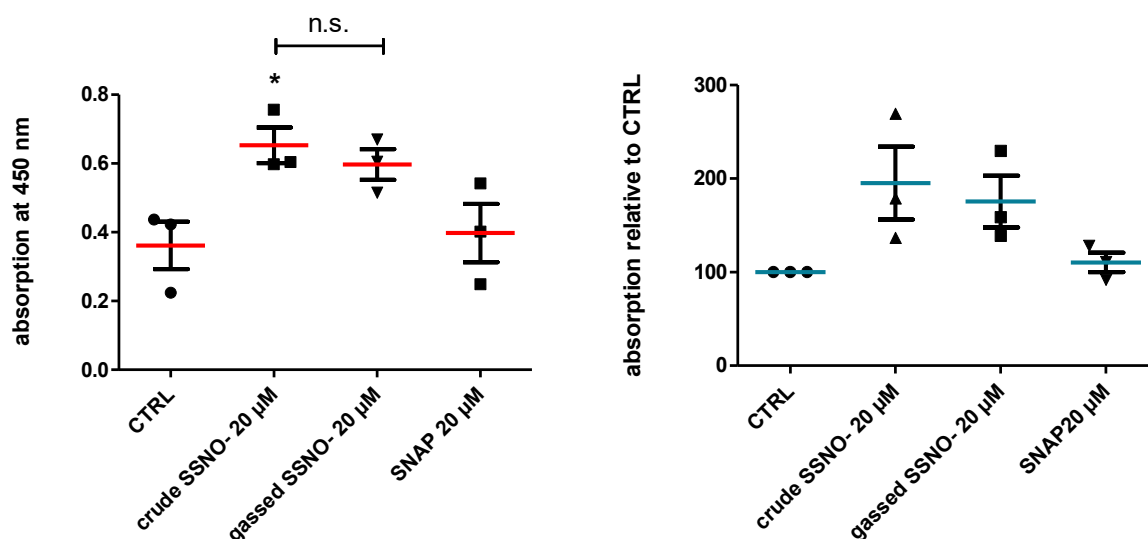


Fig. 33 Transcription factor binding assay of nuclear extracts from HUVECs treated with crude and gassed SSNO<sup>-</sup>. The graphic shows the absorbance at 450 nm corresponding to activated nuclear Nrf2 levels and absorbance relative to CTRL. Treatment for 1 h with crude and gassed SSNO<sup>-</sup> showed 1.95 ±0.39 fold and 1.76 ±0.28 fold increased absorbance with significant differences for crude SSNO<sup>-</sup>. Each measurement was performed in duplicates. Scatter is shown as SEM. Statistical significance was tested by one-way ANOVA followed by Tukey post hoc multiple comparison test (n=3; \*P<0.05, \*\*P<0.01)

Treatment for 1 h with crude and gassed SSNO<sup>-</sup> showed increased absorbance. ARE binding was augmented 1.95 ±0.39 fold by 20 μM crude SSNO<sup>-</sup> and 1.76 ±0.28 fold by 20 μM of gassed SSNO<sup>-</sup>. Significant differences to control were only observed with crude SSNO<sup>-</sup>. Differences between crude and gassed SSNO<sup>-</sup> were not significant in direct comparison.

In addition to ARE binding, the effects of gassed and non-gassed SSNO<sup>-</sup> on transcription of phase II detoxifying enzyme Hmox1 was detected after 6 h of treatment using reverse transcription real time PCR.

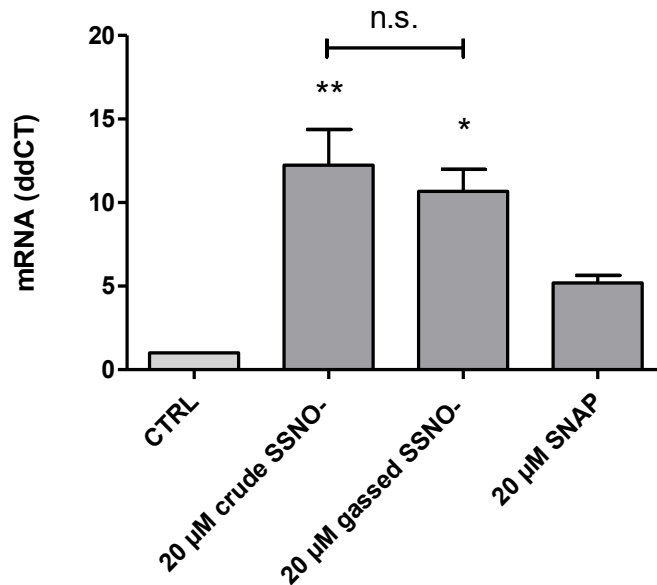


Fig. 34 Real time RT-PCR of RNA extracts from HUVECs treated for 6 h with SSNO<sup>-</sup> with and without gassing with nitrogen for 10 min. Cellular mRNA concentrations were detected by real time RT-PCR (10 ng cDNA per well) using primers for Hmox1 (Hs01110250\_m1) as target genes and 18S (Hs03003631\_g1) as housekeeping gene. CT values were analyzed according to  $\Delta\Delta CT$  method. Bars represent the mean  $\pm$ SEM. Statistical significance was tested by one-way ANOVA followed by Tukey post hoc multiple comparison test (n=3; \*P<0.05, \*\*P<0.01)

Treatment for 6 h with crude and gassed SSNO<sup>-</sup> showed increased Hmox1 gene expression.

Hmox1 mRNA levels were significantly increased  $12.25 \pm 2.13$  fold by 20  $\mu$ M crude SSNO<sup>-</sup> and  $10.68 \pm 1.31$  fold by 20  $\mu$ M gassed SSNO<sup>-</sup>. Differences between crude and gassed SSNO<sup>-</sup> were not significant in direct comparison.

#### 4.7.5 Influence of nitric oxide and polysulfides on Nrf2 activation by SSNO<sup>-</sup>

To further investigate the influence of NO released by SSNO<sup>-</sup> and the polysulfide compounds of SSNO<sup>-</sup> HUVECs were incubated with a nitric oxide scavenger (cPTIO) or with L-cysteine for polysulfide decomposition in addition to the gassed SSNO<sup>-</sup> treatment. After preparation of nuclear extracts activated Nrf2 levels were determined using the transcription factor binding assay. Fig. 35 shows the absorbance at 450 nm and absorbance relative to control corresponding to activated nuclear Nrf2 levels.

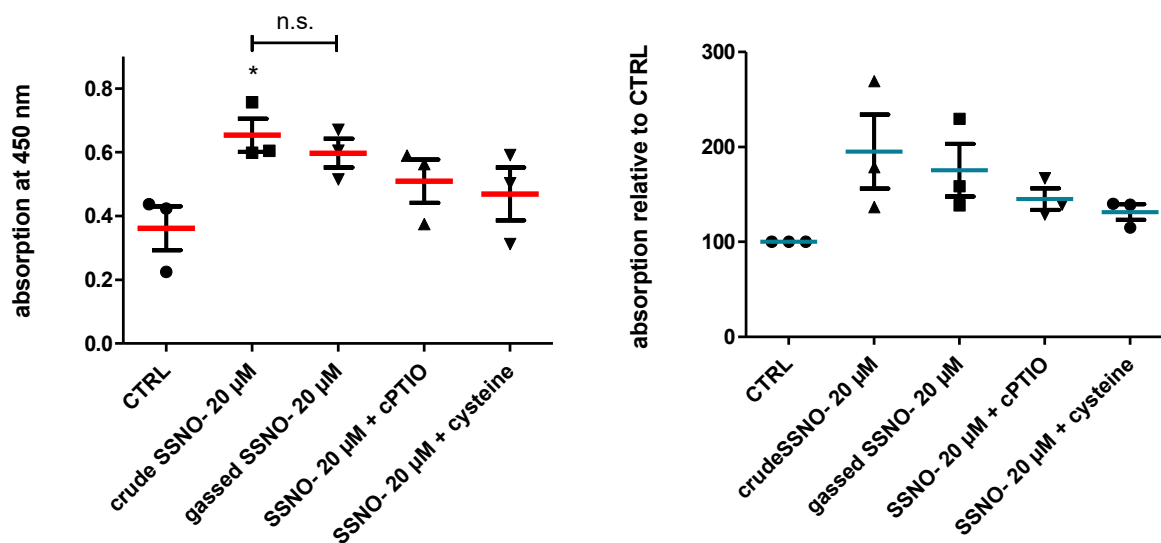


Fig. 35 Transcription factor binding assay of nuclear extracts from HUVECs treated with SSNO<sup>-</sup> (after gassing with nitrogen for 10 min) and additionally with 200 μM L-cysteine or 100 μM cPTIO. The graphic shows the absorbance at 450 nm corresponding to activated nuclear Nrf2 levels and absorbance relative to CTRL. Treatment for 1 h with gassed SSNO<sup>-</sup> showed 1.95 ± 0.39 increased absorbance compared to CTRL. Coincubation with cysteine decreases absorbance by 0.441 and cPTIO decreases absorbance by 0.305 compared to 20 μM gassed SSNO<sup>-</sup> treatment. Each measurement was performed in duplicates. Scatter is shown as SEM. Statistical significance was tested by one-way ANOVA followed by Tukey post hoc multiple comparison test (n=3; \*P<0.05, \*\*P<0.01)

Treatment for 1 h with crude and gassed SSNO<sup>-</sup> showed increased absorbance. ARE binding was augmented 1.95 ± 0.39 fold by 20 μM crude SSNO<sup>-</sup> and 1.76 ± 0.28 fold by 20 μM of gassed SSNO<sup>-</sup>. Significant differences to control were only observed with crude SSNO<sup>-</sup>. Differences between crude and gassed SSNO<sup>-</sup> were not significant. Coincubation with cysteine decreases absorbance by 0.441 and coincubation with cPTIO decreases absorbance by 0.305 compared to 20 μM gassed SSNO<sup>-</sup> treatment, even though not significant.

Importantly, western blots of nuclear extracts could prove that Nrf1 levels were not increased by SSNO<sup>-</sup>. Therefore, changes in ARE binding as assessed by transcription factor binding assays (see above) were due to increased Nrf2 activity and not Nrf1. Fig. 36 shows one representative western blot putting the focus on the influence of cPTIO and L-cysteine on Nrf2 activation and translocation. Fig. 37 shows the densitometry analysis of western blots (n=3).

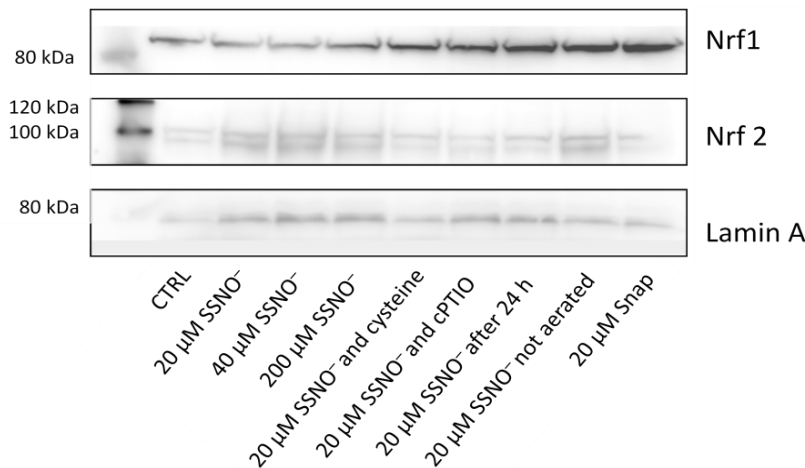


Fig. 36 Western blot of nuclear extracts from HUVECs treated with SSNO<sup>-</sup> in different concentrations with or without co-incubation with cPTIO or L-cysteine. The graphic shows bands at 100 kDa after staining with Anti-Nrf2 (ab63252) corresponding to activated nuclear Nrf2. Treatment for 1 h with SSNO<sup>-</sup> shows increased incidence of Nrf2 in the nucleus in a concentration dependent manner whereas co-incubation with cPTIO or L-cysteine led to decreased western blot signal in the nucleus. The second staining was made with Lamin A (ab8980) as a loading control. Slots were loaded with 15 μg protein.

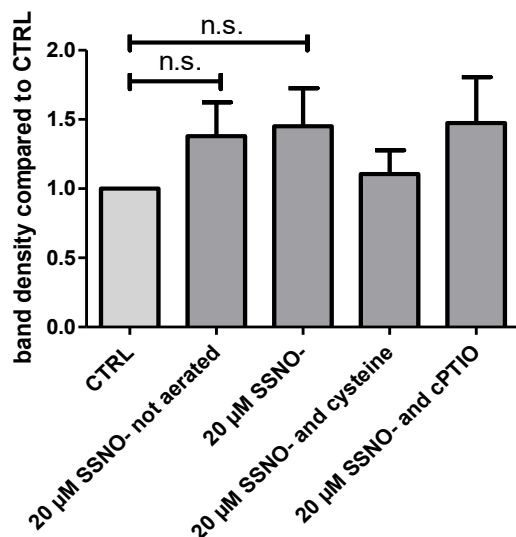


Fig. 37 Densitometry analysis of western blots of nuclear extracts from HUVECs treated with gassed and not gassed SSNO<sup>-</sup> with and without co-incubation of 200 μM L-cysteine or 100 μM cPTIO. The graphic shows the band density of the treatments compared to control. Treatment for 1 h with SSNO<sup>-</sup> and co-incubation with cPTIO showed up to 1.5 fold increased incidence of Nrf2 in the nucleus. Scatter is shown as SEM (n=3) Statistical significance was tested by non-paired, two tailed t-test.

In addition to nuclear Nrf2 activation effects of cPTIO and cysteine on mRNA expression of Hmox1 were detected by reverse transcription real time PCR. Fig. 38 shows the logarithmized CT values compared to housekeeping genes and compared to CTRL gene expression ( $\Delta\Delta\text{CT}$ ) of Hmox1.

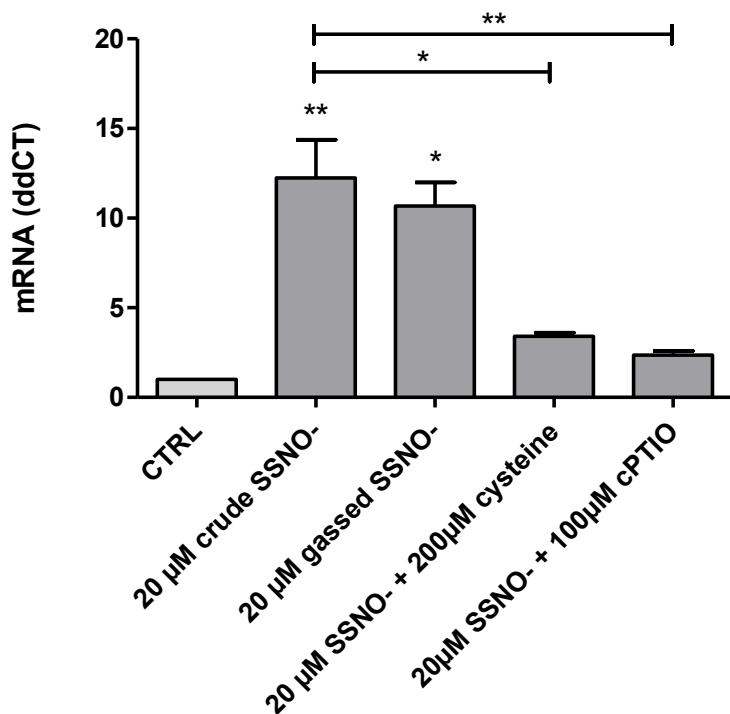


Fig. 38 Real time RT-PCR of RNA extracts from HUVECs treated for 6 h with SSNO<sup>-</sup> after gassing with nitrogen for 10 min and co incubation with cysteine or cPTIO. Cellular mRNA concentration was detected by real time RT-PCR (10 ng cDNA per well) using primers for Hmox1 (Hs01110250\_m1) as target genes and 18S (Hs03003631\_g1) as housekeeping gene. CT values were analyzed according to  $\Delta\Delta\text{CT}$  method. Bars represent the mean  $\pm$ SEM. Statistical significance was tested by one-way ANOVA followed by Tukey post hoc multiple comparison test (n=3; \*P<0.05, \*\*P<0.01)

Treatment for 6 h with crude and gassed SSNO<sup>-</sup> showed increased Hmox1 gene expression. Hmox1 mRNA levels were significantly increased  $12.25 \pm 2.13$  fold by 20  $\mu\text{M}$  crude SSNO<sup>-</sup> and  $10.68 \pm 1.31$  fold by 20  $\mu\text{M}$  gassed SSNO<sup>-</sup>. Differences between crude and gassed SSNO<sup>-</sup> were not significant. Upon coincubation with cysteine Hmox1 gene expression was only increased  $3.41 \pm 0.19$  fold and only  $2.36 \pm 0.22$  fold with cPTIO. Differences between crude/gassed SSNO<sup>-</sup> and cysteine /cPTIO were significant in Tukey post hoc multiple comparison test.

#### 4.7.6 Concentration dependent treatment of HUVECs with gassed SSNO<sup>-</sup>

To detect a concentration dependent influence of SSNO<sup>-</sup> on Nrf2 signaling, cells were treated with concentrations of 2  $\mu$ M up to 200  $\mu$ M for 1 hour. After preparation of nuclear extracts activated Nrf2 levels were determined using the transcription factor binding assay. Fig. 39 shows the absorbance at 450 nm and absorbance relative to control corresponding to activated nuclear Nrf2 levels.

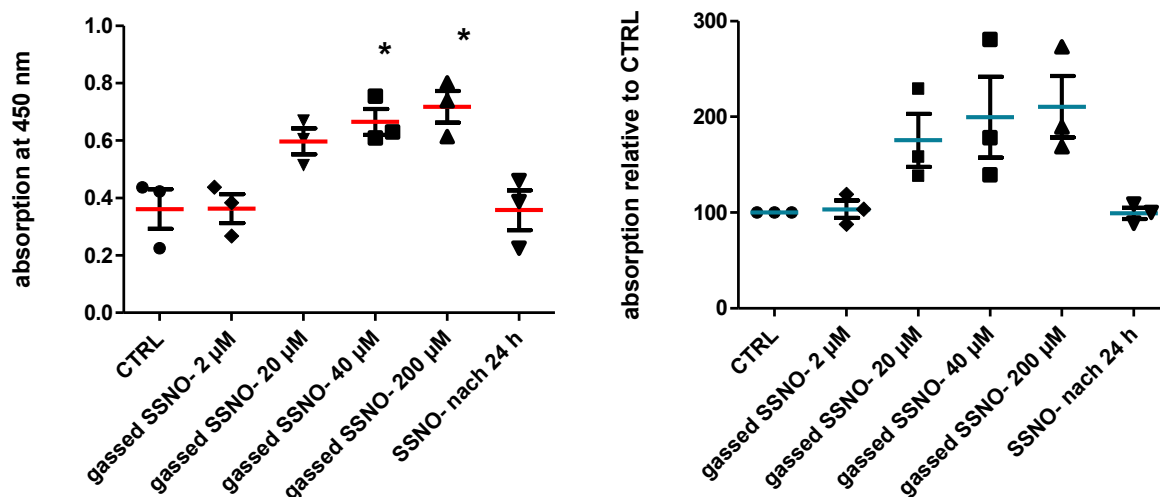


Fig. 39 Transcription factor binding assay of nuclear extracts from HUVECs treated with SSNO<sup>-</sup> after gassing with nitrogen for 10 min. The graphic shows the absorbance at 450 nm corresponding to activated nuclear Nrf2 levels and absorbance relative to control. Treatment for 1 h with gassed SSNO<sup>-</sup> shows increased absorbance in a concentration dependent manner with high significance. Each measurement was performed in duplicates. Scatter is shown as SEM. Statistical significance was tested by one-way ANOVA followed by Tukey post hoc multiple comparison test (n=3; \*P<0.05, \*\*P<0.01)

Treatment for 1 h with gassed SSNO<sup>-</sup> showed increased absorbance in a concentration dependent manner. ARE binding was augmented  $1.76 \pm 0.28$  fold by 20  $\mu$ M of gassed SSNO<sup>-</sup>,  $1.99 \pm 0.42$  fold by 40  $\mu$ M and  $2.11 \pm 0.31$  fold by 200  $\mu$ M of gassed SSNO<sup>-</sup>. At a concentration of 2  $\mu$ M SSNO<sup>-</sup> hardly affected Nrf2 binding activity. Significant differences to control were only observed at concentrations of 40  $\mu$ M and 200  $\mu$ M. Nevertheless a concentration dependent increase can be recognized. Decomposed SSNO<sup>-</sup> (incubated for 24 h protected from light) did not affect Nrf2 activation.

Importantly, western blots of nuclear extracts could prove that Nrf1 levels were not increased by SSNO<sup>-</sup>. Therefore, changes in ARE binding as assessed by transcription factor binding assays (see above) were due to increased Nrf2 activity and not Nrf1. Fig. 40 shows one representative western blot putting the focus on concentration dependent Nrf2 activation and translocation. Fig. 37 shows the densitometry analysis of western blots (n=3).

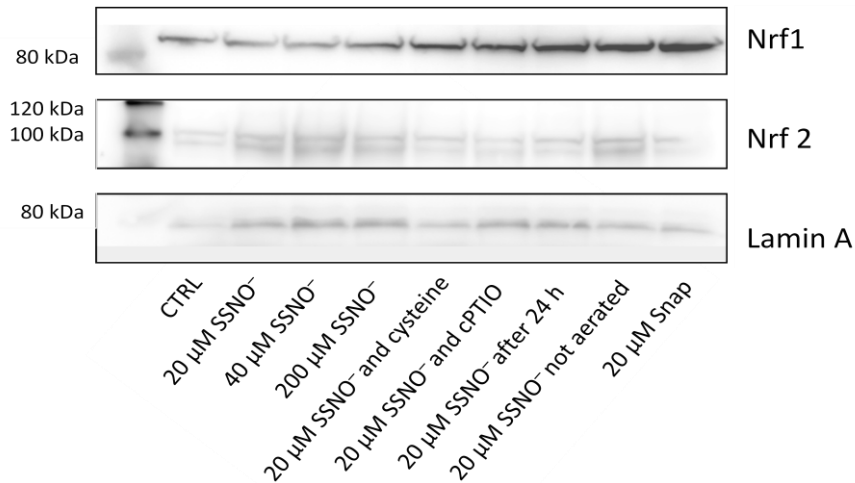


Fig. 40 Western blot of nuclear extracts from HUVECs treated with SSNO<sup>-</sup> in different concentrations. The graphic shows bands at 100 kDa after staining with Anti-Nrf2 (ab63252) corresponding to activated nuclear Nrf2. Treatment for 1 h with SSNO<sup>-</sup> shows increased Nrf2 translocation to the nucleus in a concentration dependent manner. The second staining was made with Lamin A (ab8980) as a loading control. Slots were loaded with 15 μg protein.

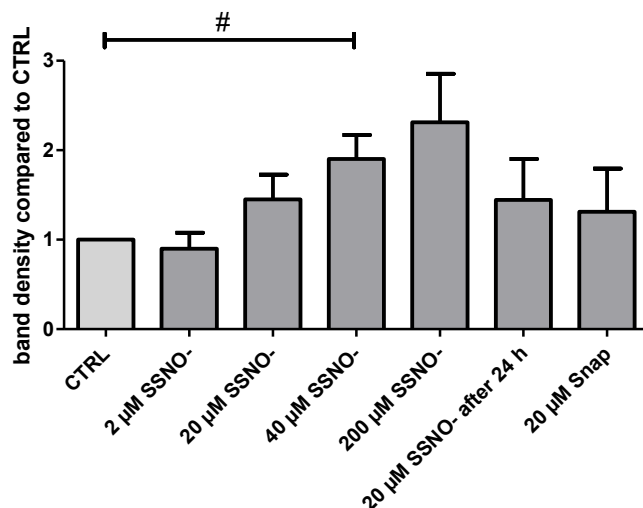


Fig. 41 Densitometry analysis of western blots of nuclear extracts from HUVECs treated with gassed SSNO<sup>-</sup> in concentrations from 2 μM up to 200 μM compared to CTRL and to 24h old SSNO<sup>-</sup>. The graphic shows the average band density of the treatments compared to control. Treatment for 1 h with gassed SSNO<sup>-</sup> showed up to 2.3 fold increased incidence of Nrf2 in the nucleus in a strongly concentration dependent manner. Scatter is shown as SEM (n=3). Statistical significance was tested by one tailed T-test (# indicates P<0.05).

In addition to ARE binding effects of increasing concentrations of SSNO<sup>-</sup> on mRNA expression of Hmox1 was detected by reverse transcription real time PCR. Ct values were compared by  $\Delta\Delta$ CT method. Fig. 42 shows the logarithmized CT values compared to housekeeping genes and compared to CTRL gene expression ( $\Delta\Delta$ CT) of Hmox1.

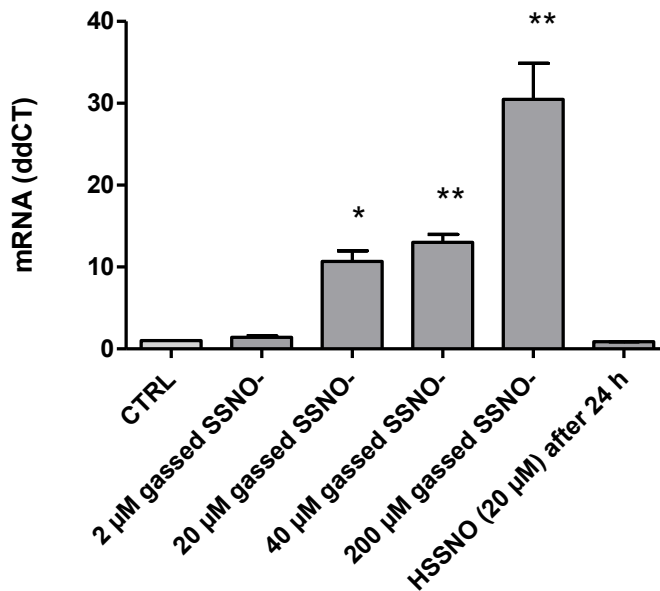


Fig. 42 Real time RT-PCR of RNA extracts from HUVECs treated for 6 h with SSNO<sup>-</sup> after gassing with nitrogen for 10 min. Cellular mRNA concentration was detected by real time RT-PCR (10 ng cDNA per well) using primers for Hmox1 (Hs01110250\_m1) as target genes and 18S (Hs03003631\_g1) as housekeeping gene. CT values were analyzed according to  $\Delta\Delta$ CT method. Each measurement was performed in duplicates. Scatter is shown as SEM. Statistical significance was tested by one-way ANOVA followed by Tukey post hoc multiple comparison test (n=3; \*P<0.05, \*\*P<0.01)

Treatment for 6 h with gassed SSNO<sup>-</sup> showed increased Hmox1 gene expression in a concentration dependent manner. Hmox1 mRNA levels were significantly increased 10.68 ±1.31 fold by 20 μM gassed SSNO<sup>-</sup>. At a concentration of 40 μM of gassed SSNO<sup>-</sup> Hmox1 expression was increased 13.01 ±0.97 fold and 30.48 ±4.39 fold at a concentration of 200 μM. Decomposed SSNO<sup>-</sup> (incubated for 24 h protected from light) did not affect Hmox1 expression.

## 4.8 Comparison of HS, NO and SSNO<sup>-</sup> effects on Nrf2 signaling

### 4.8.1 Nrf2 activation by nitroxyl, S-nitrosothiol, NO, sulfide and SSNO<sup>-</sup>

In order to compare the effect sizes on Nrf2 activation by nitroxyl, S-nitrosothiol, NO, sulfide and SSNO<sup>-</sup> mixtures raw data were normalized. ARE binding data were first compared to untreated control within the same experiment as  $\Delta\%$  of control [(sample-CTRL)/CTRL]. Hereafter data were pooled and rearranged for better comparability.

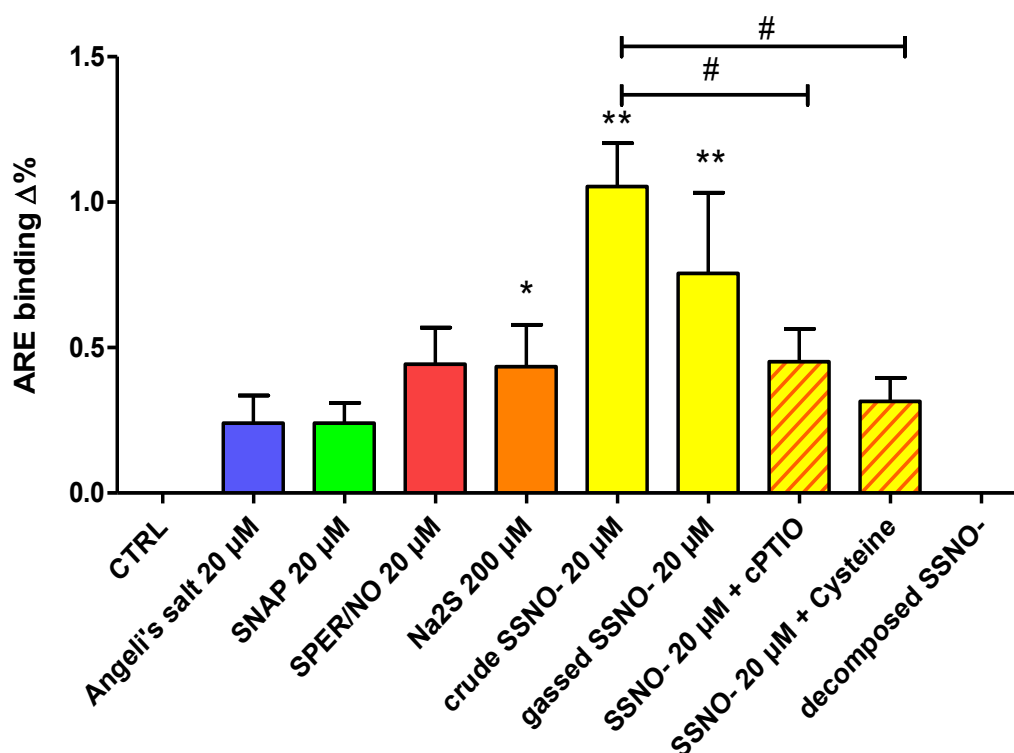


Fig. 43 Compared Nrf2 activation by nitroxyl, S-nitrosothiol, NO, sulfide and SSNO<sup>-</sup>. In order to compare the effect sizes on Nrf2 activation by nitroxyl, S-nitrosothiol, NO, sulfide and SSNO<sup>-</sup> mixtures raw data were normalized as  $\Delta\%$  of control [(sample-CTRL)/CTRL]. Hereafter data were pooled and rearranged for better comparability. Treatment of endothelial cells with SSNO<sup>-</sup> led to the strongest and most significant activation of Nrf2 among all substances analyzed. Each measurement was performed in duplicates. Scatter is shown as SEM. Statistical significance was tested by one-way ANOVA followed by Tukey post hoc multiple comparison test (n=3; \*P<0.05, \*\*P<0.01), or as T-test (# indicates P<0.05).

Treatment of endothelial cells with SSNO<sup>-</sup> led to the strongest and most significant activation of Nrf2 among all substances analyzed. Upon coincubation with a NO scavenger (cPTIO) and with millimolar concentrations of reducing thiols (cysteine) we found that SSNO<sup>-</sup> signaling is significantly decreased indicating that it is in large parts dependent on NO<sup>•</sup> release and polysulfide formation. By comparison to the effects of NO redox congeners we found NO<sup>-</sup> to exert only weak ARE binding indicating that the NO<sup>-</sup> donor SULFI/NO is unlikely to mediate SSNO<sup>-</sup> derived effects on Nrf2 signaling. As described before (chapter 4.5) sulfide alone only exerted effects on Nrf2 signaling at concentrations of more than 100  $\mu\text{M}$ .

#### 4.8.2 Hmox1 expression by nitroxyl, S-nitrosothiol, NO, sulfide and SSNO<sup>-</sup>

To compare Hmox1 expression by nitroxyl, S-nitrosothiol, NO, sulfide and SSNO<sup>-</sup> reverse transcription real time PCR was performed after 6 h treatment of HUVECs with all substances used. Data were first compared to housekeeping gene expression and then to untreated control expression using ( $\Delta\Delta\text{CT}$  method – see chapter 3.6 and 3.9). Hereafter all data were pooled for better comparability between experiments.

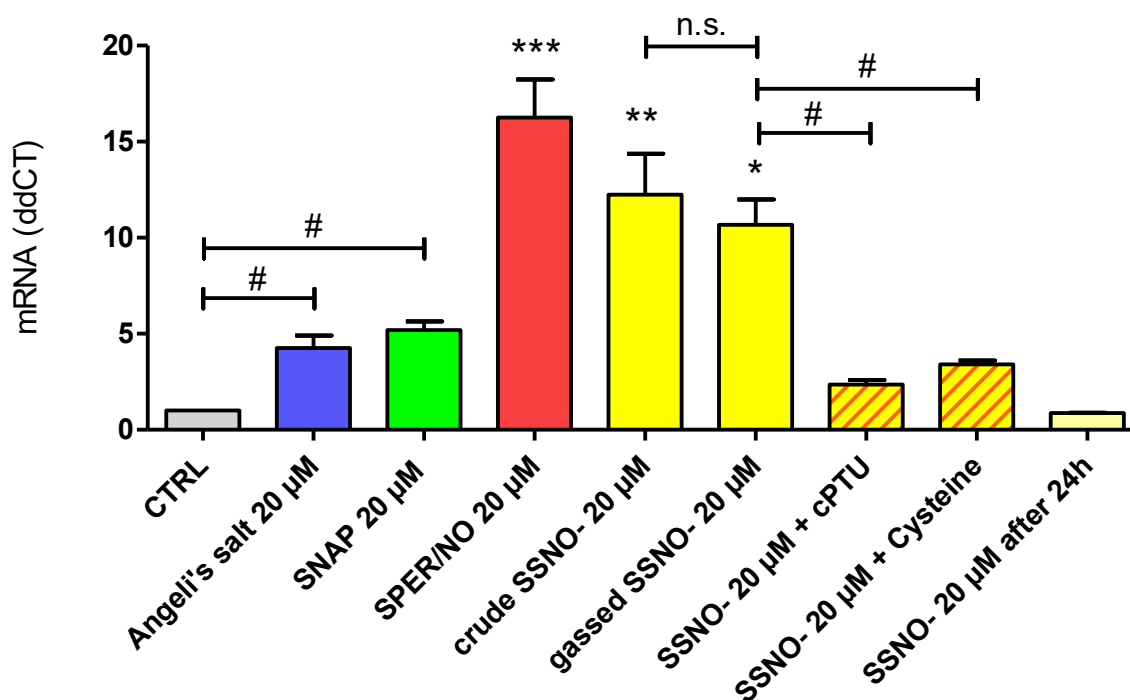


Fig. 44 compared Hmox1 expression by nitroxyl, S-nitrosothiol, NO, sulfide and SSNO<sup>-</sup>. Pooled data of real time RT-PCR of RNA extracts from HUVECs treated for 6 h with SSNO<sup>-</sup> mixes and NO redox congeners. Cellular mRNA concentration was detected by real time RT-PCR (10 ng cDNA per well) using primers for Hmox1 (Hs01110250\_m1) as target genes and 18S (Hs03003631\_g1) as housekeeping gene. CT values were analyzed according to  $\Delta\Delta\text{CT}$  method. Each measurement was performed in duplicates. Scatter is shown as SEM. Statistical significance was tested by one-way ANOVA followed by Tukey post hoc multiple comparison test (n=3; \*P<0.05, \*\*P<0.01) Additional direct comparison was performed by unpaired, two tailed t-test (# indicates P<0.05).

SPER/NO at a concentration of 20 μM showed the highest and significant increase in cellular mRNA levels of Hmox-1 (16.26 ± 1.97 fold expression compared to untreated control). Crude and gassed SSNO<sup>-</sup> also augmented Hmox1 gene expression significantly (12.25 ± 2.13 fold by 20 μM crude SSNO<sup>-</sup> and 10.68 ± 1.31 fold by 20 μM gassed SSNO<sup>-</sup>). Differences between crude and gassed SSNO<sup>-</sup> were not significant. Upon coincubation with cysteine Hmox1 gene expression was only increased 3.41 ± 0.19 fold and only 2.36 ± 0.22 fold with cPTIO. Differences between crude/gassed SSNO<sup>-</sup> and cysteine /cPTIO were significant in single comparison two-tailed T-tests.

Augmentations of cellular Hmox1 mRNA levels by Angeli's salt and SNAP were less potent and not significant in Tukey post hoc multiple comparison test, but in single comparison two-tailed T-tests compared to control ( $4.26 \pm 0.64$  fold expression by Angeli's salt vs.  $5.19 \pm 0.46$  fold expression by SNAP).

## 5 Discussion

### 5.1 Major findings

This study investigated on the role of Nrf2 signaling as a converging node in defense against redox induced damage in human primary endothelial cells. Since Keap1-Nrf2-interaction is a susceptible target of electrophiles and other redox active molecules this work aimed to compare the effects of (1) (-)-epicatechin, (2)  $\text{NO}^\cdot$ ,  $\text{NO}^-$  and  $\text{NO}^+$ , (3) sulfide, (4) the crosstalk of NO and sulfide and (5) nitrosopersulfide ( $\text{SSNO}^-$ ) on Nrf2 activation and translocation to the nucleus, ARE binding and transcription of phase II detoxifying enzymes. This led to the following major findings.

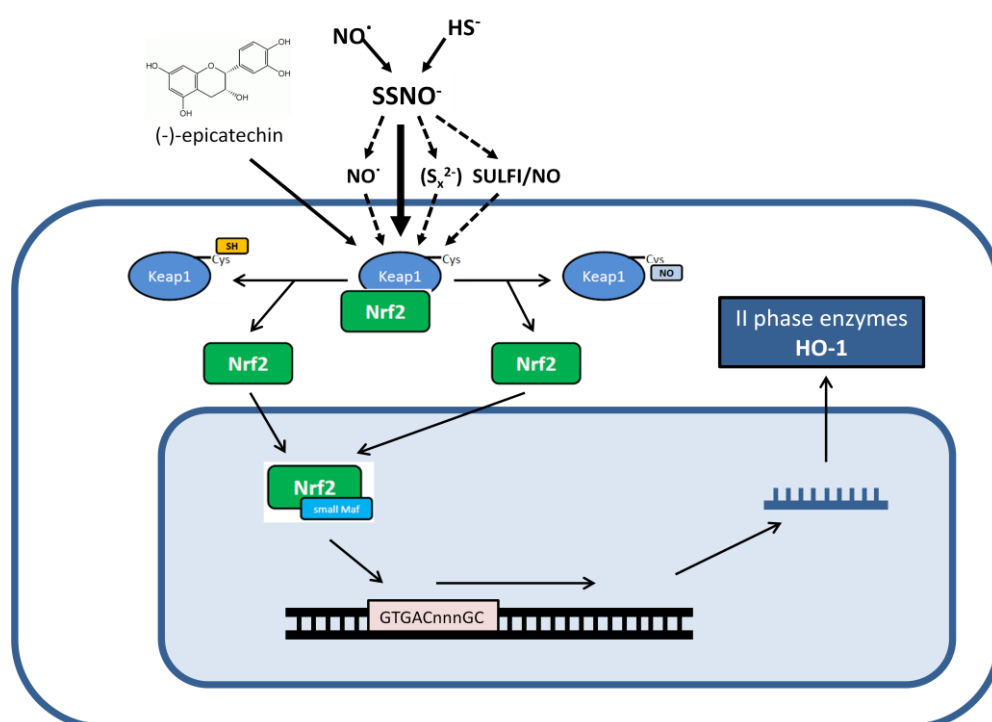


Fig. 45 major hypothesis - Nrf2 as a converging node of redox sensing and signaling in HUVECs induced by (-)-epicatechin, NO species, sulfide and S-nitrosothiols

1) (-)-epicatechin induced Nrf2 activation, translocation into the nucleus and ARE binding in human primary endothelial cells. In consequence transcription of Hmox1, Nqo1 and Gclc was augmented at low micromolar concentrations but very weak as compared to the other substances.

2)  $\text{NO}^\cdot$ ,  $\text{NO}^-$  and  $\text{NO}^+$  led to dose responsive and significantly increased nuclear Nrf2 levels and ARE binding as well as higher cellular Hmox1 levels. In direct comparison  $\text{NO}^\cdot$  (SPER/NO) had much stronger effects than its redox congeners.

3) Sulfide only affected Nrf2 activation, translocation and ARE binding in human primary endothelial cells at concentrations of >100  $\mu\text{M}$ . Exposure to  $\text{Na}_2\text{S}$  induced stronger Nrf2 activation than treatment with the slow sulfide releasing compound GYY 4137.

4) Crosstalk of NO and sulfide however led to diverging results. While the Nrf2 activation of the  $\text{NO}^+$  donor SNAP was attenuated by sulfide, co-incubation with sulfide did not affect  $\text{NO}^\cdot$  (SPER/NO and DEA/NO) derived Nrf2 activation.

5) Following the protocol of Cortese-Krott et al. (Cortese-Krott, Fernandez et al. 2014) stable solutions of  $\text{SSNO}^-$  were obtained monitored by UV-visible spectrophotometry and sulfide in excess was removed. Treatment of endothelial cells with  $\text{SSNO}^-$  led to the strongest and most significant activation of Nrf2 and transcription of Hmox1 mRNA among all substances analyzed.  $\text{SSNO}^-$  formation was recently described to be accompanied with dinitrososulfite formation ( $[\text{ONN}(\text{O})-\text{SO}_3]^{2-}$  or “SULFI/NO”). In addition, it releases NO and  $\text{S}_2^{2-}$  upon decomposition, which allows polysulfide ( $\text{S}_x^{2-}$ ) formation (Cortese-Krott, Kuhnle et al. 2015). Upon coincubation with NO scavengers (cPTIO) this work found that  $\text{SSNO}^-$  signaling is in large parts dependent on  $\text{NO}^\cdot$  release. Nrf2 binding activity and Hmox1 gene expression were also significantly decreased upon coincubation with millimolar concentrations of cysteine indicating that polysulfides contribute to Nrf2 activation of the  $\text{SSNO}^-$  mix. Taking the effects of NO redox congeners into consideration, it was found that  $\text{NO}^-$  only activates ARE binding very weakly indicating that the  $\text{NO}^-$  donor SULFI/NO is unlikely to mediate  $\text{SSNO}^-$  derived effects on Nrf2 signaling.

## **5.2 Methods measuring Nrf2 activation – advantages and limitations**

In this study Nrf2 signaling was measured at different sections of its pathway. First, Nrf2 translocation and activation were detected via transcription factor binding assays. DNA binding activity of Nrf2 is detected colorimetric with an ELISA-based kit allowing sensitive and specific quantification.

To obtain further specificity activated Nrf2 concentration was determined in nuclear extracts by western blotting. As suggested by Lau et al. (Lau, Tian et al. 2013) we compared bands at 100 kDa which is described to be the apparent molecular weight of Nrf2 in its biologically active form. Western blots were analyzed by densitometry for quantification using the software imageJ.

Downstream signaling was detected by reverse transcription real time PCR of Hmox1 mRNA to achieve better comparability to previous studies on Nrf2 signaling (Naughton, Hoque et al. 2002, Buckley, Marshall et al. 2003, Foresti, Hoque et al. 2003). Nqo1 and Gclc mRNA levels were determined additionally in some experiments.

To exclude influence of other signaling pathways gene silencing of Nrf2 and Keap1 (iNrf2) via siRNA transfection was planned. However, this could not yet be established for HUVECs (see chapter 4.2.3) and should be substance of subsequent studies. Nevertheless, Nrf2 could be identified to be a crucial factor in the surveyed signaling pathway.

## **5.3 Influence of (-)-epicatechin on Nrf2 signaling in human endothelial cells**

This study could show that (-)-epicatechin has a significant impact on Nrf2 signaling in HUVECs. Nrf2 activation and translocation to the nucleus could be detected in a concentration dependent fashion whereas cellular mRNA levels of phase II detoxifying enzymes (Hmox1, Gclc and Nqo1) showed highest increase upon treatment with micromolar concentrations.

These results indicate that Nrf2 signaling is triggered by (-)-epicatechin.

These effects are likely to emerge even at micromolar concentrations as shown after oral administration of flavanols (Ottaviani, Momma et al. 2011). For neurons and astrocytes Nrf2 activation and Hmox1 expression was already shown after treatment with (-)-epicatechin in cell culture (Bahia, Rattray et al. 2008) and animal experiments (Shah, Li et al. 2010). Effects could be abolished in Nrf2 knock-out mice (Shah, Li et al. 2010) indicating that Hmox1 expression was mainly induced by (-)-epicatechin dependent Nrf2 activation.

What seemed to be rather surprising in this study was to find maximum mRNA increase of Hmox1 levels upon treatment with 1  $\mu$ M (-)-epicatechin, whereas higher concentration had lower effects on transcription of phase II detoxifying enzymes. In contrast Nrf2 translocation followed (-)-epicatechin application in a concentration dependent manner. Nevertheless, these findings could be compared to those of Ramirez Sanchez et al. (Ramirez-Sanchez, Maya et al. 2010) who could find effects of (-)-epicatechin on eNOS activation and nitric oxide synthesis at low micromolar concentrations.

To distinguish whether Nrf2 plays the key role of protecting endothelial cells from oxidative stress Nrf2, Keap1 and Hmox-1 knockdown was planned to be performed by siRNA techniques. Since we were not yet able to establish successful knockdown for HUVECs (see chapter 4.2.3) this would be subject to subsequent studies.

However, since evidence that (-)-epicatechin accounts for Nrf2 activation in endothelial cells was missing so far this work gives an important new insight to the possible mechanisms of cellular signaling and antioxidant activity of (-)-epicatechin *in vitro* which might provide antioxidant and cytoprotective effects in the vasculature.

#### **5.4 Influence of nitroxyl, S-nitrosothiols and NO on Nrf2 signaling in human endothelial cells**

In this study activation of Nrf2 by nitroxyl, S-nitrosothiol and NO were compared in human primary endothelial cells. After treatment of HUVECs with chemicals releasing NO<sup>•</sup> (SPER/NO; DEA/NO), an S-nitrosothiol (SNAP) and a nitroxyl donor (Angeli's salt) quantitative analysis of ARE binding assays and reverse transcription real time PCR of phase II enzyme Hmox1 were performed. Hereby, treatment with SPER/NO showed the strongest increase in ARE binding (44% at 20  $\mu$ M and 105% at 100  $\mu$ M) and the most distinct increase in Hmox1 expression (16.26 fold expression at 20  $\mu$ M). Angeli's salt and SNAP also augmented Nrf2 activation in a concentration dependent fashion but in less potent way (24% at 20  $\mu$ M Angeli's salt and 24% at 20  $\mu$ M SNAP). Similar results were shown for Hmox1 expression (see chapter 4.4.1)

These findings go in line with other publications where NO and other nitrogen derivatives were already shown to activate Nrf2 signaling in different cell lines (Buckley, Marshall et al. 2003). Naughton et al. described interaction of heme with nitroxyl and nitric oxide leading to Nrf2 derived HO-1 augmentation in cardiac cells (Naughton, Hoque et al. 2002).

Also, a significant increase in Hmox1 mRNA levels could be shown after treatment of BAEC with SNAP, SNP and DETA/NO (Foresti, Hoque et al. 2003). SPER/NO was also found out to affect Nrf2 activation as well as HO-1 and total GSH levels in BAEC (Buckley, Marshall et al. 2003). Similar findings could be made by peroxyxynitrite releasing treatments of BAEC (Buckley and Whorton 2000) with SIN-1. In addition, NO<sup>•</sup> and peroxyxynitrite interaction with Nrf2 was described for macrophages (Abbas, Breton et al. 2011) and rat aortic SMC (Liu, Peyton et al. 2007).

However, Nrf2 activation by NO in human endothelial cells and direct comparison of the effects of NO<sup>•</sup>, NO<sup>-</sup> and NO<sup>+</sup> on Nrf2 signaling in the same cellular model was missing so far.

What seems rather surprising in this study is the weakly induced ARE binding and Hmox1 expression by the s-nitrosothiol SNAP. Since S-nitrosylation of Cys151 in Keap1 was reported to be a major mechanism of Nrf2 signaling (McMahon, Lamont et al. 2010), SNAP was expected to account for stronger effects.

There are limitations for comparability of the NO<sup>•</sup>, NO<sup>-</sup> and NO<sup>+</sup> donors used due to differences in mechanisms and kinetics of release. Nevertheless, differences observed in this study were distinct and significant enough to conclude that NO<sup>•</sup> is more potent in activating Nrf2 and inducing Hmox1 expression than its redox congeners NO<sup>-</sup> and NO<sup>+</sup>.

Taken together, this work showed Nrf2 activation and increase in cellular mRNA levels of phase II enzyme Hmox1 in HUVECs by all three substances. By direct comparison of NO<sup>•</sup>, NO<sup>-</sup> and NO<sup>+</sup> strongest effects were shown for SPER/NO indicating NO<sup>•</sup> to be the most potent Nrf2 activator of those three.

## **5.5 Influence of sulfide on Nrf2 signaling in human endothelial cells**

This study could show weak activation of Nrf2 by sulfide in human primary endothelial cells. By quantitative analysis of ARE binding assays and reverse transcription real time PCR this study compared Nrf2 activation and Hmox1 gene expression by Na<sub>2</sub>S and the slow sulfide releasing compound GYY 4137.

Both substances were found to be weak activators of Nrf2 signaling leading to increased ARE binding and Hmox1 expression but only at concentrations of 100μM and above. Noticeably, Na<sub>2</sub>S induced more Nrf2 signaling than the slow sulfide releasing agent GYY 4137, which showed only weak increase in ARE binding.

That seems rather surprising on first sight, since DeLeon and Olson reported limitations of direct sulfide application in cell culture experiments by volatilization and oxidation (Olson 2012) leading to a half-time of sulfide of 5 min in 24-well plates (measured by H<sub>2</sub>S polarographic electrode) (DeLeon, Stoy et al. 2012). Therefore we expected GYY 4137 to exert more influence on sulfide mediated effects than Na<sub>2</sub>S. However, taking in account that application of 200 μM Na<sub>2</sub>S leads to less than 40 μM of dissolved bioactive H<sub>2</sub>S under physiological conditions as calculated according to Olson (Olson 2012), the high concentrations of Na<sub>2</sub>S applied, which were necessary to have significant effects on Nrf2 signaling in the experimental settings of this study seem to be realistic in its biological environment and therefore transferable to *in vivo* models.

Findings of this study also go well in line with other publications. In hearts of mice treated with Na<sub>2</sub>S Calvert et al. described increased levels of nuclear Nrf2 and increased protein expression of thioredoxin and heme Hmox1 (Calvert, Jha et al. 2009). Since HS<sup>-</sup> has been reported to S-sulfhydrate cysteine residues in proteins (Mustafa, Gadalla et al. 2009) and since covalent modulation of cysteine residues in Keap1 lead to Nrf2 activation (Dinkova-Kostova, Holtzclaw et al. 2002) Nrf2 signaling makes a likely target of sulfide effects. Further studies could confirm sulfide-Keap1 interaction in mouse embryonic fibroblasts (MEF) (Hayes, Hourihan et al. 2012, Hourihan, Kenna et al. 2012) and could show increased mRNA expression of the modifier subunit of glutamate-cysteine ligase (GCLM), catalytic subunit of glutamate-cysteine ligase (GCLC), and glutathione reductase (GR) as well as increased levels of cellular GSH after treatment of MEF with Na<sub>2</sub>S.

Though, another approach of explaining Nrf2 activation by sulfide could be its capability of increasing NO bioavailability via 1) eNOS phosphorylation (Coletta, Papapetropoulos et al. 2012, Altaany, Yang et al. 2013) or 2) releasing NO<sup>•</sup> from S-nitrosothiols (Teng, Scott Isbell et al. 2008). Increased cellular NO levels after sulfide treatment might themselves account for Keap1 S-nitrosation (McMahon, Lamont et al. 2010) and Nrf2 activation.

Taken together the results of this study showed increased Nrf2 activation and mRNA expression of the phase II enzyme Hmox1 in human primary endothelial cells when treated with high concentrations of sulfide. Compared to the findings described in other studies we consider direct sulfide-Keap1 interaction via S-sulfhydration of cysteine residues in Keap1 the most likely mechanism of sulfide induced Nrf2 signaling in human endothelial cells. However, further comparisons of sulfide and NO interaction with Keap1 have to be made to distinguish direct sulfide-Keap1-interaction and indirect effects via increased cellular NO levels.

## 5.6 Comparison and Crosstalk of sulfide with NO

As discussed above this work could show that treatment with  $\text{NO}^\cdot$ ,  $\text{NO}^-$  and  $\text{NO}^+$  as well as with high concentrations of sulfide leads to Nrf2 activation and increased expression of cellular Hmox1 mRNA levels in HUVECs.

However, coincubation of sulfide with different NO redox congeners showed diverging effects.  $\text{NO}^\cdot$  donors (SPER/NO or DEA/NO) plus sulfide showed equipotent ARE binding as upon separate application, whereas effects of the S-nitrosothiol SNAP were attenuated by low sulfide concentrations. These findings suggest that there may be direct chemical interactions of S-nitrosothiols and sulfide leading to decreased reactivity towards cysteine residues of Keap1. In contrast,  $\text{NO}^\cdot$  and sulfide either do not interact chemically or form products that are equipotent to  $\text{NO}^\cdot$  in Keap1 inhibition.

Cortese-Krott et al. reported similar observation of the S-nitrosothiol/sulfide crosstalk. They found that NO and sulfide would inhibit each other in sGC activation in RFL-6 cells whenever concentrations of sulfide were lower than those of NO. In contrast, effects were increased if sulfide exceeded NO concentrations (Cortese-Krott, Fernandez et al. 2014). In the same publication they described formation of two compounds from NO sulfide reaction. They reported that HSNO and its deprotonated form  $\text{SNO}^-$  were formed when concentrations of sulfide were lower than those of NO. In case of sulfide exceeding concentrations of NO nucleophilic attacks of sulfide became more dominant leading to formation of nitrosopersulfide ( $\text{SSNO}^-$ ) as shown by UV-visible spectroscopy and mass spectrometry. They supposed that HSNO was not able to deliver sufficient amounts of NO to activate sGC. Therefore low concentrations of sulfide inhibit NO effects. On the other hand  $\text{SSNO}^-$  could be shown to release significant amounts of  $\text{NO}^\cdot$  and exert  $\text{NO}^\cdot$  mediated effects (Cortese-Krott, Fernandez et al. 2014).

Taken together this study could show that (1) especially at low concentrations  $\text{NO}^\cdot$  is a more potent activator of Nrf2 than S-nitrosothiols, nitroxyl and sulfide and (2) Effects of S-nitrosothiols on Nrf2 activation in endothelial cells are inhibited upon coincubation with low sulfide concentrations. The later result goes well in line with the findings of Cortese-Krott et al. who reported similar effects of a NO-sulfide crosstalk on sGC activation in RFL-6 cells. Therefore, direct chemical interaction of sulfide and NO appears to be a likely explanation for their interdependent effects and further studies on HSNO/ $\text{SNO}^-$  and  $\text{SSNO}^-$  formation should be done.

## 5.7 Formation of SSNO<sup>-</sup> and influence on Nrf2 signaling

In this study SSNO<sup>-</sup> was synthesized from sulfide and the S-nitrosothiol SNAP at physiological conditions monitored by UV–visible spectroscopy following the protocol of Cortese-Krott et al. (Cortese-Krott, Fernandez et al. 2014). HUVECs were incubated with the obtained SSNO<sup>-</sup> mixtures to investigate on their biological effects.

Hereby this work showed (1) a concentration dependent activation of Nrf2 by SSNO<sup>-</sup> mix in ARE binding assays, western blots of nuclear extracts and Hmox1 gene expression; (2) SSNO<sup>-</sup> induced Nrf2 binding activity significantly stronger than NO and/or sulfide whereas expression of Hmox1 mRNA levels by SSNO<sup>-</sup> was increased equipotent to NO<sup>•</sup> (3) Effects on Nrf2 activation by crude SSNO<sup>-</sup> showed no significant difference to the effects of the SSNO<sup>-</sup> mixture where sulfide in excess was removed by gassing with N<sub>2</sub> (4) Effects of SSNO<sup>-</sup> on Nrf2 binding activity and Hmox1 expression were strongly attenuated by coincubation with NO scavenger cPTIO and in presence of 1 mM cysteine (L-Cys).

### 5.7.1 SSNO<sup>-</sup> increases Nrf2 binding activity and Hmox1 gene expression in human endothelial cells

While SSNO<sup>-</sup> was recently characterized as a strong NO<sup>•</sup> releasing agent and therefore a potent vasodilator *in vivo* and *in vitro* (Berenyiova, Grman et al. 2015, Cortese-Krott, Kuhnle et al. 2015) this study was the first one to investigate on its influence on redox signaling in endothelial cells. Hereby Keap1-Nrf2-interaction could be identified as a very susceptible target of the reaction product of sulfide and NO<sup>•</sup>. This work showed that treatment of HUVECs with SSNO<sup>-</sup> leads to a significant and concentration dependent translocation and activation of Nrf2, which then leads to a significant and concentration dependent increase in Hmox1 gene expression. These findings add a whole new spectrum of transcriptional signaling to the characteristics of SSNO<sup>-</sup> and it must be of great interest to elucidate the underlying molecular mechanism, since also byproducts of SSNO<sup>-</sup> formation and decomposition might contribute to its effects on Nrf2 due to their chemical characteristics.

As described by Seel and Wagner and by Cortese et al. SSNO<sup>-</sup> formation from NO/S-nitrosothiols and sulfide is accompanied by formation of dinitrososulfite ([ONN(O)–SO<sub>3</sub>]<sup>2-</sup> or “SULFI/NO”) at physiological pH (Seel and Wagner 1988, Cortese-Krott, Kuhnle et al. 2015). Additionally SSNO<sup>-</sup> decomposes to NO<sup>•</sup> and persulfides, of which the later lead to formation of polysulfides (S<sub>x</sub><sup>2-</sup>), colloidal sulfur (S<sub>8</sub>) and sulfide (Cortese-Krott, Kuhnle et al. 2015).

Since all of those substances were described to effect Nrf2 activation (McMahon, Lamont et al. 2010, Kimura 2014) or are at least able to interact with cysteine residues of Keap1 it was necessary to distinguish to what amount each of them contributes to the SSNO<sup>-</sup> mediated effects.

### **5.7.2 Sulfide in excess does not contribute to SSNO<sup>-</sup> mediated effects on Nrf2**

Amongst all substances analyzed in this work SSNO<sup>-</sup> showed the strongest and most significant increase in Nrf2 activation. Therefore it is of great interest how these effects are mediated. Since this study amongst others (Calvert, Jha et al. 2009, Hayes, Hourihan et al. 2012, Yang, Zhao et al. 2013) showed that sulfide at concentrations of >100 μM increases ARE binding it was important to identify whether excess sulfide, which was necessary as an educt of SSNO<sup>-</sup> formation, is accounting for Nrf2 activation.

By gassing the solution with N<sub>2</sub> for 10 minutes sulfide could be completely remove from the SSNO<sup>-</sup> mixture as described in Cortese-Krott et al. 2014 and in chapter 3.3. This gassed SSNO<sup>-</sup> solution had the same impact on both Nrf2 activation and Hmox1 expression with no significant differences to crude SSNO<sup>-</sup>. Thus, excess sulfide is not likely to mediate SSNO<sup>-</sup> derived effects.

### **5.7.3 SULFI/NO is not likely to account for SSNO<sup>-</sup> derived effects on Nrf2 signaling**

In this study, nitroxyl exerted very weak effects on Nrf2 signaling in HUVECs as compared to treatment with NO donors like SPER/NO and DEA/NO or the SSNO<sup>-</sup> mixture (see chapter 4.8.1). Treatment of endothelial cells with the potent nitroxyl donor Angeli's salt only lead to weak increases in Nrf2 binding activity or in Hmox1 gene expression as compared to its redox congeners.

SULFI/NO has been described as a weak nitroxyl and a very weak NO<sup>•</sup> donor in comparison to DEA/NO and Angeli's salt (Cortese-Krott, Kuhnle et al. 2015). Therefore, the small S/N hybrid molecule was not able to exert NO<sup>•</sup> mediated biological effects on cellular cGMP levels. These effects could only be induced after nitroxyl was converted to NO<sup>•</sup> by addition of superoxide dismutase (SOD).

In conclusion, SULFI/NO has already been shown to exert its effects mainly by nitroxyl release. This work, however, could show that nitroxyl only exerts weak effects on Nrf2 binding activity and on Hmox1 gene expression. Therefore, effects of the SSNO<sup>-</sup> mixture on Nrf2 activation are unlikely mediated by the weak nitroxyl donor SULFI/NO although subsequent experiments, in which SULFI/NO is administered directly to the cells, should be made to confirm this.

#### 5.7.4 Nitric oxide plays a crucial role in SSNO<sup>-</sup> signaling

This study showed that NO<sup>·</sup> is a distinct activator of Nrf2 in human endothelial cells as compared to other NO redox congeners and sulfide (see chapter 4.4). Treatment of HUVECs with SPER/NO increased Nrf2 binding activity and Hmox1 gene expression significantly. Comparing the effects of SSNO<sup>-</sup> and SPER/NO we find that SSNO<sup>-</sup> is more potent in Nrf2 activation whereas SPER/NO was equipotent in increasing expression of Hmox1 mRNA. A possible reason for this might be Hmox1 mRNA stabilization by NO, which was described for human fibroblast cells (Bouton and Demple 2000).

Additionally, this work showed that SSNO<sup>-</sup> mediated effects on ARE binding were strongly attenuated upon coincubation with the NO<sup>·</sup> scavenger cPTIO and Hmox1 expression was almost completely abolished. These findings suggest that NO<sup>·</sup> accounts for large parts of SSNO<sup>-</sup> bioactivity.

Cortese-Krott et al. characterized SSNO<sup>-</sup> as a potent NO<sup>·</sup> donor as assessed by chemiluminescence. Besides, they could show NO<sup>·</sup> (released by SSNO<sup>-</sup>) mediated effects on sGC in RFL-6 cells and reported decreases in blood pressure after acute administration of SSNO<sup>-</sup> to rats (Cortese-Krott, Kuhnle et al. 2015). Effects of SSNO<sup>-</sup> on cGMP levels were abolished upon coincubation with the NO<sup>·</sup> scavenger cPTIO and the inhibitor of sGC ODT indicating that these effects are mediated by NO<sup>·</sup>.

Berenyiova et al. (Berenyiova, Grman et al. 2015) were also able to show biological effects of the NO/HS crosstalk. Following the procedure of Cortese-Krott et al. (Cortese-Krott, Fernandez et al. 2014) they prepared solutions from GSNO and Na<sub>2</sub>S. By measuring relaxation of precontracted isolated rings of rat thoracic aorta they described a more than twofold higher potency of the reaction products than the one of the educts GSNO and sulfide by themselves (Berenyiova, Grman et al. 2015). They also described attenuation of these effects by sGC inhibition via ODQ and by nitric oxide scavenging via cPTIO whereas prior acidification or coincubation with N-acetylcysteine (1 mM) or methemoglobin (20 μM heme) lead to almost complete abolishment of the effects on vasodilation (Berenyiova, Grman et al. 2015). These findings also suggest that the observed effects are in large parts dependent of NO released by SSNO<sup>-</sup>.

Taken together, this work and other publications showed that (1) SSNO<sup>-</sup> is a potent NO<sup>•</sup> donor upon decomposition (Seel and Wagner 1988, Cortese-Krott, Kuhnle et al. 2015), (2) NO<sup>•</sup> accounts for major parts of SSNO<sup>-</sup> bioactivity on sGC activation (Berenyiova, Grman et al. 2015, Cortese-Krott, Kuhnle et al. 2015) and (3) this study showed that SSNO<sup>-</sup> effects on Nrf2 activation and Hmox1 gene expression are significantly attenuated upon coincubation with NO<sup>•</sup> scavengers. Therefore, NO<sup>•</sup> release emerges to play a key role in mediating effects of SSNO<sup>-</sup> on Nrf2 signaling.

#### **5.7.5 Polysulfides contribute to SSNO<sup>-</sup> derived effects on Nrf2 signaling**

In recent studies polysulfides were described as potential signaling molecules able to modulate proteins via S-sulfhydration (Kimura 2014). Since Keap1 was also described to be a target of S-sulfhydration (Yang, Zhao et al. 2013) polysulfides might as well contribute to Nrf2 activation by the SSNO<sup>-</sup> mixture.

To investigate on the influence of polysulfides endothelial cells were coincubated with the SSNO<sup>-</sup> mix and 1 mM of cysteine. Millimolar amounts of reducing thiols were described to mediate polysulfide decomposition without affecting SSNO<sup>-</sup> decomposition (Cortese-Krott, Kuhnle et al. 2015).

Hereby Nrf2 binding activity and Hmox1 gene expression by SSNO<sup>-</sup> were significantly reduced. These findings indicate that polysulfides also account for SSNO<sup>-</sup> mediated Nrf2 activation.

#### **5.7.6 What does account for SSNO<sup>-</sup> derived signaling?**

Taken together these findings show activation of Nrf2 by SSNO<sup>-</sup> the reaction products of nitric oxide and sulfide. Interference by the presence of sulfide in excess could be excluded by complete removal of sulfide from the solution. Since there are three main bioactive reaction products of NO and sulfide (SSNO<sup>-</sup>, SULFI/NO and polysulfides) this work aimed to compare effects of the obtained solution to effects of their educts and NO redox congeners. As displayed here (1) SULFI/NO is unlikely to mediate the effects on Nrf2 signaling, since it is a weak NO<sup>•</sup> donor and Angeli's salt (a more potent NO<sup>•</sup> releasing agent) was a very weak Nrf2 activator compared to the SSNO<sup>-</sup> mix. (2) NO<sup>•</sup> accounts for large parts of Nrf2 activation by SSNO<sup>-</sup>, which was characterized as a potent NO<sup>•</sup> donor. Effects on Hmox1 mRNA levels by SSNO<sup>-</sup> were equipotent to those of the NO<sup>•</sup> donor SPER/NO and were significantly attenuated by application of the NO<sup>•</sup> scavenger cPTIO. Activation of Nrf2 and translocation to the nucleus was also attenuated by cPTIO. (3) Polysulfides contribute to Nrf2 activation by the SSNO<sup>-</sup> mix since ARE binding and phase II gene expression are significantly decreased when polysulfides are decomposed upon coincubation with millimolar concentrations of cysteine.

## 5.8 Could SSNO<sup>-</sup> be formed endogenously and exert effects on Nrf2 *in vivo*?

In this study Keap1-Nrf2-interaction was shown to be a susceptible target of SSNO<sup>-</sup> and its decomposition products in human endothelial cells. Since Nrf2 is considered as a key major switch in redox and stress signaling, and since SSNO<sup>-</sup> emerges to influence endothelial redox homeostasis, there is great importance to the question whether SSNO<sup>-</sup> is likely to be formed *in vivo*.

To answer this question Cortese-Krott et al. proposed that it is worth to have a look at the reaction of superoxide (O<sub>2</sub><sup>•-</sup>) with NO<sup>•</sup>. This radical-radical reaction occurs at a rate close to the diffusion-controlled limit and leads to formation of peroxynitrite (<sup>-</sup>OONO), which is the oxygen analogon of SSNO<sup>-</sup> and therefore shares many biochemical characteristics. They described that discovery of enzymes generating O<sub>2</sub><sup>•-</sup> in proximity to endogenous sources of NO<sup>•</sup> provided the biochemical premises that peroxynitrite acts as a signaling molecule although previously it was considered too unstable and unlikely to be formed in tissues as described in more detail in Cortese-Krott, Butler et al. (2016) and references therein.



In the same publication Cortese-Krott et al. speculated that in parallel to peroxynitrite, SSNO<sup>-</sup> might be formed by a radical-radical reaction *in vivo* since it is in equilibrium with its products of homolysis S<sub>2</sub><sup>•-</sup> and NO<sup>•</sup> (see equation 2). This source of SSNO<sup>-</sup> appears to be likely since cysteine persulfides and glutathione persulfides serve as possible precursors and were found in micromolar concentrations in tissues (Ida, Sawa et al. 2014). Assuming this formation close to effects sites and increased local availability SSNO<sup>-</sup> would be able to act as a signaling molecule *in vivo*. Therefore, finding methods to detect SSNO<sup>-</sup> or its precursors and decomposition product S<sub>2</sub><sup>•-</sup> *in vitro* and *in vivo* poses the next challenge to be solved.

## 5.9 Conclusion, significance and outlook

Nitric oxide has unique biochemical characteristics that enable it to be an eligible signaling molecule and provide large scope to interact with other small molecules (Hill, Dranka et al. 2010). So does sulfide, which was also shown to be interacting and interdependent on NO. These special characteristics and their involvements in each other explain the recently growing interest in gasotransmitter signaling and imply a complex interplay that is currently under expanded investigation. Crosstalk of sulfide and NO<sup>•</sup> or S-nitrosothiols is especially interesting since very recently there are many reactive and biologically active reaction products described such as SNO<sup>-</sup>, SSNO<sup>-</sup>, SULFI/NO or polysulfides (Cortese-Krott, Fernandez et al. 2014, Cortese-Krott, Kuhnle et al. 2015) that still need to be further studied.

Nrf2 is abundant in almost all tissues and cells of the human body (Chan, Han et al. 1993, Moi, Chan et al. 1994, McMahon, Itoh et al. 2001) and considered to play a crucial role in mediating antioxidant response (Kobayashi and Yamamoto 2006) and therefore maintaining redox homeostasis. Since both nitric oxide (Naughton, Hoque et al. 2002) and sulfide (Calvert, Jha et al. 2009) were described to activate Nrf2-Keap1-signaling, this pathway is established as a converging node of gasotransmitter and electrophile sensing and signaling.

This study provided novel direct comparison of Nrf2 activation by electrophiles, nitric oxide, hydrogen sulfide and its reaction product SSNO<sup>-</sup> in endothelial cells.

Taken together we find proof that among all substances under investigation NO<sup>•</sup> and SSNO<sup>-</sup> exert the most distinct effects on Nrf2 signaling whereas effects of SSNO<sup>-</sup> are likely to be mediated by its products of homolysis NO<sup>•</sup> and S<sub>2</sub><sup>•-</sup>. Therefore, these molecules emerge to play a key role in NO and sulfide derived redox signaling. While NO<sup>•</sup> is already established as a signaling molecule SSNO<sup>-</sup> was only recently discovered and endogenous sources, metabolism and concentrations *in vivo* must still be elucidated. However, as described by Cortese-Krott et al. (see chapter 5.8) endogenous formation of SSNO<sup>-</sup> might occur as radical-radical reactions in parallel to <sup>-</sup>OONO since sources of S<sub>2</sub><sup>•-</sup> are available *in vivo*, even close to effect sites.

Therefore, SSNO<sup>-</sup> might come out as an important endogenous mediator of NO<sup>•</sup> and sulfide effects on Nrf2 signaling in the future. Thus, finding methods to detect SSNO<sup>-</sup> or its precursors or decomposition product S<sub>2</sub><sup>•-</sup> poses the next challenge to be solved.

The molecular mechanisms of Keap1 modification by SSNO<sup>-</sup> should also be subject to future research. Since SSNO<sup>-</sup> signaling was shown to involve NO<sup>•</sup> and polysulfides in this study, it is of great interest whether cysteine residues are target of S-nitrosation or S-sulfhydration. Both mechanisms have been described previously and are should be eligible for SSNO<sup>-</sup> signaling.



## 6 Literature

- Abbas, K., J. Breton, A.-G. Planson, C. Bouton, J. Bignon, C. Seguin, S. Riquier, M. B. Toledano and J.-C. Drapier (2011). "Nitric oxide activates an Nrf2/sulfiredoxin antioxidant pathway in macrophages." Free Radical Biology and Medicine **51**(1): 107-114.
- Ali, M. Y., C. Y. Ping, Y. Y. Mok, L. Ling, M. Whiteman, M. Bhatia and P. K. Moore (2006). "Regulation of vascular nitric oxide in vitro and in vivo; a new role for endogenous hydrogen sulphide?" Br J Pharmacol **149**(6): 625-634.
- Altaany, Z., G. Yang and R. Wang (2013). "Crosstalk between hydrogen sulfide and nitric oxide in endothelial cells." Journal of cellular and molecular medicine.
- Andersen, J. K. (2004). "Oxidative stress in neurodegeneration: cause or consequence?" Nature Medicine **10 Suppl**: S18-25.
- Bahia, P. K., M. Rattray and R. J. Williams (2008). "Dietary flavonoid (-)epicatechin stimulates phosphatidylinositol 3-kinase-dependent anti-oxidant response element activity and up-regulates glutathione in cortical astrocytes." Journal of Neurochemistry **106**(5): 2194-2204.
- Baird, L. and A. T. Dinkova-Kostova (2011). "The cytoprotective role of the Keap1-Nrf2 pathway." Arch Toxicol **85**(4): 241-272.
- Berenyiova, A., M. Grman, A. Mijuskovic, A. Stasko, A. Misak, P. Nagy, E. Ondriasova, S. Cacanyiova, V. Brezova, M. Feelisch and K. Ondrias (2015). "The reaction products of sulfide and S-nitrosoglutathione are potent vasorelaxants." Nitric Oxide: Biology and Chemistry / Official Journal of the Nitric Oxide Society **46**: 123-130.
- Bouton, C. and B. Demple (2000). "Nitric oxide-inducible expression of heme oxygenase-1 in human cells. Translation-independent stabilization of the mRNA and evidence for direct action of nitric oxide." J Biol Chem **275**(42): 32688-32693.
- Bradford, M. M. (1976). "A rapid and sensitive method for the quantitation of microgram quantities of protein utilizing the principle of protein-dye binding." Anal Biochem **72**: 248-254.
- Bredt, D. S. and S. H. Snyder (1990). "Isolation of nitric oxide synthetase, a calmodulin-requiring enzyme." Proc Natl Acad Sci U S A **87**(2): 682-685.
- Brossette, T., C. Hundsdörfer, K.-D. Kröncke, H. Sies and W. Stahl (2011). "Direct evidence that (-)-epicatechin increases nitric oxide levels in human endothelial cells." European journal of nutrition **50**(7): 595-599.
- Buckley, B. J., Z. M. Marshall and A. R. Whorton (2003). "Nitric oxide stimulates Nrf2 nuclear translocation in vascular endothelium." Biochemical and Biophysical Research Communications **307**(4): 973-979.
- Buckley, B. J. and A. R. Whorton (2000). "Adaptive responses to peroxynitrite: increased glutathione levels and cystine uptake in vascular cells." American Journal of Physiology - Cell Physiology **279**(4): C1168-C1176.
- Calvert, J. W., S. Jha, S. Gundewar, J. W. Elrod, A. Ramachandran, C. B. Pattillo, C. G. Kevil and D. J. Lefer (2009). "Hydrogen sulfide mediates cardioprotection through Nrf2 signaling." Circulation research **105**(4): 365-374.
- Canning, P., F. J. Sorrell and A. N. Bullock (2015). "Structural basis of KEAP1 interactions with Nrf2." Free Radic Biol Med.
- Chan, J. Y., X. L. Han and Y. W. Kan (1993). "Isolation of cDNA encoding the human NF-E2 protein." Proceedings of the National Academy of Sciences of the United States of America **90**(23): 11366-11370.
- Chang, C.-F., S. Cho and J. Wang (2014). "(-)-Epicatechin protects hemorrhagic brain via synergistic Nrf2 pathways." Annals of Clinical and Translational Neurology **1**(4): 258-271.
- Chen, Y. T., R. L. Zheng, Z. J. Jia and Y. Ju (1990). "Flavonoids as superoxide scavengers and antioxidants." Free Radical Biology & Medicine **9**(1): 19-21.

Cleasby, A., J. Yon, P. J. Day, C. Richardson, I. J. Tickle, P. A. Williams, J. F. Callahan, R. Carr, N. Concha, J. K. Kerns, H. Qi, T. Sweitzer, P. Ward and T. G. Davies (2014). "Structure of the BTB domain of Keap1 and its interaction with the triterpenoid antagonist CDDO." PLoS One **9**(6): e98896.

Cohen, M. V., X. M. Yang and J. M. Downey (2006). "Nitric oxide is a preconditioning mimetic and cardioprotectant and is the basis of many available infarct-sparing strategies." Cardiovasc Res **70**(2): 231-239.

Coletta, C., A. Papapetropoulos, K. Erdelyi, G. Olah, K. Módis, P. Panopoulos, A. Asimakopoulou, D. Gerö, I. Sharina, E. Martin and C. Szabo (2012). "Hydrogen sulfide and nitric oxide are mutually dependent in the regulation of angiogenesis and endothelium-dependent vasorelaxation." Proceedings of the National Academy of Sciences of the United States of America **109**(23): 9161-9166.

Cooper, C. E. and C. Giulivi (2007). "Nitric oxide regulation of mitochondrial oxygen consumption II: Molecular mechanism and tissue physiology." Am J Physiol Cell Physiol **292**(6): C1993-2003.

Cortese-Krott, M. M., A. R. Butler, J. D. Woollins and M. Feelisch (2016). "Inorganic sulfur-nitrogen compounds: from gunpowder chemistry to the forefront of biological signaling." Dalton Trans **45**(14): 5908-5919.

Cortese-Krott, M. M., B. O. Fernandez, M. Kelm, A. R. Butler and M. Feelisch (2015). "On the chemical biology of the nitrite/sulfide interaction." Nitric Oxide: Biology and Chemistry / Official Journal of the Nitric Oxide Society **46**: 14-24.

Cortese-Krott, M. M., B. O. Fernandez, J. L. T. Santos, E. Mergia, M. Grman, P. Nagy, M. Kelm, A. Butler and M. Feelisch (2014). "Nitrosopersulfide (SSNO(-)) accounts for sustained NO bioactivity of S-nitrosothiols following reaction with sulfide." Redox biology **2**: 234-244.

Cortese-Krott, M. M., G. G. Kuhnle, A. Dyson, B. O. Fernandez, M. Grman, J. F. DuMond, M. P. Barrow, G. McLeod, H. Nakagawa, K. Ondrias, P. Nagy, S. B. King, J. E. Saavedra, L. K. Keefer, M. Singer, M. Kelm, A. R. Butler and M. Feelisch (2015). "Key bioactive reaction products of the NO/H<sub>2</sub>S interaction are S/N-hybrid species, polysulfides, and nitroxyl." Proc Natl Acad Sci U S A **112**(34): E4651-4660.

Cortese-Krott, M. M., A. Rodriguez-Mateos, R. Sansone, G. G. Kuhnle, S. Thasian-Sivarajah, T. Krenz, P. Horn, C. Krisp, D. Wolters, C. Heiss, K. D. Kroncke, N. Hogg, M. Feelisch and M. Kelm (2012). "Human red blood cells at work: identification and visualization of erythrocytic eNOS activity in health and disease." Blood **120**(20): 4229-4237.

Cortese-Krott, M. M., C. V. Suschek, W. Wetzel, K.-D. Kröncke and V. Kolb-Bachofen (2009). "Nitric oxide-mediated protection of endothelial cells from hydrogen peroxide is mediated by intracellular zinc and glutathione." American journal of physiology. Cell physiology **296**(4): C811-820.

Cortese, M. M., C. V. Suschek, W. Wetzel, K.-D. Kröncke and V. Kolb-Bachofen (2008). "Zinc protects endothelial cells from hydrogen peroxide via Nrf2-dependent stimulation of glutathione biosynthesis." Free Radical Biology and Medicine **44**(12): 2002-2012.

DeLeon, E. R., G. F. Stoy and K. R. Olson (2012). "Passive loss of hydrogen sulfide in biological experiments." Anal Biochem **421**(1): 203-207.

Denninger, J. W. and M. A. Marletta (1999). "Guanylate cyclase and the .NO/cGMP signaling pathway." Biochim Biophys Acta **1411**(2-3): 334-350.

Dhakshinamoorthy, S., A. K. Jain, D. A. Bloom and A. K. Jaiswal (2005). "Bach1 competes with Nrf2 leading to negative regulation of the antioxidant response element (ARE)-mediated NAD(P)H:quinone oxidoreductase 1 gene expression and induction in response to antioxidants." J Biol Chem **280**(17): 16891-16900.

Dhakshinamoorthy, S., D. J. Long and A. K. Jaiswal (2000). "Antioxidant regulation of genes encoding enzymes that detoxify xenobiotics and carcinogens." Current Topics in Cellular Regulation **36**: 201-216.

Dinkova-Kostova, A. T., W. D. Holtzclaw, R. N. Cole, K. Itoh, N. Wakabayashi, Y. Katoh, M. Yamamoto and P. Talalay (2002). "Direct evidence that sulfhydryl groups of Keap1 are the sensors regulating induction of phase 2 enzymes that protect against carcinogens and oxidants." Proc Natl Acad Sci U S A **99**(18): 11908-11913.

Dinkova-Kostova, A. T., M. A. Massiah, R. E. Bozak, R. J. Hicks and P. Talalay (2001). "Potency of Michael reaction acceptors as inducers of enzymes that protect against carcinogenesis depends on their reactivity with sulfhydryl groups." Proc Natl Acad Sci U S A **98**(6): 3404-3409.

Du, J., Y. Hui, Y. Cheung, G. Bin, H. Jiang, X. Chen and C. Tang (2004). "The possible role of hydrogen sulfide as a smooth muscle cell proliferation inhibitor in rat cultured cells." Heart Vessels **19**(2): 75-80.

DuMond, J. F. and S. B. King (2011). "The chemistry of nitroxyl-releasing compounds." Antioxid Redox Signal **14**(9): 1637-1648.

Filipovic, M. R., J. L. Miljkovic, T. Nauser, M. Royzen, K. Klos, T. Shubina, W. H. Koppenol, S. J. Lippard and I. Ivanović-Burmazović (2012). "Chemical characterization of the smallest S-nitrosothiol, HSNO; cellular cross-talk of H<sub>2</sub>S and S-nitrosothiols." Journal of the American Chemical Society **134**(29): 12016-12027.

Fink, G. and Fink (2000). Encyclopedia of Stress, Three-Volume Set.

Foresti, R., M. Hoque, S. Bains, C. J. Green and R. Motterlini (2003). "Haem and nitric oxide: synergism in the modulation of the endothelial haem oxygenase-1 pathway." The Biochemical Journal **372**(Pt 2): 381-390.

Fraga, C. G. and P. I. Oteiza (2011). "Dietary flavonoids: Role of (-)-epicatechin and related procyanidins in cell signaling." Free Radical Biology & Medicine **51**(4): 813-823.

Fukutomi, T., K. Takagi, T. Mizushima, N. Ohuchi and M. Yamamoto (2014). "Kinetic, thermodynamic, and structural characterizations of the association between Nrf2-DLGex degron and Keap1." Mol Cell Biol **34**(5): 832-846.

Goehring, M. and J. Messner (1950). "Zur Kenntnis der schwefligen Säure. III Das Sulfinimid und seine Isomeren." Zeitschrift für anorganische und allgemeine Chemie **268**(1-2): 47-56.

Haenen, G. R., J. B. Paquay, R. E. Korthouwer and A. Bast (1997). "Peroxyxynitrite scavenging by flavonoids." Biochemical and Biophysical Research Communications **236**(3): 591-593.

Haigis, M. C. and B. A. Yankner (2010). "The aging stress response." Molecular Cell **40**(2): 333-344.

Hayes, J. D., J. M. Hourihan and J. G. Kenna (2012). "The gasotransmitter hydrogen sulfide induces Nrf2-target genes by inactivating the Keap1 ubiquitin ligase substrate adaptor through formation of a disulfide bond between Cys-226 and Cys-613." Antioxidants & redox signaling.

Hill, B. G., B. P. Dranka, S. M. Bailey, J. R. Lancaster, Jr. and V. M. Darley-Usmar (2010). "What part of NO don't you understand? Some answers to the cardinal questions in nitric oxide biology." J Biol Chem **285**(26): 19699-19704.

Hong, F., M. L. Freeman and D. C. Liebler (2005). "Identification of sensor cysteines in human Keap1 modified by the cancer chemopreventive agent sulforaphane." Chem Res Toxicol **18**(12): 1917-1926.

Hosoki, R., N. Matsuki and H. Kimura (1997). "The possible role of hydrogen sulfide as an endogenous smooth muscle relaxant in synergy with nitric oxide." Biochem Biophys Res Commun **237**(3): 527-531.

Hourihan, J. M., J. G. Kenna and J. D. Hayes (2012). "The Gasotransmitter Hydrogen Sulfide Induces Nrf2-Target Genes by Inactivating the Keap1 Ubiquitin Ligase Substrate Adaptor Through Formation of a Disulfide Bond Between Cys-226 and Cys-613." Antioxidants & Redox Signaling **19**(5): 465-481.

Hrabie, J. A. and L. K. Keefer (2002). "Chemistry of the nitric oxide-releasing diazeniumdiolate ("nitrosohydroxylamine") functional group and its oxygen-substituted derivatives." Chem Rev **102**(4): 1135-1154.

Ida, T., T. Sawa, H. Ihara, Y. Tsuchiya, Y. Watanabe, Y. Kumagai, M. Suematsu, H. Motohashi, S. Fujii, T. Matsunaga, M. Yamamoto, K. Ono, N. O. Devarie-Baez, M. Xian, J. M. Fukuto and T. Akaike (2014). "Reactive cysteine persulfides and S-polythiolation regulate oxidative stress and redox signaling." Proc Natl Acad Sci U S A **111**(21): 7606-7611.

Ignarro, L. J., G. M. Buga, K. S. Wood, R. E. Byrns and G. Chaudhuri (1987). "Endothelium-derived relaxing factor produced and released from artery and vein is nitric oxide." Proc Natl Acad Sci U S A **84**(24): 9265-9269.

Ishii, T., K. Itoh, S. Takahashi, H. Sato, T. Yanagawa, Y. Katoh, S. Bannai and M. Yamamoto (2000). "Transcription factor Nrf2 coordinately regulates a group of oxidative stress-inducible genes in macrophages." The Journal of Biological Chemistry **275**(21): 16023-16029.

Itoh, K., T. Chiba, S. Takahashi, T. Ishii, K. Igarashi, Y. Katoh, T. Oyake, N. Hayashi, K. Satoh, I. Hatayama, M. Yamamoto and Y. Nabeshima (1997). "An Nrf2/small Maf heterodimer mediates the induction of phase II detoxifying enzyme genes through antioxidant response elements." Biochemical and biophysical research communications **236**(2): 313-322.

Itoh, K., K. Igarashi, N. Hayashi, M. Nishizawa and M. Yamamoto (1995). "Cloning and characterization of a novel erythroid cell-derived CNC family transcription factor heterodimerizing with the small Maf family proteins." Molecular and Cellular Biology **15**(8): 4184-4193.

Itoh, K., T. Ishii, N. Wakabayashi and M. Yamamoto (1999). "Regulatory mechanisms of cellular response to oxidative stress." Free Radical Research **31**(4): 319-324.

Itoh, K., N. Wakabayashi, Y. Katoh, T. Ishii, K. Igarashi, J. D. Engel and M. Yamamoto (1999). "Keap1 represses nuclear activation of antioxidant responsive elements by Nrf2 through binding to the amino-terminal Neh2 domain." Genes & Development **13**(1): 76-86.

Jaiswal, A. K. (2004). "Nrf2 signaling in coordinated activation of antioxidant gene expression." Free Radical Biology & Medicine **36**(10): 1199-1207.

Jones, S. P. and R. Bolli (2006). "The ubiquitous role of nitric oxide in cardioprotection." J Mol Cell Cardiol **40**(1): 16-23.

Kajimura, M., R. Fukuda, R. M. Bateman, T. Yamamoto and M. Suematsu (2010). "Interactions of multiple gas-transducing systems: hallmarks and uncertainties of CO, NO, and H<sub>2</sub>S gas biology." Antioxidants & redox signaling **13**(2): 157-192.

Kang, N. J., K. W. Lee, D. E. Lee, E. A. Rogozin, A. M. Bode, H. J. Lee and Z. Dong (2008). "Cocoa procyanidins suppress transformation by inhibiting mitogen-activated protein kinase kinase." The Journal of Biological Chemistry **283**(30): 20664-20673.

Kaspar, J. W., S. K. Niture and A. K. Jaiswal (2009). "Nrf2:INrf2 (Keap1) signaling in oxidative stress." Free radical biology & medicine **47**(9): 1304-1309.

Katoh, Y., K. Itoh, E. Yoshida, M. Miyagishi, A. Fukamizu and M. Yamamoto (2001). "Two domains of Nrf2 cooperatively bind CBP, a CREB binding protein, and synergistically activate transcription." Genes Cells **6**(10): 857-868.

Keefer, L. K. (2011). "Fifty years of diazeniumdiolate research. From laboratory curiosity to broad-spectrum biomedical advances." ACS Chem Biol **6**(11): 1147-1155.

Kimura, H. (2014). "Signaling Molecules: Hydrogen Sulfide and Polysulfide." Antioxidants & redox signaling.

Kobayashi, A., M. I. Kang, H. Okawa, M. Ohtsuji, Y. Zenke, T. Chiba, K. Igarashi and M. Yamamoto (2004). "Oxidative stress sensor Keap1 functions as an adaptor for Cul3-based E3 ligase to regulate proteasomal degradation of Nrf2." Mol Cell Biol **24**(16): 7130-7139.

Kobayashi, M., K. Itoh, T. Suzuki, H. Osanai, K. Nishikawa, Y. Katoh, Y. Takagi and M. Yamamoto (2002). "Identification of the interactive interface and phylogenetic conservation of the Nrf2-Keap1 system." Genes to Cells: Devoted to Molecular & Cellular Mechanisms **7**(8): 807-820.

Kobayashi, M. and M. Yamamoto (2006). "Nrf2-Keap1 regulation of cellular defense mechanisms against electrophiles and reactive oxygen species." Advances in Enzyme Regulation **46**: 113-140.

Koike, S., Y. Ogasawara, N. Shibuya, H. Kimura and K. Ishii (2013). "Polysulfide exerts a protective effect against cytotoxicity caused by t-butylhydroperoxide through Nrf2 signaling in neuroblastoma cells." FEBS letters **587**(21): 3548-3555.

Lau, A., W. Tian, S. A. Whitman and D. D. Zhang (2013). "The predicted molecular weight of Nrf2: it is what it is not." Antioxidants & redox signaling **18**(1): 91-93.

Levitt, M. D., M. S. Abdel-Rehim and J. Furne (2011). "Free and acid-labile hydrogen sulfide concentrations in mouse tissues: anomalously high free hydrogen sulfide in aortic tissue." Antioxid Redox Signal **15**(2): 373-378.

Li, L., M. Whiteman, Y. Y. Guan, K. L. Neo, Y. Cheng, S. W. Lee, Y. Zhao, R. Baskar, C.-H. Tan and P. K. Moore (2008). "Characterization of a novel, water-soluble hydrogen sulfide-releasing molecule (GYY4137): new insights into the biology of hydrogen sulfide." Circulation **117**(18): 2351-2360.

Liu, W., D. Wang, K. Liu and X. Sun (2012). "Nrf2 as a converging node for cellular signaling pathways of gasotransmitters." Medical hypotheses **79**(3): 308-310.

Liu, X.-m., K. J. Peyton, D. Ensenat, H. Wang, M. Hannink, J. Alam and W. Durante (2007). "Nitric oxide stimulates heme oxygenase-1 gene transcription via the Nrf2/ARE complex to promote vascular smooth muscle cell survival." Cardiovascular Research **75**(2): 381-389.

Liu, Y.-H., M. Lu, L.-F. Hu, P. T. H. Wong, G. D. Webb and J.-S. Bian (2012). "Hydrogen sulfide in the mammalian cardiovascular system." Antioxidants & redox signaling **17**(1): 141-185.

Lo, S. C., X. Li, M. T. Henzl, L. J. Beamer and M. Hannink (2006). "Structure of the Keap1:Nrf2 interface provides mechanistic insight into Nrf2 signaling." EMBO J **25**(15): 3605-3617.

Lukosz, M., S. Jakob, N. Büchner, T.-C. Zschauer, J. Altschmied and J. Haendeler (2010). "Nuclear redox signaling." Antioxidants & redox signaling **12**(6): 713-742.

Mackenzie, G. G., A. M. Adamo, N. P. Decker and P. I. Oteiza (2008). "Dimeric procyanidin B2 inhibits constitutively active NF-kappaB in Hodgkin's lymphoma cells independently of the presence of IkappaB mutations." Biochem Pharmacol **75**(7): 1461-1471.

Mackenzie, G. G., F. Carrasquedo, J. M. Delfino, C. L. Keen, C. G. Fraga and P. I. Oteiza (2004). "Epicatechin, catechin, and dimeric procyanidins inhibit PMA-induced NF-kappaB activation at multiple steps in Jurkat T cells." FASEB J **18**(1): 167-169.

Mackenzie, G. G. and P. I. Oteiza (2006). "Modulation of transcription factor NF-kappaB in Hodgkin's lymphoma cell lines: effect of (-)-epicatechin." Free Radical Research **40**(10): 1086-1094.

McCullough, M. L., J. J. Peterson, R. Patel, P. F. Jacques, R. Shah and J. T. Dwyer (2012). "Flavonoid intake and cardiovascular disease mortality in a prospective cohort of US adults." The American Journal of Clinical Nutrition **95**(2): 454-464.

McMahon, M., K. Itoh, M. Yamamoto, S. A. Chanas, C. J. Henderson, L. I. McLellan, C. R. Wolf, C. Cavin and J. D. Hayes (2001). "The Cap'n'Collar basic leucine zipper transcription factor Nrf2 (NF-E2 p45-related factor 2) controls both constitutive and inducible expression of intestinal detoxification and glutathione biosynthetic enzymes." Cancer Research **61**(8): 3299-3307.

McMahon, M., D. J. Lamont, K. A. Beattie and J. D. Hayes (2010). "Keap1 perceives stress via three sensors for the endogenous signaling molecules nitric oxide, zinc, and alkenals." Proc Natl Acad Sci U S A **107**(44): 18838-18843.

McMahon, M., N. Thomas, K. Itoh, M. Yamamoto and J. D. Hayes (2004). "Redox-regulated turnover of Nrf2 is determined by at least two separate protein domains, the redox-sensitive Neh2 degron and the redox-insensitive Neh6 degron." J Biol Chem **279**(30): 31556-31567.

McMahon, M., N. Thomas, K. Itoh, M. Yamamoto and J. D. Hayes (2006). "Dimerization of substrate adaptors can facilitate cullin-mediated ubiquitylation of proteins by a "tethering" mechanism: a two-site interaction model for the Nrf2-Keap1 complex." The Journal of biological chemistry **281**(34): 24756-24768.

Moi, P., K. Chan, I. Asunis, A. Cao and Y. W. Kan (1994). "Isolation of NF-E2-related factor 2 (Nrf2), a NF-E2-like basic leucine zipper transcriptional activator that binds to the tandem NF-E2/AP1 repeat of the beta-globin locus control region." Proceedings of the National Academy of Sciences of the United States of America **91**(21): 9926-9930.

Moore, P. K., M. Bhatia and S. Moolchhala (2003). "Hydrogen sulfide: from the smell of the past to the mediator of the future?" Trends Pharmacol Sci **24**(12): 609-611.

Motohashi, H., F. Katsuoka, J. D. Engel and M. Yamamoto (2004). "Small Maf proteins serve as transcriptional cofactors for keratinocyte differentiation in the Keap1-Nrf2 regulatory pathway." Proc Natl Acad Sci U S A **101**(17): 6379-6384.

Müller, R. P., M. Nonella, P. Russegger and J. R. Huber (1984). "UV-, VIS- and IR-light-induced isomerization of HSNO in a low-temperature matrix." Chemical Physics **87**(3): 351-361.

Mulvihill, E. E. and M. W. Huff (2010). "Antiatherogenic properties of flavonoids: implications for cardiovascular health." The Canadian Journal of Cardiology **26 Suppl A**: 17A-21A.

Mustafa, A. K., M. M. Gadalla, N. Sen, S. Kim, W. Mu, S. K. Gazi, R. K. Barrow, G. Yang, R. Wang and S. H. Snyder (2009). "H<sub>2</sub>S signals through protein S-sulfhydration." Sci Signal **2**(96): ra72.

Naughton, P., M. Hoque, C. J. Green, R. Foresti and R. Motterlini (2002). "Interaction of heme with nitroxyl or nitric oxide amplifies heme oxygenase-1 induction: involvement of the transcription factor Nrf2." Cellular and Molecular Biology (Noisy-Le-Grand, France) **48**(8): 885-894.

Nehlig, A. (2013). "The neuroprotective effects of cocoa flavanol and its influence on cognitive performance." British Journal of Clinical Pharmacology **75**(3): 716-727.

Nioi, P., T. Nguyen, P. J. Sherratt and C. B. Pickett (2005). "The carboxy-terminal Neh3 domain of Nrf2 is required for transcriptional activation." Mol Cell Biol **25**(24): 10895-10906.

Nishida, M., T. Sawa, N. Kitajima, K. Ono, H. Inoue, H. Ihara, H. Motohashi, M. Yamamoto, M. Suematsu, H. Kurose, A. van der Vliet, B. A. Freeman, T. Shibata, K. Uchida, Y. Kumagai and T. Akaike (2012). "Hydrogen sulfide anion regulates redox signaling via electrophile sulfhydration." Nat Chem Biol **8**(8): 714-724.

Olson, K. R. (2012). "A practical look at the chemistry and biology of hydrogen sulfide." Antioxidants & redox signaling **17**(1): 32-44.

Ondrias, K., A. Stasko, S. Cacanyiova, Z. Sulova, O. Krizanova, F. Kristek, L. Malekova, V. Knezl and A. Breier (2008). "H<sub>2</sub>S and HS(-) donor NaHS releases nitric oxide from nitrosothiols, metal nitrosyl complex, brain homogenate and murine L1210 leukaemia cells." Pflugers Arch **457**(2): 271-279.

Ottaviani, J. I., T. Y. Momma, C. Heiss, C. Kwik-Urbe, H. Schroeter and C. L. Keen (2011). "The stereochemical configuration of flavanols influences the level and metabolism of flavanols in humans and their biological activity in vivo." Free radical biology & medicine **50**(2): 237-244.

Ottaviani, J. I., T. Y. Momma, G. K. Kuhnle, C. L. Keen and H. Schroeter (2012). "Structurally related (-)-epicatechin metabolites in humans: assessment using de novo chemically synthesized authentic standards." Free radical biology & medicine **52**(8): 1403-1412.

Padmanabhan, B., K. I. Tong, T. Ohta, Y. Nakamura, M. Scharlock, M. Ohtsuji, M. I. Kang, A. Kobayashi, S. Yokoyama and M. Yamamoto (2006). "Structural basis for defects of Keap1 activity provoked by its point mutations in lung cancer." Mol Cell **21**(5): 689-700.

Palmer, R. M., A. G. Ferrige and S. Moncada (1987). "Nitric oxide release accounts for the biological activity of endothelium-derived relaxing factor." Nature **327**(6122): 524-526.

Paravicini, T. M. and R. M. Touyz (2006). "Redox signaling in hypertension." Cardiovascular Research **71**(2): 247-258.

Rachakonda, G., Y. Xiong, K. R. Sekhar, S. L. Stamer, D. C. Liebler and M. L. Freeman (2008). "Covalent modification at Cys151 dissociates the electrophile sensor Keap1 from the ubiquitin ligase CUL3." Chem Res Toxicol **21**(3): 705-710.

Ramirez-Sanchez, I., L. Maya, G. Ceballos and F. Villarreal (2010). "(-)-epicatechin activation of endothelial cell endothelial nitric oxide synthase, nitric oxide, and related signaling pathways." Hypertension **55**(6): 1398-1405.

Rassaf, T., M. Feelisch and M. Kelm (2004). "Circulating NO pool: assessment of nitrite and nitroso species in blood and tissues." Free Radical Biology & Medicine **36**(4): 413-422.

Riccio, D. A. and M. H. Schoenfisch (2012). "Nitric oxide release: part I. Macromolecular scaffolds." Chem Soc Rev **41**(10): 3731-3741.

Rothe, F., P. L. Huang and G. Wolf (1999). "Ultrastructural localization of neuronal nitric oxide synthase in the laterodorsal tegmental nucleus of wild-type and knockout mice." Neuroscience **94**(1): 193-201.

Ruijters, E. J. B., A. R. Weseler, C. Kicken, G. R. M. M. Haenen and A. Bast (2013). "The flavanol (-)-epicatechin and its metabolites protect against oxidative stress in primary endothelial cells via a direct antioxidant effect." European journal of pharmacology.

Rushmore, T. H., M. R. Morton and C. B. Pickett (1991). "The antioxidant responsive element. Activation by oxidative stress and identification of the DNA consensus sequence required for functional activity." The Journal of Biological Chemistry **266**(18): 11632-11639.

Rushmore, T. H., M. R. Morton and C. B. Pickett (1991). "The antioxidant responsive element. Activation by oxidative stress and identification of the DNA consensus sequence required for functional activity." J Biol Chem **266**(18): 11632-11639.

Saito, R., T. Suzuki, K. Hiramoto, S. Asami, E. Naganuma, H. Suda, T. Iso, H. Yamamoto, M. Morita, L. Baird, Y. Furusawa, T. Negishi, M. Ichinose and M. Yamamoto (2015). "Characterizations of Three Major Cysteine Sensors of Keap1 in Stress Response." Mol Cell Biol **36**(2): 271-284.

Schreck, R., P. Rieber and P. A. Baeuerle (1991). "Reactive oxygen intermediates as apparently widely used messengers in the activation of the NF-kappa B transcription factor and HIV-1." EMBO J **10**(8): 2247-2258.

Schroeter, H., C. Heiss, J. Balzer, P. Kleinbongard, C. L. Keen, N. K. Hollenberg, H. Sies, C. Kwik-Urbe, H. H. Schmitz and M. Kelm (2006). "(-)-Epicatechin mediates beneficial effects of flavanol-rich cocoa on vascular function in humans." Proceedings of the National Academy of Sciences of the United States of America **103**(4): 1024-1029.

Seel, F. and M. Wagner (1988). "Über die Umsetzung von Sulfiden mit Stickstoffmonoxid in Wäßrigen Lösungen." Zeitschrift für anorganische und allgemeine Chemie **558**(1): 189-192.

Shah, Z. A., R.-c. Li, A. S. Ahmad, T. W. Kensler, M. Yamamoto, S. Biswal and S. Doré (2010). "The flavanol (-)-epicatechin prevents stroke damage through the Nrf2/HO1 pathway." Journal of cerebral blood flow and metabolism: official journal of the International Society of Cerebral Blood Flow and Metabolism **30**(12): 1951-1961.

Shukla, V., S. K. Mishra and H. C. Pant (2011). "Oxidative stress in neurodegeneration." Advances in Pharmacological Sciences **2011**: 572634.

Sichel, G., C. Corsaro, M. Scalia, A. J. Di Bilio and R. P. Bonomo (1991). "In vitro scavenger activity of some flavonoids and melanins against O<sub>2</sub>(-)." Free Radical Biology & Medicine **11**(1): 1-8.

Siedlar, M., B. Mytar, A. Krzeszowiak, J. Baran, M. Hyszko, I. Ruggiero, J. Wieckiewicz, J. Stachura and M. Zembala (1999). "Demonstration of iNOS-mRNA and iNOS in human monocytes stimulated with cancer cells in vitro." J Leukoc Biol **65**(5): 597-604.

Sies, H. (1985). Oxidative Stress.

Sies, H. (1986). "Biochemie des oxidativen Stress." Angewandte Chemie **98**(12): 1061-1075.

Sies, H. (1993). "Strategies of antioxidant defense." Eur J Biochem **215**(2): 213-219.

Sies, H. (2015). "Oxidative stress: a concept in redox biology and medicine." Redox Biol **4**: 180-183.

Sivarajah, A., M. C. McDonald and C. Thiemermann (2006). "The production of hydrogen sulfide limits myocardial ischemia and reperfusion injury and contributes to the cardioprotective effects of preconditioning with endotoxin, but not ischemia in the rat." Shock **26**(2): 154-161.

Stocker, R. and J. F. Keaney, Jr. (2004). "Role of oxidative modifications in atherosclerosis." Physiological reviews **84**(4): 1381-1478.

Teng, X., T. Scott Isbell, J. H. Crawford, C. A. Bosworth, G. I. Giles, J. R. Koenitzer, J. R. Lancaster, J. E. Doeller, W. K. D and P. P. R (2008). "Novel method for measuring S-nitrosothiols using hydrogen sulfide." Methods Enzymol **441**: 161-172.

Thomas, D. D., X. Liu, S. P. Kantrow and J. R. Lancaster, Jr. (2001). "The biological lifetime of nitric oxide: implications for the perivascular dynamics of NO and O<sub>2</sub>." Proc Natl Acad Sci U S A **98**(1): 355-360.

Toh, J. Y., V. M. H. Tan, P. C. Y. Lim, S. T. Lim and M. F. F. Chong (2013). "Flavonoids from fruit and vegetables: a focus on cardiovascular risk factors." Current Atherosclerosis Reports **15**(12): 368.

Tong, K. I., B. Padmanabhan, A. Kobayashi, C. Shang, Y. Hirotsu, S. Yokoyama and M. Yamamoto (2007). "Different electrostatic potentials define ETGE and DLG motifs as hinge and latch in oxidative stress response." Mol Cell Biol **27**(21): 7511-7521.

Trachootham, D., J. Alexandre and P. Huang (2009). "Targeting cancer cells by ROS-mediated mechanisms: a radical therapeutic approach?" Nature Reviews. Drug Discovery **8**(7): 579-591.

van der Veen, R. C., T. A. Dietlin, L. Pen and J. D. Gray (1999). "Nitric oxide inhibits the proliferation of T-helper 1 and 2 lymphocytes without reduction in cytokine secretion." Cell Immunol **193**(2): 194-201.

Wakabayashi, N., A. T. Dinkova-Kostova, W. D. Holtzclaw, M. I. Kang, A. Kobayashi, M. Yamamoto, T. W. Kensler and P. Talalay (2004). "Protection against electrophile and oxidant stress by induction of the phase 2 response: fate of cysteines of the Keap1 sensor modified by inducers." Proc Natl Acad Sci U S A **101**(7): 2040-2045.

Wang, R. (2003). "The gasotransmitter role of hydrogen sulfide." Antioxid Redox Signal **5**(4): 493-501.

Wang, R. (2012). "Physiological implications of hydrogen sulfide: a whiff exploration that blossomed." Physiological reviews **92**(2): 791-896.

Whiteman, M., L. Li, I. Kostetski, S. H. Chu, J. L. Siau, M. Bhatia and P. K. Moore (2006). "Evidence for the formation of a novel nitrosothiol from the gaseous mediators nitric oxide and hydrogen sulphide." Biochem Biophys Res Commun **343**(1): 303-310.

Yang, G., K. Zhao, Y. Ju, S. Mani, Q. Cao, S. Puukila, N. Khaper, L. Wu and R. Wang (2013). "Hydrogen sulfide protects against cellular senescence via S-sulphydration of Keap1 and activation of Nrf2." Antioxidants & redox signaling **18**(15): 1906-1919.

Zhang, D. D. (2006). "Mechanistic studies of the Nrf2-Keap1 signaling pathway." Drug metabolism reviews **38**(4): 769-789.

Zhang, D. D. and M. Hannink (2003). "Distinct cysteine residues in Keap1 are required for Keap1-dependent ubiquitination of Nrf2 and for stabilization of Nrf2 by chemopreventive agents and oxidative stress." Mol Cell Biol **23**(22): 8137-8151.

Zhang, Y. and N. Hogg (2005). "S-Nitrosothiols: cellular formation and transport." Free Radical Biology and Medicine **38**(7): 831-838.

Zhao, Y., T. D. Biggs and M. Xian (2014). "Hydrogen sulfide (H<sub>2</sub>S) releasing agents: chemistry and biological applications." Chem Commun (Camb) **50**(80): 11788-11805.